Università degli Studi di Ferrara

DOCTORAL COURSE IN

BIOMEDICAL SCIENCES AND BIOTECHNOLOGY

CYCLE XXXI

DIRECTOR Prof. Paolo Pinton

The Chronic Challenge: Strategies to Improve Biocompatibility and Performance of Implanted Neural Devices.

Research funded by Fondazione Istituto Italiano di Tecnologia

Scientific/Disciplinary Sector (SDS) BIO/09

Candidate

Dott.ssa Francesca Ciarpella

Supervisor

Prof. Luciano Fadiga

Years 2015/2018

To my Family,
always with me.

With love.

ACKNOWLEDGEMENTS

I would like to thank my supervisor Professor Luciano Fadiga, for giving me the opportunity to join this PhD program and to carry out the works of this thesis.
I would also like to thank Professor Davide Ricci for his patience in the review process of my thesis and for all the comments and suggestions. His precious support, all his teachings and advice have always guided me during these years.
Thanks to all the collaborators and especially thanks to all the lab's people, each of you is part of this work and you have been part of all my days.

Formalities apart.
There are people that I would like to thank with my heart.
Emanuela, Rosanna, Elena. Colleagues, friends, women, subjects! All of this is dedicated to you. *Done is better than perfect*. You have been my strength and you know it better than me. We shared something that we only know and that I don't need to explain. Without you this thesis would not have been possible. My joy, my daily support. You already know what you left me inside.

Thanks to my old Friends. There is an invisible thread that binds us and I am sure that its strength will make us always find each other. You are my second Family.

Thanks to all the people who have gone through my life and my days in these three years. Thanks to who was beside me and to who is still here.

Thanks to who believed in me and to who will continue to do so.

Thanks to You, my Love and my Pain.

LIST OF CONTENTS

Introduction 3

1. Brain computer interfaces 3

2. Intracortical devices 7

3. Tissue reaction 10

4. Strategies to improve intracortical electrodes performance 17

4.1 Materials improvements 17

4.2 Bioactive modifications 20

5. Concept of biocompatibility of neural probes 23

Bibliography 25

Chapter 1

Cell-coated Intracortical Microelectrodes: Methods to Improve the Biocompatibility of Chronic Implants 34

1.Experimental section 36

1.1 Isolation and characterization of rat aortic endothelial cells (RAEC) 36

1.2 Cell culture on electrode substrates 37

1.3 Electrochemical characterization of the electrodes 38

1.4 Immunofluorescence cells labeling 38

1.5 Animal surgery and *in vivo* chronic implants 39

1.6 Neural Recordings and Evaluation of the Signal-To-Noise ratio 40

1.7 Histology and quantitative analysis 41

2. Results and Discussion 44

2.1 Wire coated with endothelial cells: Bio-hybrid manufacturing 44

2.2 Electrochemical properties and recording capability of the bio-hybrid device 47

2.3 Check of *in vivo* cell presence 48

2.4 Improving intracortical microelectrodes 50

2.4.1 Inflammatory response: coated vs uncoated microelectrodes 50

2.4.2 Neuronal response: coated vs uncoated microelectrodes 55

3. Conclusions 58

Bibliography 60

Chapter 2

How Flexibility and Probe Size Influence Chronic Performance: *In Vivo* Study on Polyimide-based Intracortical Arrays 62

1. Experimental section 65

1.1 Electrodes fabrication and design 65

1.2 Electrochemical characterization of the electrodes 66

1.3 Animal surgery and array implantation for histological evaluation 66

1.4 Histology and quantitative analysis 68

1.5 Animal surgery and array implantation for signal recording 69

1.6 *In vivo* impedance measurements 70

1.7 Neural recording and evaluation of Signal-To-Noise ratio 70

2. Results and discussion 72

2.1 Implantation of small and flexible polyimide-based arrays 72

2.2 Electrochemical properties of small and flexible arrays 73

2.3 Functional properties and recording quality of small and flexible arrays 74

2.4 Immunofluorescence and foreign body reaction 76

3. Conclusions 83

Bibliography 85

Chapter 3

Biocompatibility of Innovative Neural Electrode Materials 86

3.1 Highly Stable Glassy Carbon Interfaces for Long-Term Neural Stimulation and Low-Noise Recording of Brain Activity. 90

3.2 A Direct Comparison of Glassy Carbon and PEDOT-PSS Electrodes for High Charge Injection and Low Impedance Neural Interfaces. 92

3.3 Incorporation of Silicon Carbide and Diamond-Like Carbon as Adhesion Promoters Improves *In Vitro* and *In Vivo* Stability of Thin-Film Glassy Carbon Electrocorticography Arrays. 94

3.4 Single Walled Carbon Nanohorns for Neural Sensing and Stimulation. 97

3.5 Drug Delivery System based on Tauroursodeoxycholic Acid and PEDOT. 99

3.6 pHEMA Encapsulated PEDOT-PSS-CNT Microsphere for Recording Single Unit Activity in the Brain. 101

Conclusions and Future Perspective 105

INTRODUCTION

1. BRAIN COMPUTER INTERFACES

With the term *neural interface,* one refers to a device able to establish a direct communication between the nervous system and the external world by stimulating and recording the electrical activity from nearby neurons. Therefore, a *brain computer interface* (BCI), also referred to as *brain machine interface* (BMI), is a hardware/software bidirectional communication system that interconnects the brain to an external device[1] allowing control trough feedback.

The term "brain-computer Interface" (BCI) was first introduced during the pioneering work of J. Vidal in the early 1970's. By this term he referred to the possibility of utilizing brain signals in a man-computer dialogue and, at the same time, of developing novel tools for studying the neurophysiological phenomena that govern the production and the control of detectable neuroelectric events [2].

BCIs, mainly non-invasive, have contributed to various fields of research, spacing from medical to educational, entertainment and security applications (Figure **1**). In particular, healthcare could take great advantage through the analysis of brain signals in all associated phases including prevention, detection, diagnosis, rehabilitation and restoration[3].

At present, implantation of invasive macro- and micro-devices into the brain is increasingly used for treatment of neurological disorders, so that the most immediate high-impact goal of BMI research is to provide communication capabilities to severely disabled people who are totally paralyzed or 'locked in' by neurological neuromuscular disorders, such as amyotrophic lateral sclerosis, stroke or neural injuries. In the clinical environment, neural prostheses are used for a variety of treatment applications, including counteracting the devastating deficits in motor function due to Parkinson's disease, intervening in seizure activity induced in intractable epilepsy, and returning sensory function to individuals who have lost vision or hearing[1]. Another purpose of BMIs is to restore motor and somatosensory function to paralyzed patients by directly controlling an assistive device through signals recorded from the brain. Likewise, innovative designs are being explored to reconnect a patient's residual peripheral nerves with electrode arrays for direct control of prostheses in amputees. Outside the clinic, neural prostheses are invaluable research

tools used to reveal the role of specific neurons and activation patterns in natural and pathological functions[4].

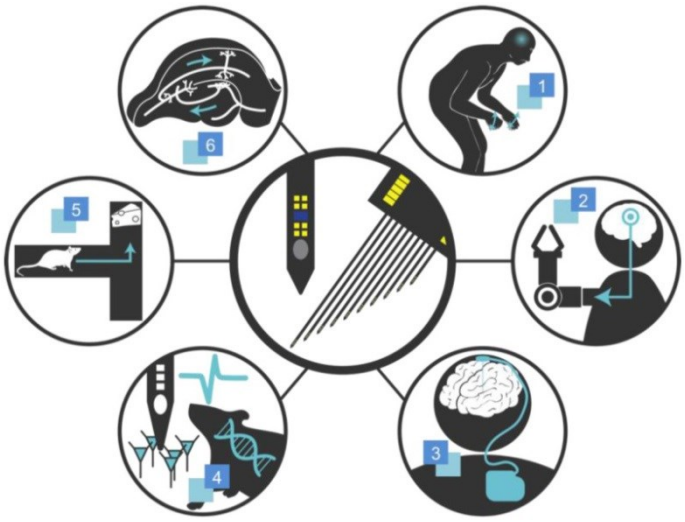

Figure 1. Graphical overview of applications of the neural probe technology. 1. Parkinson's Disease; 2. Neuroprosthetics; 3. Brain Pacemaker; 4. Investigation of Brain Diseases; 5. Cognitive Experiments; 6. Brain Mapping (*from Kook G et al., 2016*[5]).

Different neurophysiological signals are known to be correlated with neuronal activity in the brain and, thus, they could be recorded and used to drive a BCI. The signal source can be of different biophysical nature and we can categorize the signals in three major groups: electrophysiological, magnetic (i.e. related to very small magnetic fields produced by the electrical activity of the brain), and metabolic.[6] Electrophysiological activity is generated by ions movements across the neural membrane following neurotransmitter release and recognition by neurons, the basic information processing in the central nervous system (CNS). The intracellular current, known as primary current, is a dipole conducting current from a source to a sink through the dendritic trunk. Conservation of electric charges implies that the primary currents are enclosed by extracellular current flows, which are known as secondary currents.

There are different types of recording electrode devices that have been developed to access different forms of neural information through varying levels of invasiveness (Figure **2**).
Most current BMIs obtain the relevant information from the brain activity through electroencephalography (EEG)[7]. EEG is by far the most widely used non-invasive approach, owing to its high temporal resolution, relative low cost and minimal risk for the users. BCIs based on EEG consist of a set of sensors that acquire EEG signals from

different brain areas. The quality of these signals is affected by distance and the transmission through scalp, skull, and many other biological layers as well as background noise. A better control signal for complex BMI applications could come from invasive devices that, by penetrating into specific regions of the brain, allow high spatial resolution in detecting or stimulating particular groups of neurons.

The spatial resolution refers to the brain volume from which neuron-derived information is detected and combined in the sensor. For instance, EEG recordings reflect the resulting effect of changes in a huge number of local neural electrical fields oriented perpendicular to the skull, whereas implanted intracortical (or subcortical) recordings are able to focus on individual neuronal action potentials from groups of simultaneously recorded neurons. Hence the intracortical signals result more efficient than EEG signals.

Most of our knowledge on brain structure and functionalities rely on the use of invasive devices, such as intracortical electrodes, that require to be implanted under the skull: the associated significant health risks limit their use to experimental settings and several issues have to be still addressed before they become suitable for long-term applications. There are two major invasive modalities in BCI research: electrocorticography (ECoG), performed using electrodes placed on the surface of the cortex, usually under the dura mater (subdural ECoG), and intracortical neuron recording systems which rely on electrodes implanted inside the cortex. ECoG is a recording method that combines together the accuracy of invasiveness and the safety of a relatively non-invasive technique. It requires the placement of a grid or strip of electrodes over the cortex, measuring the same signals as in EEG, but closer to the source. The absence of the insulating features of skull and dura mater, results in greater signal amplitude, wider detectable frequency range, and better topographical resolution. Several studies report the use of ECoG recordings in BMI approaches like in motor tasks and speech process classification as well as for seizure localization in epilepsy patients[3,8].

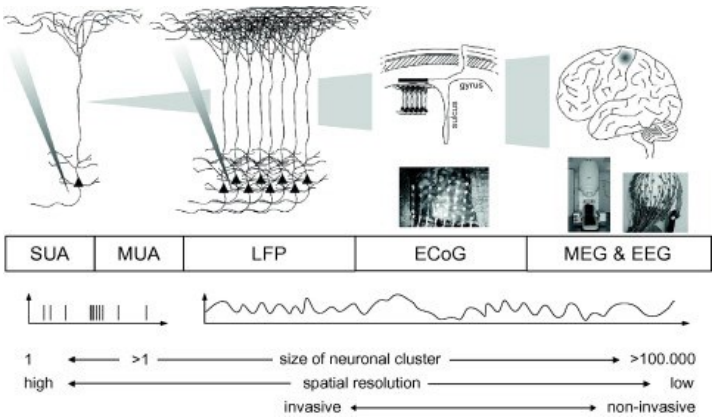

Figure 2. Schematic overview of the recording techniques SUA/MUA, LFP, ECoG, and MEG (magnetoencephalography)/EEG showing (from top to bottom): the spatial scale at which signals are recorded, the characteristic of the signal (discrete vs. analog), and the correspondence to different scales (*from Waldert S et al., 2009*[9]).

The intracortical method represents the most invasive BCI method since it requires the implant of microelectrode arrays inside the brain to capture neuronal activity. Three types of signals can be obtained by intracortical neural recordings: single-unit activity (SUA), multi-unit activity (MUA), and local field potentials (LFPs). SUA is obtained by high-pass filtering (> 300 Hz) the signal recorded from a single neuron while MUA is related to the signals coming from multiple neurons. On the contrary, LFPs are extracted by low-pass filtering (< 300 Hz) the neuron activity signal detected near the electrode tip. LFPs are analog signals whereas SUA and MUA measure the spiking activity of single neurons and can be reduced to discrete events in time[9]. Intracortical neuron recording provides much higher spatial and temporal resolution than EEG recording, and for best possible results one would require achieving stable communication with as many as possible individual neurons with a high degree of signal-to-noise ratio (SNR) for specific time periods, from hours to years. However, signal quality may be affected by the reaction of cerebral tissue to the implanted microelectrode and by changes in the device sensitivity, which may be progressively damaged over time. This may reduce the detection and decoding efficacy of BMIs and performance of closed-loop neuro stimulation systems in which the stimulus is conditioned on a recorded neural signal. Signal loss and instability are due to a variety of reasons, both of biological and non-biological origin, but the neural injury and inflammation that accompany device implantation are the key contributing factors. Neuronal loss, signatures of neurodegeneration, and activation of neuronal cell death pathways have been observed in the tissue surrounding devices implanted in the CNS[10].

A more detailed description of intracortical devices and their failure modalities will be given in the next section.

Summing up, neural interfaces communicate with the nervous system via implantable electrodes that transduce electric signals from and to bioelectric neural sources. For all applications the challenge is to obtain a stable, long-term communication between the device and the neuronal population of interest.

To reach this aim, there is the need to develop innovative bioengineering approaches to create neural probes that are biologically "transparent" and biocompatible, support seamless integration with neurons and remain functional for a long period of time.

2. INTRACORTICAL DEVICES

The intracortical acquisition technique represents the most invasive method, implanting single electrodes or an array of multiple electrodes under the brain cortex surface. Different kinds of intracortical microelectrodes have been designed to interface with cortical neurons but the way how microelectrodes extract electrical signals generated from target neurons is similar.

The first portion of the circuit involves the cortical column and the complex set of presynaptic inputs that innervate the target neurons addressed by the microelectrodes. These inputs can be both excitatory and inhibitory. If a sufficiently large excitatory postsynaptic potential is created, an action potential is then generated through depolarization of the axon hillock. The ion-based signal then travels through the extracellular space to the electrode-recording site. Since the information travels primarily through diffusion mechanisms, the signal strength that is picked up by the microelectrodes is mainly influenced by the distance and the impedance of the extracellular space.

At the recording site, the electric potential produced by the ion-based signal is recorded as a voltage change. Signals can then be amplified and analyzed using various acquisition and processing techniques. Once analyzed, appropriate algorithms are applied to translate the signal into device commands/orders that carry out the user's volitional intent.

Originally, neural interfaces were developed as a basic science tool, and as such, have been used extensively to increase our understanding of how the nervous system works. Since 1940's metal wires were used in acute electrophysiology experiments to record electrical signals from single neurons[11]. These early devices were made of a penetrating tine with an

exposed conducting tip capable of electrically interacting with nearby neurons. The traditional Ag/AgCl based electrodes were then replaced with other metals such as stainless steel, tungsten and platinum, more effective and safer for long term recording applications.

The most widely used penetrating microelectrode is the standard insulated tungsten wire and starting from its simplicity and effectiveness, early devices were made of multiple electrodes combined in a single integrated electrode array (Figure **3A**).

Over the years, several new electrode designs and materials were introduced leading to the development of microwire electrodes from iridium (Ir, because of its stiffness), platinum (Pt) and platinum-iridium- alloys (Pt/Ir) as well as to the incorporation of either glass or poly (monochloro-p-xylene) (Parylene-C) coatings to insulate the shaft of microwire electrodes[12] leaving exposed only the very tip. Despite the capability to detect neuronal signals for months, the performance of these devices decreases over time, limiting their use in neuroprosthetic applications. This drop of recording capability is widely associated to the inflammatory-mediated device encapsulation that electrically isolates the device from the surrounding tissue, increasing impedance values.

Advancements in semiconducting materials and improvements in micromachining capabilities drove the development of silicon-based microelectrodes. By the 1980's, the work by Wise and colleagues at the University of Michigan led to the development of what is commonly referred to as the "Michigan (MI)-style microlectrode". They present multiple recording sites placed along single or multiple planar shanks (Figure **3B**), with the advantage over traditional metal microwire devices to allow simultaneous recordings from different sites at well-controlled tissue depth[13].

Normann and colleagues developed an alternative silicon-based microelectrode, which due to its origin at the University of Utah is referred to as the UEA. Instead of the thin film design of the MI-style arrays, the UEA uses glass reflow, dicing and etching to create an array of well-defined penetrating electrode tines[14]. As for the MI-style electrodes, several microfabrication processes are used in the creation of UEA microelectrodes and significant development efforts have been devoted to improve their performance. The Utah array consists of 100 densely packed silicon shanks protruding 1.0-1.5 mm from a flat rectangular base (Figure **3C**). The base of every single microelectrode is surrounded by a glass trench and the whole structure (but the recording pads) is covered by parylene as insulating material. The electrode active sites are located on the shank tips and are metalized with activated iridium oxide. The UEA is the only high-density, penetrating recording electrode approved by the US Food and Drug Administration and that has

received the CE mark for use in Europe. The ability of the UEA to record the neural signals needed for chronic rehabilitative applications has been demonstrated by a number of groups[15] and it has been used in several clinical trials[16] and in research with epilepsy patients[17].

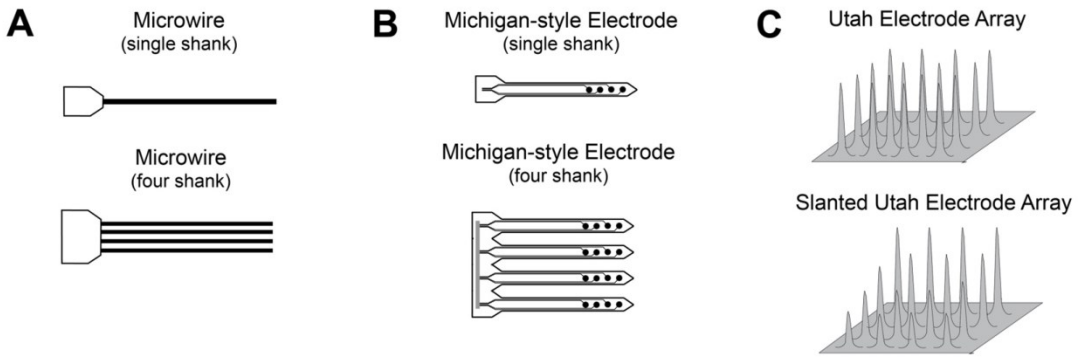

Figure 3. Schematic representation of microelectrode array technologies design, including A) Microwires, B) Michigan-style Microelectrodes, C) Utah Electrode Arrays (UEA) (*modified from Jorfi M et al., 2015*[18]).

The first experiments making use of intracortical devices were performed on experimental animals. Multielectrode arrays have been used to record neural activity from the motor cortex in monkeys or rats during learned movements. Monkeys have also been used to move a brain-controlled robotic arm in a computer-generated 3D virtual setting and, more recently, to investigate the control of prosthetic devices for direct real-time interaction with the physical environment[1,19]. Studies using invasive recording techniques with human subjects have been limited to severely disabled people. A patient affected by amyotrophic lateral sclerosis (ALS) has been able to move a cursor on a computer screen to select presented items after implanting a single electrode into the motor cortex[20].

Regarding the application of intracortical neuron recording in BCI systems, microelectrode arrays such as the Utah intracortical electrode array have been reported as a suitable means of providing simultaneous and proportional control of a large number of external devices[21]. Also, Kennedy *et al.* employed cortical control signals to design a BCI that allowed users to control cursor movement and flexion of a cyber-digit finger on a virtual hand[22].

Despite the substantial success obtained using intracortical microelectrodes in neural interface applications, a number of failure modes likely influence chronic recording stability and quality. The most important problem is of biological and physiological origin:

the brain reacts with a neuro-inflammatory response to the chronically implanted device as well as versus the local traumatic injury. This key factor will be explained in detail in the following sections. Among other mechanisms that induce intracortical device failure there are: direct mechanical damage of the electrode, during or following insertion; corrosion of electrical contacts that impacts recording site stability but also can generate toxic species modifying the biocompatibility of chronically implanted devices; the degradation of passivation layers and insulating coatings that reduces the electrode ability to detect local ionic signals[23,24]. Indeed, both traditional microwires and silicon-based electrode array systems require an insulation layer to shield the electrodes from unwanted electrical signals. The large majority of the devices surface area is represented by the insulating materials and thus these layers must be non-toxic and should minimize the foreign body reaction (FBR). One of the most common insulating materials is polyimide, that is also useful to improve the mechanical mismatch between rigid electrode and soft brain tissue[25]. As previously discussed, traditional microelectrodes are made of stiff materials such as silicon or metal and although this characteristic allows an easy implantation, on the other side it increases the negative effects of a foreign body presence into the brain. A great effort has been made in material science to overcome this and other limitations due to shape and size, which will be discussed later.

3. TISSUE REACTION

In order to design recording electrodes that minimize or avoid the tissue response of the central nervous system, it is necessary to understand the biological mechanisms behind it.
The extent and nature of the FBR could differ dramatically between studies most likely due to type of implant, sterilization method, species studied, implantation method, choice of electrode design and materials used. In any case, implantation of neural probes into the brain will always induce some trauma. The FBR can be described as any (immunological) tissue reaction in response to the presence or insertion of an implant and it is characterized by the involvement of different molecular and cellular species and their interaction with the non-biological component such as the microelectrode.
The FBR leads to the deterioration of both the electrode, manifested as a loss of neural recording capability, and the surrounding tissue and a series of events characterize and influence the duration and the performance of the implant starting from the time of surgery.

When the electrode is stiff enough to be implanted into the brain, the tissue is subjected to a deformation called dimpling by the action of mechanical forces and, due to the dense and highly vascularized nature of the nervous tissue, the disruption of the blood-brain barrier (BBB) as well as of some blood vessels is inevitable. Different studies have provided initial evidence that these factors and the mechanical trauma related to insertion techniques lead to irreversible localized traumatic brain injury and reduced recorded neuronal activity[26,27]. These events lead to an initial brain tissue damage and its extension is primarily related to the implant geometry (for example tip angle, cross sectional area and overall configuration), mechanical constants, and the applied insertion speed. In fact, the base materials used in traditional microelectrodes are significantly stiffer than the cortical tissue (Young's modulus of 6 – 7 orders of magnitude greater than that of the brain tissue, that is ~ 10 kPa) and the mechanical mismatch between the brain and the device contributes to the propagation of the neuro-inflammatory response[28]. This sustained reaction is more likely due to tissue-device interactions and the micromotion generated by respiratory and pulsatile movements plays a key role in promoting the spread of initial trauma. This concept is widely reported in the literature and several studies show that brain micromotion induces displacements in the order of tens of microns around silicon or metal device, which lead to a continuous mechanical stress around the implanted electrode[29,30]. The viability and function of the surrounding brain tissue is intimately associated with the extent of these phenomena.

Starting from the moment of insertion, the local trauma, characterized by vessel breaking and hemorrhage, triggers the coagulation and the complement system cascade. The resulting influx of monocytes and blood-serum proteins (together with albumin and fibronectin) lead to the activation of nearby glial cells, including microglia and astrocytes, that are the main cell populations involved in the inflammatory chronic tissue response[24,31–33] (Figure **4**).

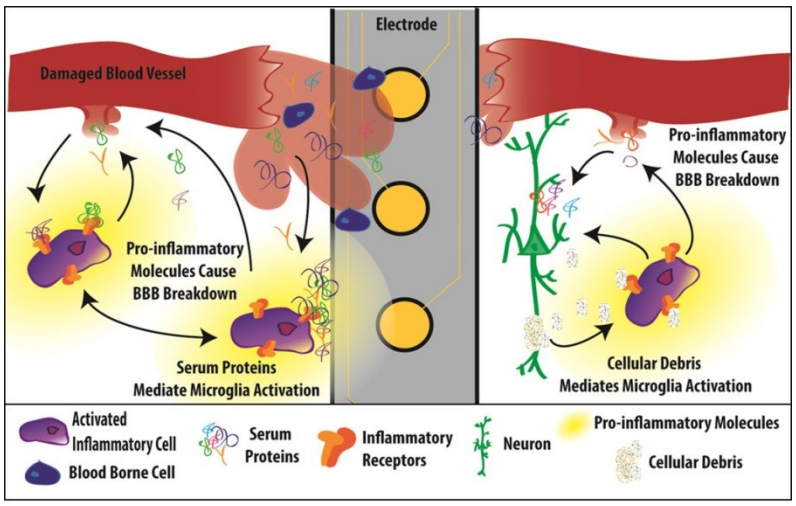

Figure 4. Schematic representation of initial local trauma after microelectrode insertion (*from Jorfi M et al., 2015*[18]).

The intensified blood flow in vessels together with the increased capillaries permeability allow fluids and blood proteins to move into injured tissue and to adhere to the electrode surface, that becomes surrounded by many serum plasma proteins and blood cells that push away the targeted neurons. The absorbed proteins impose a strong driving force on the subsequent adsorption of further proteins that activate macrophages and initiates the acute tissue response[34]. The more the electrode is coated with proteins, the more the damage increases; consequently, protein adsorption is of key importance in determining the in vivo performance of intracortical electrodes and strategies to minimize the extension of protein attachment could improve implant success.

There are several distinct molecules and cell populations involved in the inflammatory and wound healing response to devices implanted into the brain. Neurons are the most common CNS cells, representing the targets for intracortical electrodes, but they make up less than 25% of brain cells while the remaining tissue consists of glial cells, including oligodendrocytes, astrocytes and microglia. Oligodendrocytes are the myelin forming cells of the CNS, while astrocytes and microglia are the main effectors of the brain's response to injury. Astrocytes, characterized by a star-like appearance due to the cellular extensions, are important during CNS development providing growth cues to neurons. They mechanically support the mature neuronal circuits, help control the chemical environment of the neurons, buffer the neurotransmitters and ions released during neuronal signaling, and even modulate the firing activity of neurons. Specialized astrocytic extensions, termed "end feet", support capillary walls and help in the transfer of nutrients across the blood–brain barrier. Astrocytes are characterized by 8 – 10 nm diameter intermediate filaments of

polymerized glial fibrillary acid protein (GFAP), which is considered an astrocyte specific cell marker.

Microglia are the other major glial cell type involved in the brain's wound healing response, acting as cytotoxic cells killing pathogenic organisms or as phagocytes secreting proteolytic enzymes to degrade cellular debris and damaged matrix after injury or during regular cell turnover. Microglia reside in an inactive or ramified, highly branched state until "activated" via injury mediated mechanisms, as in the case of microelectrodes implantation[31].

After an initial acute phase that takes place within several hours after the insertion trauma, the glial cells progressively change their morphology, losing their physiological functions and leading to the formation of the so-called *glial scar* (Figure **5**). There is a comprehensive literature that reviews all the mechanisms underlying this tissue response[24,32,33,35–38]. Activation of the astrocytes by injury transforms the cells into a "reactive" phenotype characterized by enhanced migration, proliferation, hypertrophy, upregulation of GFAP, changes in number, in distribution of cellular organelles and glycogen deposits, and increased matrix production. Immunostaining for GFAP is one of the most common methods for evaluating the extent of "reactive gliosis".

Upon activation, also the microglia cells begin to proliferate and migrate to the implant area to release pro-inflammatory cytokines. This activation of microglia and the loss of ramified processes prevent these cells from executing their physiological 'resting state' activities, such as normal modulation of synapses. In turn, the upregulation of pro-inflammatory cytokines drives nearby neurons towards excitotoxicity and neurodegeneration. Simultaneously, the loss of nearby oligodendrocyte precursor cells (also called NG2-glia) leads to the proliferation, migration and differentiation of distant NG2-glia into astrocytes, increasing the activated astrocyte population. Moreover, astroglial reactivity around the implant leads to increased expression of connexon-43 (Cx43), an astroglial hemichannel and gap junction known to facilitate the spread of inflammation. Consecutively, inflammation leads to the recruitment of blood-borne monocytes and neutrophils through the intact BBB, and to the formation of multinucleated giant cells. In addition, this inflammation alters the expression level of matrix metalloproteinases, together leading to further breakdown of the BBB and facilitating the influx of blood-serum proteins, red blood cells and leukocytes. BBB disruption also leads to lower oxygen and nutrient delivery, as well as to impaired removal of neurotoxic waste products, including reactive oxygen species generated during the breakdown of red blood cells in the parenchyma. This increase in metabolic, oxidative and osmotic stress further

drives inflammation in nearby cells. Thus, if we look more deeply to the tissue response at the cellular and molecular levels, the scenario is very complicated with a strongly intricate network of events involving several distinct cell populations in the inflammatory and wound healing response to materials implanted in the CNS.

In this framework, the most studied cells are microglia and astrocytes, because of their prominent role in the encapsulation of devices, which represents the main event of the chronic phase. In fact, surrounding the implantation site, a region consisting of hypertrophic astrocytes as well as infiltrating fibroblast and meningeal cells has been observed, creating a dense scar-like layer that limits volume transmission. Also the activated macrophages take part to the FBR: since they cannot digest the implant materials, they fuse together into multinucleated foreign body giant cells that are often found at the end-phase of the inflammation. This dense glial scar layer, that develops around the fourth week, may take over 6 weeks to stabilize[39,40].

The glial scar insulates the electrode from nearby neurons and increases the impedance of the tissue-electrode interface, limiting the recording function of the microelectrodes. In fact, one belief is that gliosis pushes away the surrounding tissues, and this extends the distance between the electrode and its nearest target neurons, thus dramatically degrading the amplitude of the recorded signals from neurons[41,42].

However, the loss of neurons is a process not as well characterized as glial scar formation, as it seems to vary from implant to implant, and even between electrodes implanted at different sites in the same animal. Another explanation of electrode signal degradation is the formation of a “kill zone” around the implant site resulting from the initial trauma or neuro-inflammatory events[43]. This region is defined by a significantly lower or non-existent neuronal density up to some distance away from the electrode, varying between 1 μm (no dead zone) and more than 100 μm. Some research groups suggested a correlation between initial tissue damage and kill zone size, although this correlation has not been confirmed by others. Moreover, some authors suggest that some neurons around the implant die shortly after implantation and many other undergo apoptosis resulting in the gap between electrode and the targeted neurons[44].

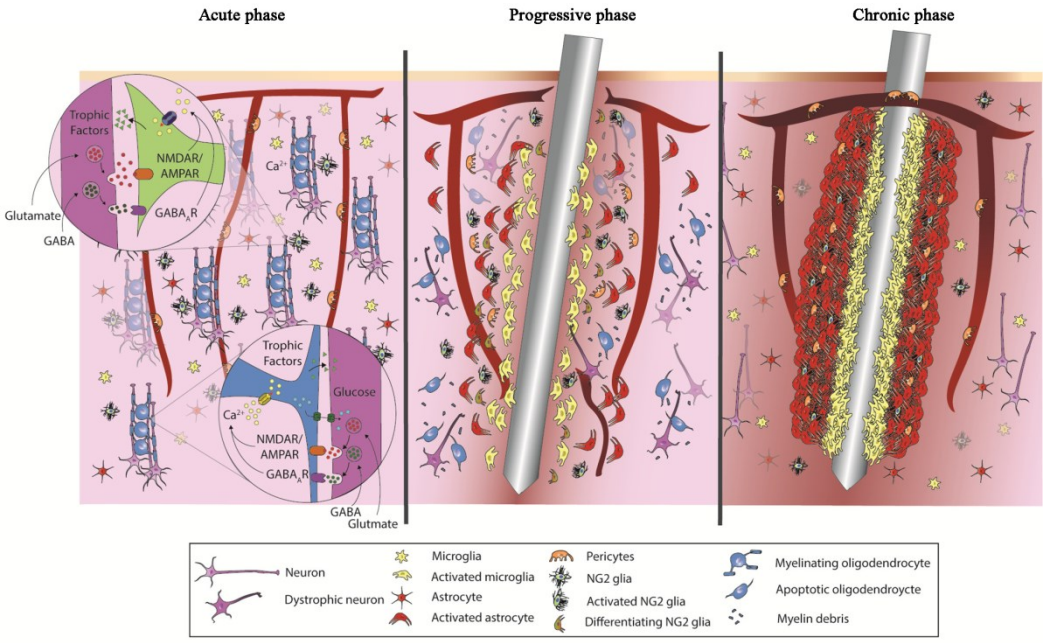

Figure 5. Visualization of foreign body response to chronically implanted electrode into the brain (*modified from Wellman SM and Kozai TDY, 2017*[32]).

To sum up, the effects of implantation could be divided in three principal groups of events that develop in time[24]:

- the surgical/acute phase, that develops in the first 24h after electrode implantation and is due to tissue dimpling during insertion, direct local tissue trauma, vascular damage and pressure effect caused by the implant volume;
- the progressive phase, that matures between one and three weeks and involves the initial electrode exposure to biological tissue and histopathological changes due to initial FBR. In this time window, the inflammatory response becomes more intense and the tissue starts remodeling with the activation of glial cells, the development of the glial scar and the displacement of neurons around the electrode;
- the chronic/persistent phase that is characterized by the long-term structural changes that occur on the recording surfaces of the electrodes combined with the chronic neuro-inflammatory response. It occurs from the fourth week and becomes stable in twelve week.

There are different methods to assess the development of the tissue reaction and we can refer to abiotic or biotic methods depending on whether we concentrate more on the probe or on tissue related aspects[5]. Currently, histological staining, assisted with immunohistochemistry (IHC) on the excised brain tissue, is the most common and reliable method to observe the FBR to the implanted neural probe, using cell-type-specific markers to quantify the inflammation level[45–47]. Astrogliosis is identified by increased GFAP

immunoreactivity and the area of inflammation is also characterized by reduced number of neurons, identified by neuronal nuclei (NeuN) staining, loss of neurofilament density as well as overexpression of inflammatory marker as ED1.

As a consequence of probe encapsulation and neurons displacement, the performance of the implanted microelectrodes decrease over time and the quality of neural spike signals is the most direct method to assess the chronic recording capability and hence the development of gliosis. Thus, a common statistical metric, the SNR, is often used to evaluate the fidelity of the chronic recording[48,49]. This is a dimensionless ratio of signal power to noise power, thus SNR of the recorded signals may decrease over time due to the chronic FBR such as insulation from the glial scar, migration of neurons away from the electrode, and lack of biocompatibility such as electrode fouling. Therefore, the SNR measurements over the duration of the implantation not only indicate chronic reliability of the neural probe but also provide insights into the state of the electrode-tissue interface.

Another method to indirectly assess the state of the chronic inflammation is the measurement of the electrical impedance of the electrode-tissue interface at multiple frequencies by electrochemical impedance spectroscopy (EIS)[50,51]. Because of its non-invasive nature, as opposed to that of biological assays, once the neural probes are implanted, changes in the electrode-tissue interface can be monitored over a long period of time using the same animal. The frequency range analyzed is typically from 10 Hz to 100 kHz, two orders of magnitude smaller and larger than 1 kHz. This is the impedance reference value for microelectrodes because the duration of the individual neural spike signal is in the range of milliseconds.

Studies showed that an increase in the impedance is observed over time as a glial scar forms and insulates the implant. Although the EIS measurement may indicate the formation of a glial scar around the implant, it does not necessarily indicate chronic viability of the neural probe and must be accompanied with other assessment methods.

As it is apparent from this description of the development of the inflammatory response over time, it is extremely important to find valid methods to limit it to the minimum by allowing the electrode to remain stable over time and a variety of approaches have been taken to solve the different stages of tissue reaction.

4. STRATEGIES TO IMPROVE INTRACORTICAL ELECTRODES PERFORMANCE

4.1 MATERIALS IMPROVEMENTS

To increase electrode viability and performance quality it is essential to control the tissue reaction against these implants and in this section I will report an overview of strategies developed to solve this problem. These methods can be categorized into two types: (i) 'improvements by material science', that affect only the implant itself and include changes in device material, geometry and size, modifications that allow for better recordings, or those that enable safer insertion and minimize the invasiveness and the tissue damage during insertion. At the same time, research is focused on stiffness reduction and on increase of flexibility to diminish the local tissue compression and the brain-device mechanical mismatch.

The other type of methods refers to (ii) 'bioactive modifications', that influence the affected tissue and include treatments with anti-inflammatory compounds, immobilized protein coatings that interact with the immediate surroundings, and attempts to resolve the inhibitory extracellular environment formed by the FBR, improving the biocompatibility at the tissue/electrode interface.

As already discussed, the immediate effects of device implantation are caused by the mechanical interaction of the device with the brain tissue and there is evidence that relates the extent of the initial trauma with microelectrode size and material rigidity. Despite high stiffness facilitates microelectrode implantation into the cortical tissue, it also impacts the biological environment leading to the breakdown of physiological tissue functions. Existing neural electrodes use conventional materials that are often not intrinsically compatible with biological systems and do not conduct integration with neural tissue. Although biocompatible metallic materials do exist, the hard, electronic, dry, and static nature of metals and metal oxides are quite foreign to biological tissue, which is soft, ionic, wet, and dynamic. Next-generation devices are designed to incorporate flexible and compliant materials to more closely mimic the neural tissue characteristics and to attenuate the persistent presence - and micromotion - of the foreign body inside the brain. In this context, it is important to distinguish between the concepts of compliance and flexibility. Compliance represents the ability of a system to deflect upon axial forces brought on it by the surrounding tissue, and so it is closely associated with the buckling force. Flexibility is more related to the nature of the material, referring to the elastic Young's modulus. Different approaches could be adopted to achieve better compliance: (i) reducing the

effective elastic modulus of the material either by using low-modulus coatings as hydrogels or by using flexible polymeric materials to build the device; (ii) modifying probe dimensions (cross-section area and length); (iii) choosing a free-floating/soft-tethered fixation mode[52].

Among flexible substrates, great attention has been obtained by polyimide[53,54], polydimethylsiloxane (PDMS)[55], parylene-C[56] and SU-8[57] or *in situ* softening materials. These last materials have received attention as microelectrodes substrates as they are sufficiently stiff to facilitate implantation into the brain, but then soften *in vivo* to better match the mechanical properties of neural tissue. This approach has been sought after, as in fact microelectrodes made from soft materials that would be ideal for reducing mechanical mismatch with the brain, cannot be easily inserted in the cortex. To overcome this issue may require either to increase their size or to adopt shuttle devices. The first study in literature concerning in situ softening materials is reported by Capadona *et al.* in 2008 where they used adaptive polymer nanocomposites inspired to sea cucumbers, able to switch from a rigid state (E = 5.1 GPa) when dry to a soft one (E = 12 MPa) after exposure to physiological condition. The authors demonstrated the ability of a device made from such material to be inserted through the *pia mater* under the cortex without the need of assisted device[58]. The *in vivo* demonstration of *in situ* softening materials for functional devices is reported in Harris *et al.* where the authors find a more rapid stabilization of neural cells around compliant implants with respect to a rigid microwire at four weeks post-implantation. However, no significant differences were observed at a long time point (eight weeks)[59]. A more recent work by Nguyen *et al.* examines the neuroinflammatory response at 16 weeks using PVAc/CNC nanocomposite implants finding a complete attenuation of glial activation compared to stiff devices[60].

An alternative way to attenuate the tissue/electrode mechanical mismatch and to reduce the stiffness of microelectrode devices is the use of soft coatings like hydrogels (HG). Hydrogels are a type of water-swollen, cross-linked hydrophilic polymers, from synthetic or natural materials such as fibrin, collagen and alginate, already extensively used in tissue engineering and drug delivery because their water content and mechanical properties can be tailored to match the biological tissue[61]. They have excellent diffusive properties for the release of growth factors, anti-inflammatory drugs, and other molecules. Hydrogels can provide an ultrasoft intermediate layer between the electrodes and the surrounding tissue, having an elastic modulus close to that of neural tissue. Used in combination with conductive polymers they are attractive materials for altering the mechanical properties of neural probes and reducing tissue response at the electrode-tissue interface[62–64]. On the

negative side, given their hydrophilic nature, swelling of HG and HG-based polymers should be taken in consideration regarding the increased risk of delamination and the displacement of neurons from the recording site, as reported by Kim *et al.*[65].

Another key factor that impacts on the compliance of microelectrodes in the surrounding tissue is the mechanism used to anchor the device to the skull. Functional intracortical microelectrodes need to be connected to the external recording and/or stimulating systems and normally they are fixed to the skull directly or via tethering cables to protect the device from external forces. This makes them more prone to induce injuries during micromotion, as opposed to non-functional free-floating electrodes that are more likely to move along with brain tissues. Histological *in vivo* studies have verified that anchored devices evoke significantly greater immune response than un-anchored devices, with increased astrogliosis[66,67]. However, it is hard to develop a free-floating system with stable and reliable connection to the device for electrical recording or stimulation, especially for chronic studies. A compromise between tethered and non-tethered fixation modes is the integration of a flexible cable able to reduce part of the strain by decreasing the relative motion between the brain and the skull[68–70].

Additional strategies to reduce the neuro-inflammatory response to intracortical implants have been focused on altering tip geometry or penetrating profile of the device to reduce surgical trauma; reducing the size to improve mechanical compliance and minimizing surface area to decrease the local number of inflammatory cells around the implant site.

Smaller devices are likely to reduce the impact of tissue displacement, changes in pressure on the tissue, steric blockage of signaling molecules caused by the implanted device volume and vasogenic edema resulting from insertion, which may affect the short- and long-term tissue responses[66,71,72]. The decreased device volume lowers the mechanical strain on the tissue due to implantation compared with that of larger devices. However, as the size of the device decreases, the yield strength decreases making the material more prone to mechanical failure[73]. Moreover, the more the size decreases the more the active surface decreases and the impedance increases leading to a lowering of the electrode performance with reduced recording capacity. To face these problems, several solutions have been suggested. A common approach to decrease the microelectrode impedance and increase their charge transfer capability is the increase of their effective surface area using conductive polymers (CPs) and nanomaterials[12]. Among CPs, the most studied polymer for intracortical microelectrode applications is poly-(3,4-ethylene dioxythiophene) (PEDOT)[74–76] while great properties are associated with the use of carbon nanotube (CNT)–based nanocomposites[77–79], in view of their remarkable strength, toughness,

electrical conductivity and surface area. As the name itself implies, nanomaterials have nanoscale dimensions and due to this, they can interact with biological systems with high degree of specificity, stimulating and interacting with target cells. Many elements of neural tissue and of neuronal and non-neuronal cells have nanoscale dimensions, thus, the unique intrinsic properties of those materials offer a great promise to seamlessly integrate with brain tissue and simulate features and functions of cells and extracellular matrix.

In summary, the performance of the electrode-tissue interface ultimately rests on the quality of the material substrate, which enables a long-lasting functional neural device. The challenge for materials science is to apply nanotechnology strategies and develop innovative biocompatible nanomaterials that mimic neural tissue characteristics, cause minimal inflammation and neuronal cell loss, and are functional for a long period of time. These conductive nanomaterials are able to provide a more-effective surface area than regular metals for signal transduction at the electrode-tissue interface, thus enhancing the electrical characteristics of neural recordings and stimulations, such as SNR and safe charge injection density. Moreover, their performance can be improved even further by incorporation of drugs and bioactive molecules or by using them in combination with HG, improving in turn the biocompatibility of neural electrodes, reducing reactive tissue response, decreasing the mechanical mismatch between stiff electrodes and soft tissue and promoting neural process outgrowth.

4.2 BIOACTIVE MODIFICATIONS

Together with changes in mechanical and electrical properties of the materials used for neural devices, recent developments have been done regarding bioactive modifications. These approaches refer to all the strategies used to increase the stability at the tissue-electrodes interface and involve different grade of device bio-functionalization, from the introduction of drug delivery/release to the addition of bio-organic constructs. The aim is to create a microenvironment increasingly similar to that of the brain, supporting local neuronal and non-neuronal cells and thus improving the electrodes performance. Since the proximity and the vitality of neurons are directly correlated with the intensity of the signal that the microelectrodes have to record, strategies that preserve the cells near recording sites could minimize the effect of the inflammatory response on electrodes performance over time. Likewise, bioactive coatings that attract or repel glial cells could potentially

anchor the electrodes in the neural tissue and prevent micromotion and the subsequent negative effect of the glial response.

In this context, the major strategies adopted to maintain neurons near the active sites of device by minimizing astrogliosis and glial cells activation include non-fouling surface modifications to prevent cell adhesion, delivery of anti-inflammatory drugs and incorporation of bioactive molecules.

All the materials used so far in medical implants elicit the inflammatory response that lead to reduction of microelectrodes performance and failure on its biological tissue integration. After implantation, a variety of proteins and molecules nonspecifically adhere to the substrate and these attract in turn other cells by specific receptors that adhere to specific peptide sequences presented by the adsorbed proteins. This scenario, which may give rise to uncontrolled cell enrollment, triggers a number of cellular responses which subsequently control inflammation, tissue formation, and incorporation of the implant into the host. Thus, to find a way to control and reduce proteins adhesion onto substrates could alter and improve the neuro-inflammatory response[80]. A method to prevent this mechanism is to develop biologically 'inert' chemical moieties on the surface of the implant, referring to the ability to resist protein adsorption and cell attachment and different surface treatment approaches exist to create non-fouling substrates[81].

Another strategy adopted to control the biotic/abiotic interface involves the implementation of microelectrodes with bioactive surface coatings[82,5]. A huge spectrum of bioactive molecules has been used to control the neuro-inflammatory response, showing temporarily successful in attenuating the immune response to intracortical microelectrodes within the brain tissue. Among these molecules, great attention has been given to anti-inflammatory drugs to minimize the initial FBR[83] and so to slow down or prevent the chronic encapsulation. Drugs can be blended within polymer coatings through non-covalent binding, such as adsorption, physical entrapment or electrostatic interactions, and covalent binding, resulting in a passive diffusion or controlled delivery that could mediate the local tissue response to implanted devices. Dexamethasone is one of the most common drug molecules used at the electrode interface and different studies report its loading in conductive polymers and HG[84–86].

The main limitation to this kind of approach is to reach a therapeutic level of the drugs. The time during which the drug is released at functional levels from the polymers depends on different factors such as binding strength, host degradation rate and diffusion mechanisms and only a percentage of the total amount of the drug loaded is actually bioactive. Moreover, high drug concentrations could impact severely the physiochemical

properties of the coating and thus diminish the electrical and mechanical properties of the overall device. Other molecules used to functionalize the electrode substrates are neurotrophic and growth factors and extracellular matrix components[12,87] like laminin, an adhesive protein that plays important roles in cell migration, differentiation and at axonal level.

Another approach emerging from tissue engineering literature is based on the development of electrodes intimately integrated with the neural tissue. This method is based on the assumption that neural tissue should grow more effectively on a brain cell-mimicking layer on the electrode surface, creating an intimate junction between device and target. This approach combines the principles of tissue engineering with electrode coatings and proposes the incorporation of neural cells within the device itself. The concept of integrating living cells with electrodes was first raised in 1980, when Ochiai *et al*. has proposed using live blue-green algae embedded in an alginate gel to act as a photoconverter of solar radiant energy to electric energy[88]. In this study, the term "living electrode" appeared for the first time. Although the good stability of this biological electrodes, in a follow up study[89], the same authors highlighted the low power conversion efficiency, preventing further development of this concept. Another study was conducted by Campbell *at al.* in 1999 using non-nucleated cells in biosensor application[90]. More recently, in 2007 Richardson-Burns *et al.* described electrodeposition of PEDOT on neuroblastoma-derived cell lines and primary mouse cortical cells grown on metal electrodes[91]. Cells survived initial short-term exposure to monomers, but apoptosis and cytoskeletal disruption was subsequently observed. Little further progresses have been done over the past five years on the concept of creating "living" electrodes that contain eukaryotic cells.

The ideal tissue engineered interface should incorporate combined coating approaches of conductive polymers, HG and attachment factors with neural cells and a more recent report by Green *et al.* show a proof of concept to the feasibility of building layered constructs of cell loaded HG over CP coated Pt electrodes[92]. The idea behind this construct is that if neuroprogenitor cells can be supported and developed towards the target tissue then the electrode will be surrounded by a functional neural layer instead of fibrotic tissue.

Several issues have to be improved to create this kind of device: the HG scaffold must be tailored to provide mechanical and biochemical properties that support the growth and differentiation of neural cells and the encapsulated cells must form functional synaptic processes with the target neurons. It has been shown that cell survival and differentiation in three dimensional scaffolds is greatly improved by seeding cells with complementary

accessory cells which would be normally present in the developing tissue[93]. As such functional living electrodes are likely to require not only neural cells but also supporting neuroglia to achieve functional networks with target tissue. Despite the substantial amount of research required to develop this technology, it has the potential to provide a pathway for maintaining neurons in close proximity with electrodes. Additionally, a fully realized tissue engineered electrode may prevent scar tissue encapsulation and provide a means of communicating with diseased or damaged cells using natural synaptic processes.

However, although several proofs of concept have been carried out, these refer to the ability of cells to integrate into *in vitro* materials. There are currently very few works that report the use of living electrodes *in vivo.* It should also be noted that although most of the works involve the use of neural (stem) cells in order to restore the damaged tissue, a better approach may not depend on the direct use of this cell type, but on the use and involvement of other cell types normally present within the nervous tissue and therefore able to mimic the surrounding tissue without triggering the inflammatory response and moreover without altering the native neural connections.

The concept of living-electrodes, and in particular the idea of bio-electrode presented in this thesis, will be discussed in more details in the next chapter, since it represents one of the strategies that has been adopted to overcome the FBR problems of intracortical microelectrodes.

5. CONCEPT OF BIOCOMPATIBILITY OF NEURAL PROBES

Nowadays improving performance of intracortical microelectrodes is one of the main aim in the field of neuroscience and biomedical engineering. Many steps forward have been made thanks to the increasingly developing technologies for production methods and materials science, however there is still no real solution for reliable and stable recording over time from the same subject. This is mainly due to the FBR and scar tissue formation around the implant that lead to neuronal loss and to hinder the electrical interface of the device - and consequently the electrophysiological signal. One of the aspects that should be implemented is thus the biocompatibility of the microelectrodes and their interaction with the neural tissue, since one of the major prerequisites for the application of neural probe is that the organism accepts the implant with minimal tissue response.

Although the word “biocompatibility” is extensively used within biomaterial science, there are still doubts regarding the meaning of this concept and about the mechanisms involved

in all the phenomena that collectively constitute biocompatibility. Usually the word biocompatibility is used to refer at biological as well as chemical and physical properties of the implants. In the neural devices field, this implies that the probe is able to remain for a long term within the neural tissue without rejection and without evoking a toxic or immunologic reaction, to remain functional without harming or destroying cells or tissues, compressing adjacent tissues or inducing any other secondary problem. However, even considering devices and materials provided with high degree of biocompatibility, there will always be a biological response and some degree of encapsulation. Thus, in place of biocompatibility we should rather talk of bio-tolerability of intracortical microelectrodes, referring to the ability of these neural implants to reside in the brain for long periods of time with only low degrees of inflammatory reactions. Therefore, three other areas have to be considered: the "biosafety", the "biofunctionality" and the "biostability"[94,95].

Biosafety means that the implant does not harm its host in any way, biofunctionality is related with the ability of the device to perform its intended function, and biostability means that the implant must not be susceptible to attack from biological fluids, proteases, macrophages or any element involved in metabolism.

All these considerations imply extreme demands on stability and function of neural implants and place unique constraints on the architecture, materials, and surgical techniques used in the implementation of intracortical microelectrodes.

As previously described, multiple strategies have been adopted to achieve this aim, and in the next chapters I will describe in detail our approaches to improve the biocompatibility of intracortical device, minimizing the FBR.

BIBLIOGRAPHY

1. Nicolas-alonso, L. F. & Gomez-gil, J. Brain Computer Interfaces, a Review. *Sensors* **12,** 1211–1279 (2012). doi:10.3390/s120201211

2. Vidal, J. J. Toward direct brain-computer communication. *Annu. Rev. Biophys. Bioeng* (1973). doi:10.1146/annurev.bb.02.060173.001105

3. Abdulkader, S. N. *et al.* Brain computer interfacing : Applications and challenges. *Egypt. Informatics J.* **16,** 213–230 (2015). doi:10.1016/j.eij.2015.06.002

4. Thompson, C. H. *et al.* Regenerative Electrode Interfaces for Neural Prostheses. *Tissue Eng. Part B* **22,** 125–135 (2016). doi:10.1089/ten.teb.2015.0279

5. Kook, G. *et al.* Neural Probes for Chronic Applications. *Micromachines* 1–20 (2016). doi:10.3390/mi7100179

6. Mak, J. N. & Wolpaw, J. R. Clinical Applications of Brain-Computer Interfaces: Current State and Future Prospects. *IEEE Rev Biomed Eng* **2,** 187–199 (2009). doi:10.1109/RBME.2009.2035356

7. Mcfarland, D. J. & Wolpaw, J. R. ScienceDirect EEG-based brain – computer interfaces. *Curr. Opin. Biomed. Eng.* **4,** 194–200 (2017). doi:10.1016/j.cobme.2017.11.004

8. Schalk, G. & Leuthardt, E. C. Brain-Computer Interfaces Using Electrocorticographic Signals. *IEEE* **4,** 140–154 (2011). doi:10.1109/RBME.2011.2172408.

9. Waldert, S. *et al.* A review on directional information in neural signals for brain-machine interfaces. *J. Physiol. - Paris* **103,** 244–254 (2009). doi:10.1016/j.jphysparis.2009.08.007

10. McConnell, GC. *et al.* Implanted neural electrodes cause chronic , local inflammation that is correlated with local neurodegeneration. *J. Neural Eng.* **6,** (2009). doi:10.1088/1741-2560/6/5/056003

11. Renshaw, B. *et al.* Activity of isocortex and hippocampus: electrical studies with micro-electrodes. *J. Neurophysiol.* **3,** (1940). doi:10.1152/jn.1940.3.1.74

12. Jorfi, M. *et al.* Progress towards biocompatible intracortical microelectrodes for neural interfacing applications. *J. Neural Eng.* **12,** (2015). doi:10.1088/1741-2560/12/1/011001

13. BeMent SL. *et al.* Solid-State Electrodes for Multichannel Multiplexed Intracortical Neuronal Recording. *IEEE* **33,** 230–241 (1986). doi:10.1109/TBME.1986.325895

14. Campbell PK. *et al.* A silicon-based , three-dimensional neural interface : Manufacturing processes for an intracortical electrode array. *IEEE* **38,** (1991). doi:10.1109/10.83588

15. Homer, ML. *et al.* Implants and Decoding for Intracortical Brain Computer Interfaces. *Annu. Rev. Biomed. Eng.* **15,** 383–405 (2013). doi:10.1146/annurev-bioeng-071910-124640

16. Perge, JA. *et al.* Intra-day signal instabilities affect decoding performance in an intracortical neural interface system. *J. Neural Eng.* **10,** 1–26 (2014). doi:10.1088/1741-2560/10/3/036004

17. Truccolo, W. *et al.* Single-neuron dynamics in human focal epilepsy. *Nat. Neurosci.* **14,** 635–641 (2011). doi:10.1038/nn.2782

18. Jorfi, M. *et al.* Progress Towards Biocompatible Intracortical Microelectrodes for Neural Interfacing Applications. *J. Neural Eng.* **12,** (2015). doi:10.1088/1741-2560/12/1/011001

19. Taylor, D. M. *et al.* Direct Cortical Control of 3D Neuroprosthetic Devices. *Science.* **296,** 1829–1833 (2002). doi:10.1126/science.1070291

20. Vansteensel, M. J. *et al.* Fully Implanted Brain–Computer Interface in a Locked-In Patient with ALS. *N. Engl. J. Med.* **375,** 2060–2066 (2016). doi:10.1056/NEJMoa1608085

21. Maynard, E. M. *et al.* The Utah Intracortical Electrode Array : a recording structure for potential brain-computer interfaces. *Electroencephalogr. Clin. Neurophysiol.* **102,** 228–239 (1997). doi:10.1016/S0013-4694(96)95176-0

22. Kennedy, P. R. *et al.* Computer Control Using Human Intracortical Local Field Potentials. *IEEE* **12,** 339–344 (2004). doi:10.1109/TNSRE.2004.834629

23. Jorfi, M. *et al.* Progress towards biocompatible intracortical microelectrodes for neural interfacing applications. *J. Neural Eng.* **12,** (2015). doi:10.1088/1741-2560/12/1/011001

24. Prodanov, D. & Delbeke, J. Mechanical and biological interactions of implants with the brain and their impact on implant design. *Frontiers in Neuroscience* (2016). doi:10.3389/fnins.2016.00011

25. Lee, K. *et al.* Polyimide-based intracortical neural implant with improved structural stiffness. *J. Micromechanics Microengineering* **14,** 32–37 (2004). doi:10.1088/0960-1317/14/1/305

26. Rennaker, R. L. *et al.* A comparison of chronic multi-channel cortical implantation techniques : manual versus mechanical insertion. *J. Neurosci. Methods* **142,** 169–176 (2005). doi:10.1016/j.jneumeth.2004.08.009

27. Bjornsson, C. *et al.* Effects of insertion conditions on tissue strain and vascular damage during neuroprosthetic device insertion. *J. Neural Eng.* **3,** (2006). doi:10.1088/1741-2560/3/3/002

28. Lind, G. *et al.* The density difference between tissueand neural probes is a key factor for glial scarring. *Sci. Rep.* 1–7 (2013). doi:10.1038/srep02942

29. Muthuswamy, J. *et al.* Microactuated Neural Probes to Compensate for Brain Micromotion. *Proc. Annu. Int. Conf. IEEE EMBS* 2–5 (2003). doi:10.1109/IEMBS.2003.1279819

30. Gilletti, A. & Muthuswamy, J. Brain micromotion around implants in the rodent somatosensory cortex. *J. Neural Eng.* **3,** 189–195 (2006). doi:10.1088/1741-2560/3/3/001

31. Polikov, V. S. *et al.* Response of brain tissue to chronically implanted neural electrodes. *J. Neurosci. Methods* **148,** 1–18 (2005). doi:10.1016/j.jneumeth.2005.08.015

32. Wellman, S. M. & Kozai, T. D. Y. Understanding the Inflammatory Tissue Reaction to Brain Implants To Improve Neurochemical Sensing Performance. *ACS Chem. Neurosci.* (2017). doi:10.1021/acschemneuro.7b00403

33. Salatino, J. W. *et al.* Glial responses to implanted electrodes in the brain. *Nat. Biomed. Eng.* **1,** (2017). doi:10.1038/s41551-017-0154-1

34. Saxena, T. *et al.* The impact of chronic blood e brain barrier breach on intracortical electrode function. *Biomaterials* **34,** 4703–4713 (2013). doi:10.1016/j.biomaterials.2013.03.007

35. Wang, Y. *et al.* Foreign Body Reaction to Implantable Biosensors : Effects of Tissue Trauma and Implant Size. *J. Diabetes Sci. Technol.* **9,** (2015). doi:10.1177/1932296815601869

36. Fitch, M. T. *et al.* Cellular and Molecular Mechanisms of Glial Scarring and Progressive Cavitation : In Vivo and In Vitro Analysis of Inflammation-Induced Secondary Injury after CNS Trauma. *J. Neurosci.* **19,** 8182–8198 (1999).

37. Bergwerf, I. *et al.* Recognition of cellular implants by the brain's innate immune system. *Immunol. Cell Biol.* **89,** 511–516 (2010). doi:10.1038/icb.2010.141

38. Groothuis, J. *et al.* Brain Stimulation Physiological Challenges for Intracortical Electrodes. *Brain Stimul.* **7,** 1–6 (2014). doi:10.1016/j.brs.2013.07.001

39. Turner, J. N. *et al.* Cerebral Astrocyte Response to Micromachined Silicon Implants. *Exp. Neurol.* **156,** 33–49 (1999). doi:10.1006/exnr.1998.6983

40. Szarowski, D. H. *et al.* Brain responses to micro-machined silicon devices. *Brain Res.* **983,** 23–35 (2003).

41. Grand, L. *et al.* Short and long term biocompatibility of NeuroProbes silicon probes. *J. Neurosci. Methods* **189,** 216–229 (2010). doi:10.1016/j.jneumeth.2010.04.009

42. Georges, P. C. *et al.* Matrices with Compliance Comparable to that of Brain Tissue Select Neuronal over Glial Growth in Mixed Cortical Cultures. *Biophys. J.* **90,** 3012–3018 (2006). doi:10.1529/biophysj.105.073114

43. Biran, R. *et al.* Neuronal cell loss accompanies the brain tissue response to chronically implanted silicon microelectrode arrays. *Exp. Neurol.* **195,** 115–126 (2005). doi:10.1016/j.expneurol.2005.04.020

44. Lull, M. E. & Block, M. L. Microglial Activation and Chronic Neurodegeneration. *Neurother. J. Am. Soc. Exp. Neurother.* **7,** 354–365 (2010). doi:10.1016/j.nurt.2010.05.014.

45. Ersen, A. *et al.* Chronic Tissue Response to Untethered Microelectrode Implants in the Rat Brain and Spinal Cord. *J. Neural Eng.* **12,** 1–19 (2015). doi:10.1088/1741-2560/12/1/016019

46. Winslow, B. D. & Tresco, P. A. Quantitative analysis of the tissue response to chronically implanted microwire electrodes in rat cortex. *Biomaterials* **31,** 1558–1567 (2010). doi:10.1016/j.biomaterials.2009.11.049

47. Lee, H. C. *et al.* Histological evaluation of flexible neural implants ; flexibility limit for reducing the tissue response ? *J. Neural Eng.* **14,** (2017). doi:10.1088/1741-2552/aa68f0

48. Kozai, T. D. Y. *et al.* Comprehensive Chronic Laminar Single-Unit, Multi-Unit, and Local Field Potential Recording Performance With Planar Single Shank Electrode Arrays. *J. Neurosci. Methods* **242,** 15–40 (2016). doi:10.1016/j.jneumeth.2014.12.010

49. Czanner, G. *et al.* Measuring the signal-to-noise ratio of a neuron. *PNAS* **112,** 7141–7146 (2015). doi:10.1073/pnas.1505545112

50. Cui, X. *et al.* In vivo studies of polypyrrole / peptide coated neural probes. *Biomaterials* **24,** 777–787 (2003).

51. Liu, X. *et al.* Stability of the Interface Between Neural Tissue and Chronically Implanted Intracortical Microelectrodes. *IEEE* **7,** 315–326 (1999). doi:10.1109/86.788468

52. Lecomte, A. *et al.* A review on mechanical considerations for chronically-implanted neural probes. *J. Neural Eng.* **15,** (2018). doi:10.1088/1741-2552/aa8b4f

53. Lee, K. *et al.* Polyimide based neural implants with stiffness improvement. *Sensors Actuators B Chem.* **102,** 67–72 (2004). doi:10.1016/j.snb.2003.10.018

54. Mercanzini A. *et al.* Demonstration of cortical recording using novel flexible polymer neural probes. *Sensors Actuators A* **143,** 90–96 (2008). doi:10.1016/j.sna.2007.07.027

55. Minev, I. R. *et al.* Electronic dura mater for long-term multimodal neural interfaces. *Science* **347**, 159-163 (2015). doi:10.1126/science.1260318

56. Takeuchi, S. *et al.* Parylene flexible neural probe with micro fluidic channel. *Lab Chip* (20105). doi:10.1039/b417497f

57. Huang, S. *et al.* In vitro and in vivo characterization of SU-8 flexible neuroprobe : From mechanical properties to electrophysiological recording. *Sensors Actuators A. Phys.* **216,** 257–265 (2014). doi:10.1016/j.sna.2014.06.005

58. Capadona, J. R. *et al.* Stimuli-Responsive Polymer Nanocomposites Inspired by the Sea Cucumber Dermis. *Science.* 1370–1375 (2008). doi:10.1126/science.1153307

59. Harris, J. P. *et al.* In vivo deployment of mechanically adaptive nanocomposites for intracortical microelectrodes. *J. Neural Eng.* **8,** (2011).

60. Nguyen, J. K. *et al.* Mechanically-Compliant Intracortical Implants Reduce the Neuroinflammatory Response. *J. Neural Eng.* **11,** 1–27 (2015). doi:10.1088/1741-2560/11/5/056014

61. Fattahi, P. *et al.* A Review of Organic and Inorganic Biomaterials for Neural Interfaces. *Adv. Mater.* **26,** 1846–1885 (2014). doi:10.1002/adma.201304496

62. Lu, Y. *et al.* Biomaterials Poly (vinyl alcohol)/ poly (acrylic acid) hydrogel coatings for improving electrode – neural tissue interface. *Biomaterials* **30,** 4143–4151 (2009). doi:10.1016/j.biomaterials.2009.04.030

63. Heo, D. N. *et al.* Multifunctional hydrogel coatings on the surface of neural cuff electrode for improving electrode-nerve tissue interfaces. *Acta Biomater.* (2016). doi:10.1016/j.actbio.2016.05.009

64. Green, R. A. *et al.* Conductive Hydrogels : Mechanically Robust Hybrids for Use as Biomaterials. *Macromol. Biosci.* **12,** 494–501 (2012). doi:10.1002/mabi.201100490

65. Kim, D. *et al.* Conducting polymers on hydrogel-coated neural electrode provide sensitive neural recordings in auditory cortex. *Acta Biomater.* **6,** 57–62 (2010). doi:10.1016/j.actbio.2009.07.034

66. Thelin, J. *et al.* Implant Size and Fixation Mode Strongly Influence Tissue Reactions in the CNS. *PLoS One* **6,** (2011). doi:10.1371/journal.pone.0016267

67. Kim, Y. *et al.* Chronic response of adult rat brain tissue to implants anchored to the skull. *Biomaterials* **25,** 2229–2237 (2004).

68. Ledochowitsch, P. *et al.* Nanoflex for neural nanoprobes. *IEEE* 1278–1281 (2013). doi:10.1109/Transducers.2013.6627009

69. Sankar, V. *et al.* A highly compliant serpentine shaped polyimide interconnect for front-end strain relief in chronic neural implants. *Front. Neurol.* **4,** 1–11 (2013). doi:10.3389/fneur.2013.00124

70. Huang, R. *et al.* Integrated parylene-cabled silicon probes for neural prosthetics. *IEEE* (2008). doi:10.1109/MEMSYS.2008.4443637

71. Skousen, J. L. *et al.* Reducing surface area while maintaining implant penetrating profile lowers the brain foreign body response to chronically implanted planar silicon microelectrode arrays. *Progress in Brain Research* **194,** (2011). doi:10.1016/B978-0-444-53815-4.00009-1

72. Seymour, J. P. & Kipke D. R. Neural probe design for reduced tissue encapsulation in CNS. *Biomaterials* **28,** 3594–3607 (2007). doi:10.1016/j.biomaterials.2007.03.024

73. Kozai, T. D. Y. *et al.* Mechanical failure modes of chronically implanted planar silicon-based neural probes for laminar recording. *Biomaterials* 25–39 (2016). doi:10.1016/j.biomaterials.2014.10.040.

74. Kozai, T. D. Y. *et al.* Ultrasmall implantable composite microelectrodes with bioactive surfaces for chronic neural interfaces. *Nat. Mater.* **11,** 1065–1073 (2012).

75. Cui, X. & Martin, D. C. Electrochemical deposition and characterization of poly (3 , 4-ethylenedioxythiophene) on neural microelectrode arrays. *Sensors Actuators B Chem.* **89,** 92–102 (2003). doi:10.1016/S0925-4005(02)00448-3

76. Ludwig, K. A. *et al.* PEDOT polymer coatings facilitate smaller neural recording electrodes. *J. Neural Eng.* **8,** 1–14 (2011). doi:10.1088/1741-2560/8/1/014001

77. Baranauskas, G. *et al.* Carbon nanotube composite coating of neural microelectrodes preferentially improves the multiunit signal-to-noise ratio. *J. Neural Eng.* **8,** (2011).

78. Keefer, E. W. *et al.* Carbon nanotube coating improves neuronal recordings. *Nat. Nanotechnol.* (2008). doi:10.1038/nnano.2008.174

79. Bareket-Keren L & Hanein Y. Carbon nanotube-based multi electrode arrays for neuronal interfacing : progress and prospects. *Front. Neural circuits* **6,** 1–16 (2013). doi:10.3389/fncir.2012.00122

80. Leung, B. K. *et al.* Characterization of microglial attachment and cytokine release on biomaterials of differing surface chemistry. *Biomaterials* **29,** 3289–3297 (2008). doi:10.1016/j.biomaterials.2008.03.045

81. Raynor, J. E. *et al.* Polymer brushes and self-assembled monolayers: Versatile platforms to control cell adhesion to biomaterials (Review). *Biointerphases* **4,** (2009).

82. Aregueta-Robles UA. *et al.* Organic electrode coatings for next-generation neural interfaces. *Front. Neuroengineering* **7,** 1–18 (2014). doi:10.3389/fneng.2014.00015

83. Bedell, H. W. & Capadona, J. R. Anti-inflammatory Approaches to Mitigate the Neuroinflammatory Response to Brain-Dwelling Intracortical Microelectrodes. *J. Immunol. Sci.* **2,** 15–21 (2018).

84. Luo, X. *et al.* Carbon Nanotube Nanoreservior for Controlled Release of Anti-inflammatory Dexamethasone. *Biomaterials* **32,** 6316–6323 (2012). doi:10.1016/j.biomaterials.2011.05.020

85. Mercanzini, A. *et al.* Controlled release nanoparticle-embedded coatings reduce the tissue reaction to neuroprostheses. *J. Control. Release* **145,** 196–202 (2010). doi:10.1016/j.jconrel.2010.04.025

86. Carli, S. *et al.* Biochemically Controlled Release of Dexamethasone Covalently Bound to PEDOT. *Chem. - A Eur. J.* (2018). doi:10.1002/chem.201801499

87. Chen, S. & Allen, M. G. Extracellular matrix-based materials for neural interfacing. *Materials for neural interface* **37,** 606–613 (2012). doi:10.1557/mrs.2012.120

88. Ochiai, H. *et al.* ‘ Living electrode ’ as a long-lived photoconverter for biophotolysis of water. *Biochemistry* **77,** 2442–2444 (1980).

89. Ochiai, H. *et al.* Properties of Semiconductor Electrodes Coated with Living Films of Cyanobacteria. *Appl. Biochem. Biotechnol.* **8,** 289–303 (1983).

90. Campbell, T. E. *et al.* Incorporation of Erythrocytes into Polypyrrole to Form the Basis of a Biosensor to Screen for Rhesus (D) Blood Groups and Rhesus (D) Antibodies. *Electroanalysis* 215–222 (1999).

91. Richardson-burns, S. M. *et al.* Polymerization of the conducting polymer poly(3,4-ethylenedioxythiophene) (PEDOT) around living neural cells. *Biomaterials* **28,** 1539–1552 (2007). doi:10.1016/j.biomaterials.2006.11.026

92. Green, R. A. *et al.* Living electrodes: tissue engineering the neural interface. *Conf. Proc. IEEE Eng. Med. Biol. Soc.* (2013). doi:10.1109/EMBC.2013.6611158

93. Sidhu, K. *et al.* Alginate Microcapsule as a 3D Platform for Propagation and Differentiation of Human Embryonic Stem Cells (hESC) to Different Lineages. *Jove J. Vis. Exp.* 7–10 (2012). doi:10.3791/3608

94. Fernández, E. & Botella, P. Biotolerability of Intracortical Microelectrodes. *Adv. Biosyst.* **2,** 1–14 (2018). doi:10.1002/adbi.201700115

95. Marin, C. Biocompatibility of intracortical microelectrodes: current status and future prospects. *Front. Neuroengineering* (2010). doi:10.3389/fneng.2010.00008

CHAPTER 1

CELL-COATED INTRACORTICAL MICROELECTRODES: METHODS TO IMPROVE THE BIOCOMPATIBILITY OF CHRONIC IMPLANTS

As previously discussed in the Introduction, the use of intracortical microelectrodes for the development of *brain-machine interfaces* is limited by a series of events that directly affect both the electrode itself and the surrounding neural tissue.

In recent decades, thanks to progress in production technologies and to the advances in materials science, different solutions have been proposed to face the damage caused by invasive techniques. These strategies can involve changes in device material and configuration or address the bio-physiological level. Regarding these approaches, although many studies report the use of bioactive molecules, there are still no significant works concerning the use of an entirely biological coating that involves whole living cells instead of proteins, extracellular matrix components or anti-inflammatory compounds.

Bio-hybrid approaches have been used in the past to intervene in the foreign body reaction (FBR) to implanted devices in different fields of application such as in glucose sensors[1], cochlear prosthesis[2] and biosensor materials[3], but a limited number of studies exist for neural prostheses and their *in vivo* assessment. Among these, one of the most advanced is reported by Kennedy, who used a segment of sciatic nerve placed inside a cone electrode to encourage axonal growth into the glass cone[4]. The author was able to record neural signals over 200 days from rat[5] and monkey[6] cortex and in a later pivotal study he tested the neurotrophic cone electrode also in human clinical studies of BMIs. To this purpose, Kennedy and colleagues implanted this kind of novel electrode into the cortex of three awake patients whose consciously modulated neural signals were used to drive the movement of a computer cursor[7–9]. However, applications of this device are limited due to the complexity of the cone electrode fabrication method, and not many further progresses have been reported.

Seeding cells over the electrode surface is a method used by different groups to test the biocompatibility of the device by using neural stem cells to improve device integration within the brain tissue[10–12]. The belief is that neural stem cells and neural progenitor cells

(NPCs) could replace dead or non-functional cells following microelectrode implant and be able to integrate into the host tissue in a cytoarchitectonically and developmentally appropriate manner. Neural stem cells and NPCs are found in several neurogenic zones of the adult brain such as the sub ependymal layer and the hippocampus. Thus, they could differentiate into the main phenotypes of the nervous system like neurons.

Purcell *et al.* seeded neural stem cells encapsulated in an alginate hydrogel scaffold over a parylene neuroprosthesis and found an attenuate early foreign response after *in vivo* electrodes implantation into rats brain. Anyway, after some weeks, they found hydrogel degradation and a more accentuated tissue response probably due to the presence of graft cells debris[13]. Moreover, the capability of this electrode to record neural activity or electrode electrical properties are not reported. Likewise, Azemi *et al.* use laminin-coated probe surfaces to immobilize NPCs cells and evaluated the tissue response after 7 days electrodes implantation[14]. As before, also this study lacks functional measurements. Thus, although there are preliminary studies on the use of cellular coatings to improve the foreign tissue response, there is no significant evidence of their use in the development of functional electrodes.

In this chapter, starting from standard working electrodes, I report a method to develop a bio-hybrid interface using endothelial cells coating. Contrary to the use of neural stem cells that have the main purpose of restoring damaged tissue, endothelial cells could mimic the biological environment of the host tissue by forming a strong vessel-like coating on the prostheses, being able to cheat the glial cells and to reduce the chronic inflammatory response, evaluated up to 6 weeks.

Indeed, one of the advantages of the use of endothelial cells is the possibility to easily harvest them from the same patient undergoing the implant, opening a great prospect for clinical translational applications. This could be a promising solution to minimize the FBR, to face the failure of intracortical implants and to start a new trend in the design of more biologically integrated neuroprostheses.

To this purpose, I will present here some preliminary studies on experimental animal models in which aortic endothelial cells have been used to coat intracortical microelectrodes. A systematic study of the brain tissue response has shown an improvement of the tissue bio-tolerability over the bio-hybrid devices, that have been left in the rodents brain for long periods of time (six weeks) with only low degrees of inflammatory reactions.

1.EXPERIMENTAL SECTION

All the experimental procedures were carried out in accordance with the guidelines established by the European Communities Council (Directive 2010/63/EU of September 22nd, 2010).

1.1 ISOLATION AND CHARACTERIZATION OF RAT AORTIC ENDOTHELIAL CELLS (RAEC)

The protocol for the isolation of aortic endothelial cells (RAEC) involves the dissection of rat aortae followed by aortic ring culture until RAEC outgrowth. The experimental subject was anesthetized with a mixture of Zoletil (Virbac, France; 30 mg/kg) and Xylazine (Bayer, Germany; 5 mg/kg) administered intraperitoneally (i.p.) and then killed by anesthetic overdose.

Briefly, the full length of the thoracic aorta was removed from anesthetized adult Long-Evans rats after they were secured in supine position and washing the chest with 70% ethanol. Quickly, with a sterile technique, the thoracic cavity was opened, the aorta was separated from the spine by gently grasping the anterior end and it was cut near the abdominal branch and at the anterior end. Then, the dissected aorta was transferred to a petri dish containing phosphate-buffered saline solution (PBS) and all extraneous fat, tissue and branching vessels were removed under sterile conditions with forceps and scalpel. The lumen of the aorta was washed with complete medium (50 ml Fetal Bovine Serum, 75 μg/ml Endothelial cell growth supplement (ECGS) (Sigma-Aldrich, Italy) and 500 ml Advanced DMEM, 5 ml 1M HEPES, 5 ml L-glutamine, 5 ml penicillin/streptomycin (all from Thermo Fisher Scientific, USA) using a glass pipette and the aorta was cut into 0.5 mm rings. The aortic rings were incubated at 37 °C until an endothelial outgrowth was visible. The aortic rings were then gently removed and discarded while the cells were allowed to proliferate until 90% of confluence. Occasionally, spindle-shaped fibroblasts migrating from the aorta were present as well, but the purity of the majority of the culture was checked for the characteristic cobblestone morphology of cells. Cells were also characterized using the specific endothelial cell marker CD31. Briefly, cells were cultured over glass coverslips and fixed in cold fixative (4% PFA) for 45 minutes. Cell-coated surfaces were rinsed in cold PBS, blocked and permeabilized with 10% goat serum, 2% BSA and 0.5% Triton X-100 in PBS for 1h while gently agitated. Samples were later incubated for 90 minutes with anti-CD31 antibody (PECAM-1, mouse, 1:100; Thermo

Fisher Scientific, USA). Cells were rinsed in PBS, incubated for 3 hours with Alexa Fluor 488 goat anti-mouse (1:500; Invitrogen, Milano, Italy) and finally mounted with ProLong ™ Gold Antifade reagent with DAPI (Invitrogen, Milano, Italy).

1.2 CELL CULTURE ON ELECTRODE SUBSTRATES

Different types of materials were used to optimize the *in vitro* cell culture method and to test the effective ability of cells to grow on multiple electrode candidate substrates. Specifically, (i) polyimide capillaries, (ii) quartz insulated platinum wires, (iii) polyimide coated platinum wires and (iv) teflon coated platinum wires were used for *in vitro* cell culture, while single core quartz insulated metal microelectrodes were prepared in-house by mechanically grinding 95% platinum/5% tungsten microwires 20 µm in diameter coated with 30 µm of quartz (Thomas Recording, Giessen, Germany) and used for the *in vivo* implant experiments. As a proof of concept, preliminary *in vivo* experiments were also performed using polyimide capillaries.

In all cases, to allow cell attachment to the substrate, the wires were aligned overhanging the edge of a silicone support on a coverslip (**Figure 1**) and the entire structure was sterilized with 70% ethanol for 20 min followed by rinsing three times in PBS.

Cells were seeded on the upper coverslip of the support and allowed to adhere for 2 h in incubator. The substrates were then washed with PBS to discard non adherent cells and complete medium was added to the entire petri dish. Cells were cultured for 5 days at which time they proliferated and migrated along the wires. Before *in vivo* experiments, the cells were treated with Vybrant CM-Dil cell-labeling solution (Thermo Fisher Scientific, USA): briefly, staining medium was prepared adding the supplied dye labeling solution to the normal growth medium at a final concentration of 1:200 and was used to replace the culture medium. After incubation at 37 °C for 20 minutes, the staining medium was drained off and cells washed three times with fresh, 37 °C growth medium before using them for the implantation.

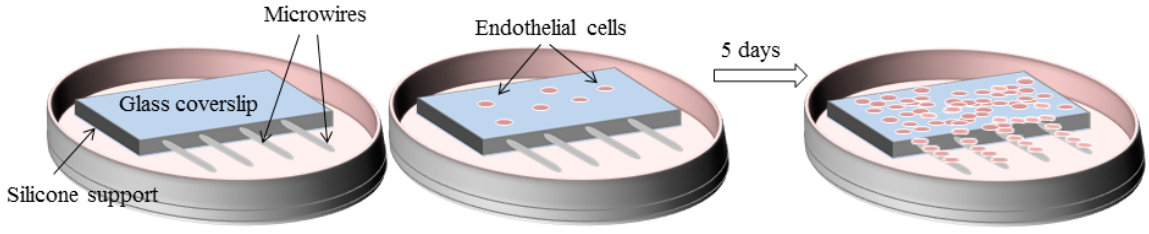

Figure 1. Schematic representation of endothelial cell culture method on microwires.

1.3 ELECTROCHEMICAL CHARACTERIZATION OF THE ELECTRODES

The electrochemical properties of the uncoated microelectrodes were studied via electrochemical impedance spectroscopy (EIS) in a physiological aqueous solution (0.9% NaCl). During the EIS measurements, a sine wave (10 mV RMS) was superimposed onto the open circuit potential while varying the frequency from 1 to 10^5 Hz. The electrochemical characterization was carried out using a potentiostat/galvanostat (Reference 600, Gamry Instruments, USA) connected to a standard electrochemical cell used in a three-electrode configuration with a platinum counter-electrode and an Ag/AgCl reference electrode. The identical measurement procedure was performed after five days of cells culturing over the same wires.

1.4 IMMUNOFLUORESCENCE CELLS LABELING

After cell seeding over the electrodes, the effective adhesion and migration of the endothelial cells along the wires were evaluated using immunofluorescence techniques. After five days of culture, cells were fixed in 4% paraformaldehyde (PFA), treated with blocking solution consisting of 4% (v/v) normal goat serum, 0.5% (v/v) Triton-X-100, 2% (w/v) bovine serum albumin (BSA) (all from Sigma Aldrich, USA) in PBS for 1 h and then incubated in the primary antibodies overnight at room temperature. The cells were stained with rabbit-anti-vimentin (1:100; Thermo Fisher Scientific, USA) followed by anti-rabbit Alexa-488 (1:500; Thermo Fisher Scientific, USA). Finally, after washing 3 times in PBS, the wires were mounted onto microscope slides, counterstained with ProLong Gold Antifade Mountant containing DAPI (Thermo Fisher Scientific, USA) and covered with a coverglass. In some cases the vital marker fluorescein diacetate (FDA, 5mg/ml; Sigma-Aldrich, Italy) was used to assess the viability of the cells over the wires. All the stainings were observed using an Olympus BX51 microscope (Melville, USA) equipped with a X-Cite R 120 fluorescence microscopy illumination system (EXFO, Canada) and a color videocamera CX-9000 (MicroBrightField, USA).

1.5 ANIMAL SURGERY AND *IN VIVO* CHRONIC IMPLANTS

To evaluate the FBR, the bio-hybrid constructs (cell coated electrodes) and the correspondent uncoated microelectrodes were chronically implanted in rats cortex. Details about number of animals and experimental condition are reported in **Table 1** and **Figure 2**. Long Evans rats were anesthetized with a mixture of Zoletil (Virbac, France; 30 mg/kg) and Xylazine (Bayer, Germany; 5 mg/kg) administered intraperitoneally (i.p.). For the entire duration of the procedure, the depth of anesthesia was monitored by testing the absence of hind limb withdrawal reflex and was maintained by additional i.m. doses of anesthetic. The body temperature was maintained at 37–38 °C with a thermostatically controlled heating pad and lacrigel (Farmigea, Italy) was placed on eyes to avoid dryness. After shaving and swabbing the head with ethanol, the anesthetized animal was placed in a stereotaxic apparatus (David Kopf Instruments, USA) equipped with ear bars (Model 957 for small animals). An approximately 2 cm long incision was made along the midline of the cranium. The underlying muscle and connective tissue were retracted to expose the skull. A small craniotomy was made in both the hemispheres. Sterile saline solution was applied while drilling to avoid local heating and to keep clean the bone surface. The exposed dura mater was wetted with saline and carefully incised using surgical micro-scissors and the tip of a 24 G syringe needle to produce an opening both in the dura and in the pia mater. Two wires, one uncoated as control and one cell-coated were then inserted in each hemisphere. Coated and uncoated wires were stereotaxically inserted for about 2 mm in depth. After insertion, the surface of the implanted tissue was protected using Kwik-Sil silicone polymer (World Precision Instruments Inc, USA) and the skin was sutured.

Time – phase	Animals	Uncoated wires	Coated wires
1 week – acute	3	6	6
3 weeks – progressive	3	6	6
6 weeks – chronic	3	6	6

Table 1. Experimental epochs, number of animals and wires used

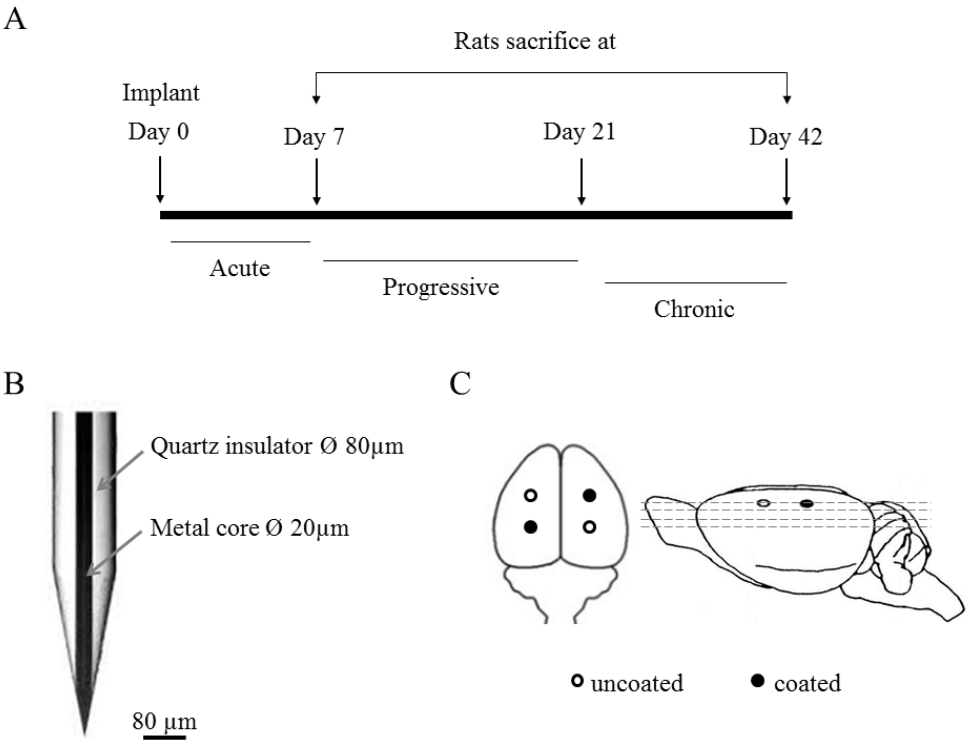

Figure 2. Experimental procedure. (A) Time line of the *in vivo* animal experiments. Acute, progressive and chronic refer to the phases of inflammatory response of the host tissue. (B) Representation of Thomas Recording microelectrode used for the creation of bio-hybrid electrodes and for the *in vivo* experiments. (C) Sketch of implants location into the rat brain. Four wires were implanted in each animal, one coated and one uncoated in both hemispheres. Horizontal sections (50 µm slices) were made for the following immunohistochemistry analysis and tissue response evaluation.

1.6 Neural Recordings and Evaluation of the Signal-To-Noise ratio

Acute neural recordings from rat cortex were performed to test the functionality of the bio-hybrid construct. Electrophysiological data were acquired for 20 min using TDT RZ-2 Processor and PZ2 preamplifier (Tucker-Davis Technologies, USA). The acquired neural traces were sampled at 24,414 Hz and bandpass filtered from 10 to 5000 Hz. To connect the microelectrodes to the headstage, a custom support for ZIF-Clip (Tucker-Davis Technologies, USA) was designed. Recorded data were stored and analyzed off-line using the Off-Line Sorter (Plexon Inc, USA) and NeuroExplorer (Nex Technologies, USA) software.

Spikes detection and evaluation of the signal-to-noise ratio (SNR) were performed with specific tools using Off-Line sorter software (Plexon Inc, USA). Each acquired trace was high-pass digitally filtered above 250 Hz. The signal was wavelet decomposed and thresholded to 3.5 standard deviations (SD) above and below the mean of the sample distribution to discriminate signal from noise. A specific tool (Threshold Scan Graph) was also used to systematically step the threshold from a starting value (5 mV) to an ending value (50 mV) and perform a waveform extraction at each threshold value, helping to adjust the correct trade-off between a large number of spikes and a high SNR.

Waveforms were clustered using T-Distribution E-M algorithm method (Off-Line Sorter). All the spikes with inter-spike-interval (ISI) smaller than the refractory period (2 ms) were removed. The SNR is computed as the ratio of (sigma squared within signal)/(sigma squared within noise), where the "signal" is taken to be all samples within extracted spikes, and the "noise" is all samples outside of extracted spikes.

1.7 HISTOLOGY AND QUANTITATIVE ANALYSIS

In order to investigate the tissue response to coated and uncoated microelectrode implants, the immunofluorescence staining was performed at 1, 3 and 6 weeks after wire implantation. At the end of each fixed time course, the animals were maintained deeply anesthetized and transcardially perfused with 300 ml of 0.9% saline solution at room temperature followed by 500 ml cold fixative solution of 2.0% PFA, 1.25% glutaraldehyde and 2.0% sucrose (all from VWR, USA), prepared in 500 ml of 0.1 M sodium phosphate buffered solution (PBS, pH 7.4). Brains were then removed, post fixed overnight at 4 °C and placed in a 30% sucrose-buffered solution until they sank. They were then frozen and 50 μm-thick horizontal sections were cut using a sliding microtome (SM2000R; Leica Microsystems, Canada). The brain sections were stained using antibodies directed against reactive astrocytes detected by the production of glial fibrillary acidic protein (GFAP); activated microglia/macrophages detected by the membrane- bound CD68-antigen (clone-ED1); neuronal nuclei (NeuN) and total number of cell nuclei (DAPI), to label the principal cell lines involved in the inflammatory tissue reaction. The adjacent sections were divided into two series, treated with blocking solution consisting of 4% (v/v) normal goat serum (Sigma Aldrich, USA), 0.5% (v/v) Triton-X-100 (Sigma Aldrich, USA), 2% (w/v) bovine serum albumin (BSA) (Sigma Aldrich, USA) in PBS for 1 h and then incubated in the primary antibodies overnight at room temperature. The first series was

stained using mouse-anti-ED1 (1:300, Millipore, USA) and rabbit-anti-NeuN (1:200, Millipore, USA) while the second one using mouse-anti-GFAP (1:500, Sigma-Aldrich, USA). After 3 rinses in PBS (10 min per rinse) the sections were incubated with anti-rabbit Alexa-488 and anti-mouse Alexa-633 conjugated secondary antibodies (1:500, Thermo Fisher Scientific, USA) for 3 hours in the dark, at room temperature. All mentioned antibodies were used diluted in the blocking solution. Finally, after washing 3 times in PBS, the two series of sections were mounted separately onto microscope slides, counterstained with ProLong Gold Anti fade Mountant containing DAPI (Thermo Fisher Scientific, USA) and covered with a coverglass. The staining was observed using a BX51 microscope with 10×, 20×, 40× objectives (Olympus, Japan) and equipped with a X-Cite 120 fluorescence microscopy illumination system (EXFO, Canada) and a color videocamera CX-9000 (MicroBrightField, USA). The images of all the fluorescence tissue slices were acquired using NeuroLucida (MicroBrightField, USA) and ImageJ software (developed at the National Institutes of Health, USA) was used for the following analysis.

Different horizontal sections were selected for each animal and images were captured at different depths along the penetrations. Fluorescent images were captured under the same illumination level so that the overall background light intensities were comparable.
For astrocytes activation (GFAP expression) the following analysis was performed. For each image, three 500 x 50 μm rectangular shape windows (ROI = region of interest) starting from the edge of the hole created by the electrode were marked, as shown in **Figure 3A**. The staining intensities within the windows were quantified by averaging the pixel across the width of the rectangle and plotting them as a function of distance from the electrodes (longitudinal axis of the rectangle) using specific tools in ImageJ. A representative GFAP intensity profile is shown in **Figure 3B**. The fluorescence intensity, directly related and proportional to glial activation, was then calculated as mean of the integrated density values of the 3 ROIs per image and used to calculate the percent increase of fluorescence with respect to the background (region far from the implant site). For each wire a single profile was plotted averaging the value of each section. Finally, the plots belonging to the same experimental group (coated and uncoated wires) at each time point were averaged together in order to obtain a single trend for each experimental group. To quantify the neuronal loss surrounding the implant, a series of concentric rings with a pitch of 80 μm, starting from the edge of the hole created by the wire, were drawn using specific plugins in ImageJ (**Figure 3C**). The number of neurons in each ring, corresponding to increasing distances from the implant, was then semi-automatically

counted using ImageJ tools. Finally, values were compared to background neuronal nuclei expression, defined as the mean value of neuronal cells within non implanted tissue region. All the counts were expressed as NeuN count per area of 50x50 μm^2. The significance of the data (*P value* < *0.05*) was evaluated performing a two-sample (coated and uncoated) unrelated two-tailed t-test for both the GFAP expression analysis and the neuronal loss evaluation.

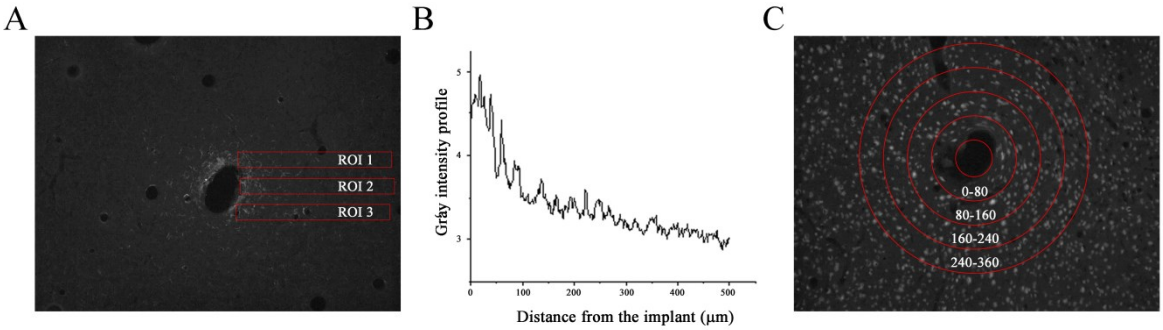

Figure 3. (A) Representative grayscale GFAP immunostaining and regions of interest (ROI - red rectangles) used for quantitative intensity analysis. (B) Example of plot profile obtained averaging values of the 3 ROI/image. (C) Representative grayscale NeuN immunostaining and concentric circles (red rings) used for quantitative analysis of neuronal nuclei density.

2. RESULTS AND DISCUSSION

2.1 WIRE COATED WITH ENDOTHELIAL CELLS: BIO-HYBRID MANUFACTURING

The bio-hybrid intracortical microelectrode was made starting from a standard commercial electrode and a culture of rat aortic endothelial cells. Vascular endothelial cells lining the internal surface of blood vessels play an active role in pro- and anti-thrombotic activities, in the inflammatory processes, by producing and by responding to cytokines, and by expressing different surface receptors and adhesion molecules to interact with other cells. Importantly, the endothelium acts as a semi-selective barrier between the vessel lumen and surrounding tissue, controlling the passage of materials and the transit of white blood cells across vascular walls. Endothelial cells are very resistant cells, constantly exposed to high hemodynamic forces, form well organized structures and are thus good candidates for our purposes. Specifically, we chose the aortic district because it is easy to reach and handle with respect to other smaller rat vessels and for the high cellular outcome of the procedure.

After aortic tissue extraction, the cells were able to grow and migrate from the explant (**Figure 4A**) and to proliferate as a continuous monolayer (**Figure 4B**), showing the characteristic cobblestone morphology and expressing the specific CD31 endothelial cell marker (**Figure 4C**). For the creation of the bio-hybrid electrodes, cells were seeded upon the upper coverslip of the silicone support where the microelectrodes wires were aligned at the edge (**Figure 4D**). The starting point of this technique was the method described by Yevick and colleagues. In this work the authors showed how epithelial cells are able to migrate in different orientations aligning their cytoskeleton in a cylindrical manner as in physiological conditions. They used glass wires of different radii to study the cell architecture and the migration rate[15]. Here, we adapted this technique as new growth method for endothelial cells in place of the previous method used by De Faveri *et al.*. In this last work, the authors used a fibrin layer to cover the same tungsten/platinum microelectrode and to perform *in vivo* implantation and acute recording, demonstrating that the coating does not alter the electrochemical properties of the electrodes and that it allows good quality recordings. They also tested the biocompatibility of the fibrin coating and the possibility to seed cells over the microelectrode surface by growing glial cells and neurons within the hydrogel. However, the adopted method required to grow the cells in suspension and therefore the coverage was not optimal. Conversely, in this work we allow the growth of adhering cells by seeding them over a coverslip, and this resulted in a very strong and confluent cell layer, increasing the quality and quantity of the cellular attachment on the

substrate. The endothelial cells migrated along the wire (**Figure 4E**) until they completely wrapped it after 5 days of culture. At this time, the formation of a confluent viable layer over the wires can be observed, as reported in **Figure 4F**, where FDA green staining show the cell vitality.

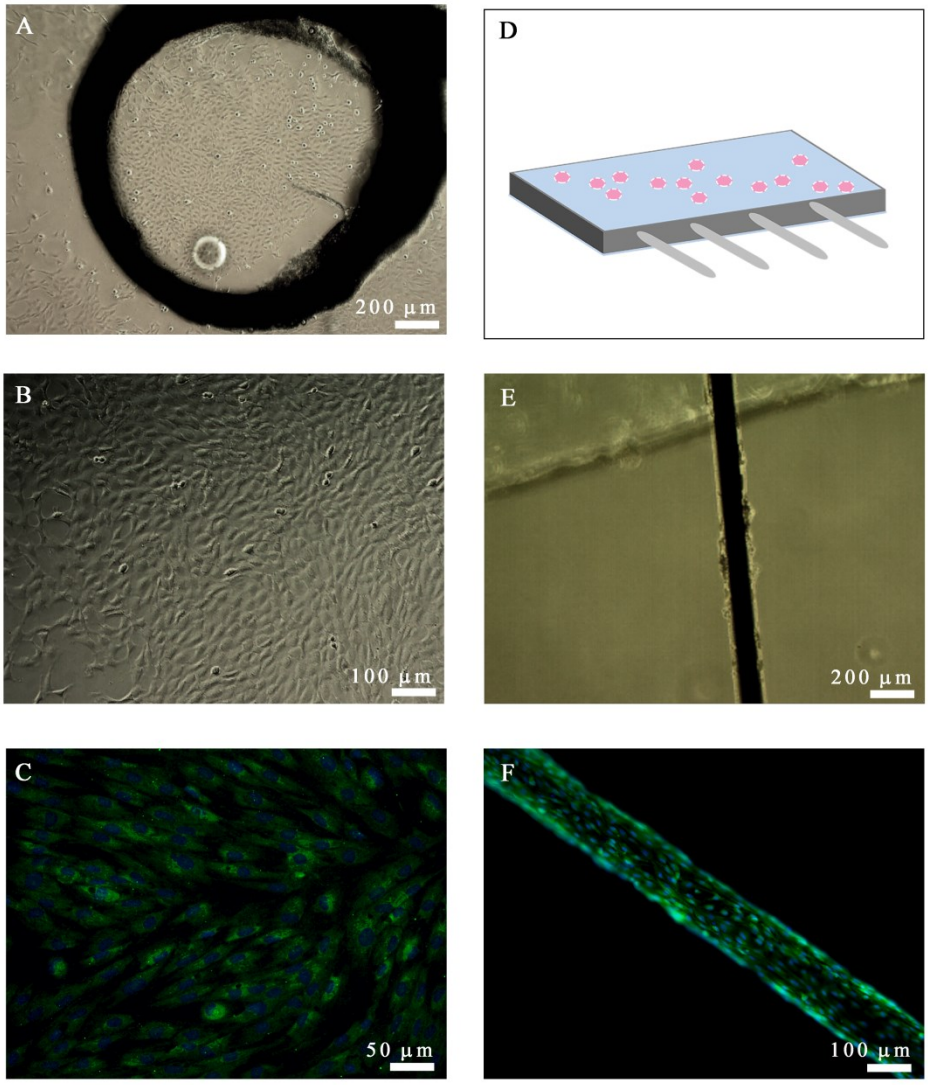

Figure 4. Cell culture and bio-hybrid realization. (A) Bright field image of aortic ring culture with endothelial cells outgrowth and (B) confluent cell monolayer before harvest and use for microelectrodes coating. (C) Immunocytochemistry characterization of endothelial cells (green: CD31; blu: DAPI). (D) Scheme of the silicone wires support: polyimide capillary as test bench and then Thomas recording microelectrodes were aligned overhanging the edge of a silicone support and the endothelial cells were seeded upon the upper coverslip. (E) Bright field image of cells migrating along the wire and (F) fluorescence image (blue: dapi, green: FDA) to check the presence of viable cells around the total length of the polyimide capillary.

Polyimide capillaries were used in a pilot experiment since they were easier to use without requiring manufacturing and, more importantly, because they could be cut by the microtome without extracting them from the brain. The efficiency of the growth method was also tested with other electrode candidate substrates (quartz insulated platinum wires, polyimide coated platinum wires and Teflon coated platinum wires) and we obtained analogous results with the development of a strong biological layer covering the entirety of the probes (**Figure 5**). Finally we progressed using real microelectrodes, in order to develop a working construct able to be used also for real applications such as animal recording studies.

We chose for our following experiments the Thomas Recording microelectrodes that are 80 µm diameter single core quartz insulated platinum/tungsten wires, in which the active metal surface is exposed by in-house mechanical grinding the end tip.

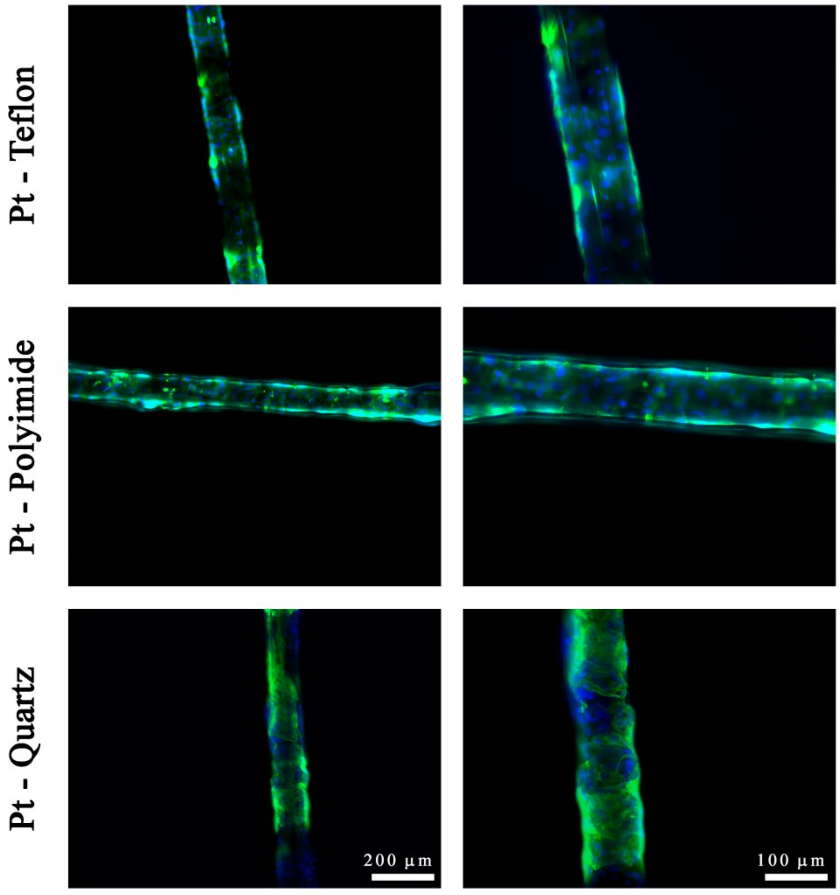

Figure 5. Representative immunofluorescence images (green: vimentin, blu: dapi) of endothelial cells cultured over different probe substrates (Teflon insulated platinum wires, Polyimide insulated platinum wires and Quartz covered platinum wires).

2.2 ELECTROCHEMICAL PROPERTIES AND RECORDING CAPABILITY OF THE BIO-HYBRID DEVICE

Thomas Recording microelectrodes were used for the creation of bio-hybrid devices and the electrochemical properties of the final products were analyzed using EIS technique in a physiological aqueous solution (0.9% NaCl). The measurements were taken before cell seeding over the microelectrodes surface and after five days of cell culturing. **Figure 6** shows the electrical impedance in the range of frequencies between 10 Hz and 100 kHz. At lower frequencies and up to about 1 KHz, center band frequency of neuronal action potentials[16], the presence of the endothelial cell layer induces a slight increment of impedance values while globally the electrochemical properties of the microelectrodes and the electrical behavior are preserved even after cellular culture procedures.

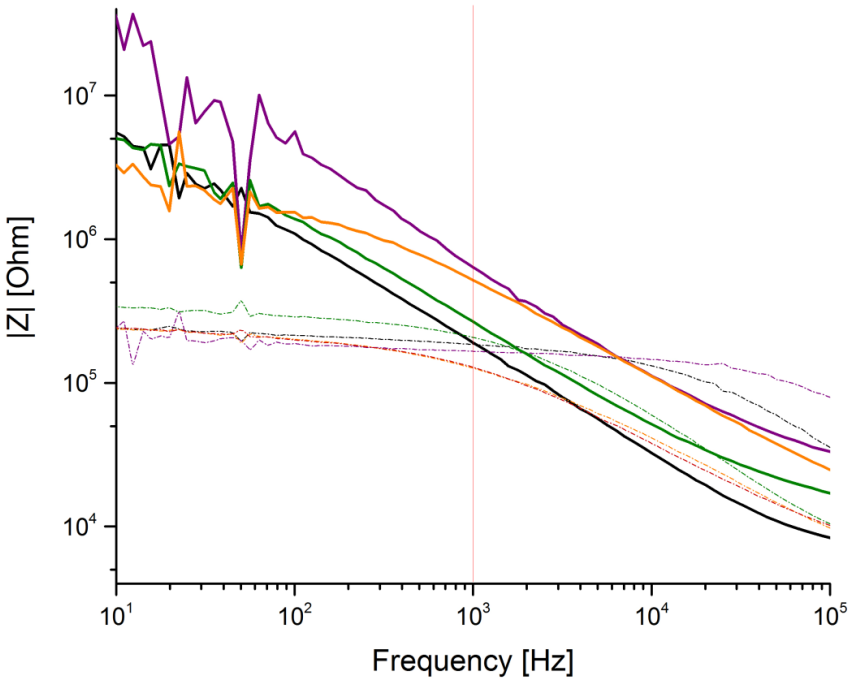

Figure 6. Electrochemical impedance spectroscopy. Impedance modulus, y-axis, with respect to the frequency window, shown in x-axis. The dotted lines correspond to the uncoated microelectrodes while the thick continuous lines correspond to the same electrodes after cells seeding. Different colors refer to different electrodes produced and analyzed. The vertical red line indicates the significant neurophysiological value of 1 kHz.

A further demonstration that the cell coatings don't represent a barrier for the electrical signals is the preservation of recording capabilities of the cell-coated device, shown in **Figure 7**. After cell seeding over the wires, we tested the ability of the electrodes to capture neuronal activity in a rat brain model. Acute recordings have shown no significant difference between the coated and uncoated devices regarding both the number of spikes and the SNR (**Table 2**).

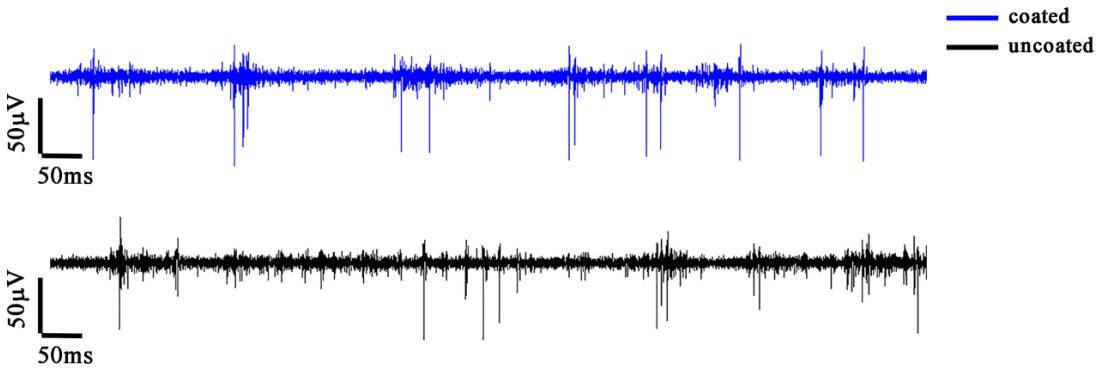

Figure 7. Examples of acutely recorded traces obtained with coated (blue) and uncoated (black) microelectrodes.

	SNR	Spikes/min
Coated	**2.069**	**4493**
Uncoated	**2.446**	**3917**

Table 2. Signal-to-noise ratio and spikes/min recorded in an acute session using coated and uncoated microelectrodes.

2.3 CHECK OF *IN VIVO* CELL PRESENCE

Most of the studies that aim to the development of cellular coatings, adopt the use of adhesion molecules such as laminin and poly-lysine to increase the efficiency of cell attachment to the substrate. In addition, several groups highlight the importance of embedding these cells within an hydrogel that can support survival and growth of the encapsulated cells and that can ensure the integrity of the coating upon insertion of the device into the brain. However, despite the hydrogel could play an important role also for improving the mechanical compliance with the soft brain tissue, issues regarding swelling,

electrical insulation and degradation should be taken into consideration. Furthermore, the presence of adhesion molecules could limit the clinical application of this kind of devices.
In our case, we succeeded in obtaining a good cellular adhesion and the formation of a thick coating without the use of any adhesion molecule. To test the stability of the cell layer, we inserted coated and uncoated microelectrodes into rat brain and we evaluated by DAPI staining the persistence of cells on the microelectrodes after brain insertion/extraction.
As illustrated in **Figure 8**, the amount of cells that remained adherent to the electrode surface is represented by blue spots, demonstrating the strength of the biological layer and its endurance to the insertion/extraction. On the contrary, no cells are visible upon the uncoated probe after extracting the wire.

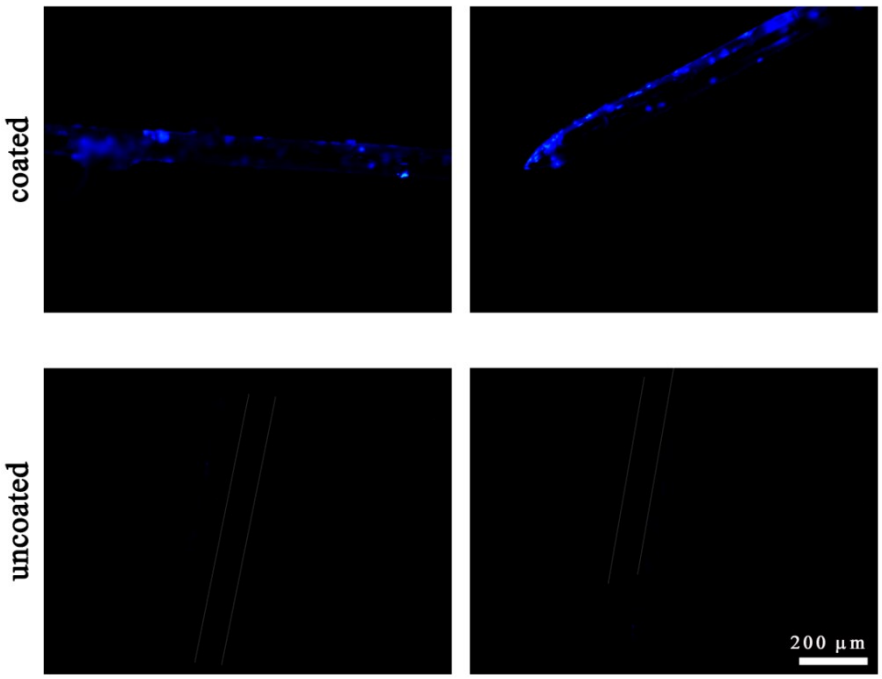

Figure 8. Representative images of coated and uncoated microelectrodes after brain insertion and extraction. In the lower panels, gray lines point out the microelectrodes shape.

As a next step, we implanted coated and uncoated probes in rat brain in order to assess their behavior *in vivo* during a chronic experiment in order to evaluate tissue response. Three animals were used for each fixed time point and four wires were implanted in each animal, one coated and one uncoated for each hemisphere (see **Figure 2C** for a schematic representation of the implant method). Although we had already verified the strength of the coating and the cell adhesion to the wires after acute implantation and probe removal, in this case, before *in vivo* implants the bio-hybrid devices were treated with Vybrant CM-Dil

cell-labeling solution, used to enable long-term *in vivo* cell tracking. This staining labels the endothelial cells adherent to the electrode and allowed monitoring their presence in the area of implant up to six weeks after microwire extraction. In **Figure 9** some representative images of brain slice tissue at different analyzed epochs are reported, showing red spots corresponding to staining of endothelial cells covering the wires. This is a further demonstration of the presence and maintenance of the cellular coating throughout the duration of the experiment and of its ability to withstand the insertion force. Moreover, the endothelial cells seem to remain in the area surrounding the insertion site therefore, even *in vivo,* they maintain a compact structure, almost reproducing a true blood vessel without spreading to nearby districts.

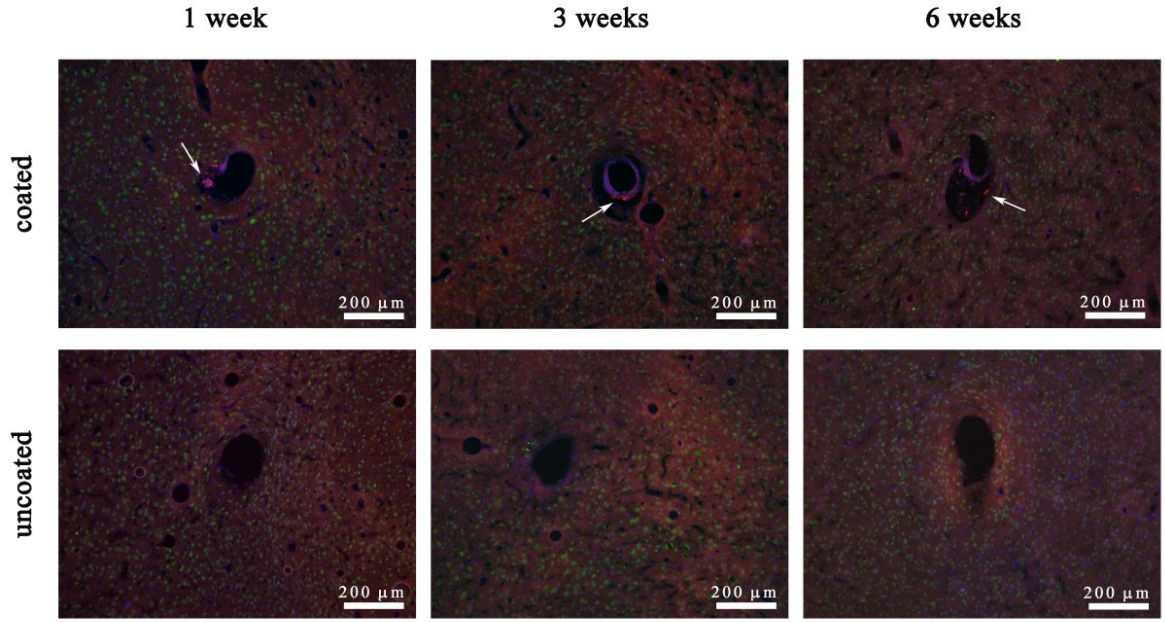

Figure 9. Representative images of brain tissue slices at 1, 3 and 6 weeks after coated (upper panel) and uncoated (lower panel) microelectrodes implant showing coating cells (indicated with arrows) remaining in the area of the insertion. Neuronal nuclei (NeuN) are shown in green.

2.4 IMPROVING INTRACORTICAL MICROELECTRODES

2.4.1 INFLAMMATORY RESPONSE: COATED VS UNCOATED MICROELECTRODES

One of the main problems related to the use of intracortical microelectrodes is the tissue reaction that over time reduces the performance of the electrodes and leads to tissue damage establishing the inflammatory cascade. To assess whether the bio-hybrid

microelectrode reduces this issue, we evaluated the inflammatory response in terms of GFAP expression by immunohistological methods. Different horizontal sections were obtained from rat brains implanted with coated and uncoated microelectrodes. Five samples for each type of wire were analyzed at different epochs in order to follow the tissue reaction progress and qualitative observations were supported by quantitative analysis. Indeed, the fluorescence intensity of GFAP immunolabeling is directly proportional to the astrocytes activation and we measure the GFAP intensity as a function of distance from the implant to quantify the overall glial reaction. The mean percentage of increased fluorescence intensity with respect to the background at different times from implant is reported in **Table 3.** Data shows a slight increase of glial reaction for uncoated microelectrodes with respect to cell-coated wires and this increase is statistically significant ($p < 0.05$) after one week from implantation.

	Fluorescence intensity increase (%) with respect to the background ± SD		
	1 week**	**3 weeks**	**6 weeks**
coated	16.9 ± 8.5	21.2 ± 16.9	18.8 ± 12
uncoated	20.2 ± 10.3	25.4 ± 21.5	20.5 ± 13.7

** difference statistically significant (two-sample, coated vs uncoated, unrelated two-tailed t-test).

Table 3. Quantitative analysis of GFAP fluorescence intensity. The intensity value for each group is reported as the mean of the integrated density values of the 3ROIs per images and used to calculate the % increase of fluorescence with respect to the background ± SD.

During the acute phase, after one week, the astrocytes were spread around the implant and presented ramified processes proximal to the electrodes traces as it can be seen at high magnification in **Figure 10**. An increase of the thickness of the glial cell processes is observed in **Figure 11** that refers to the progressive phase (3 weeks), characterized by more reactive astrocytes surrounding the area of the implants and this is more pronounced for uncoated electrodes. After six weeks (chronic phase) the tissue reaction is established and the formation of the so-called glial scar is clearly visible (**Figure 12**). The fluorescence intensity values increased progressively at this point, testifying a sustained glial cell activation. However, also after six weeks, the intensity profile for the bio-hybrid microelectrode is lower than for the uncoated one.

The trend of the GFAP intensity profile of coated and uncoated microelectrodes is shown in **Figure 10B, 11B** and **12B**. In all cases the fluorescence profile is higher for uncoated

than for coated electrodes, and decline quite sharply with distance, reaching the baseline levels at around 300 µm.

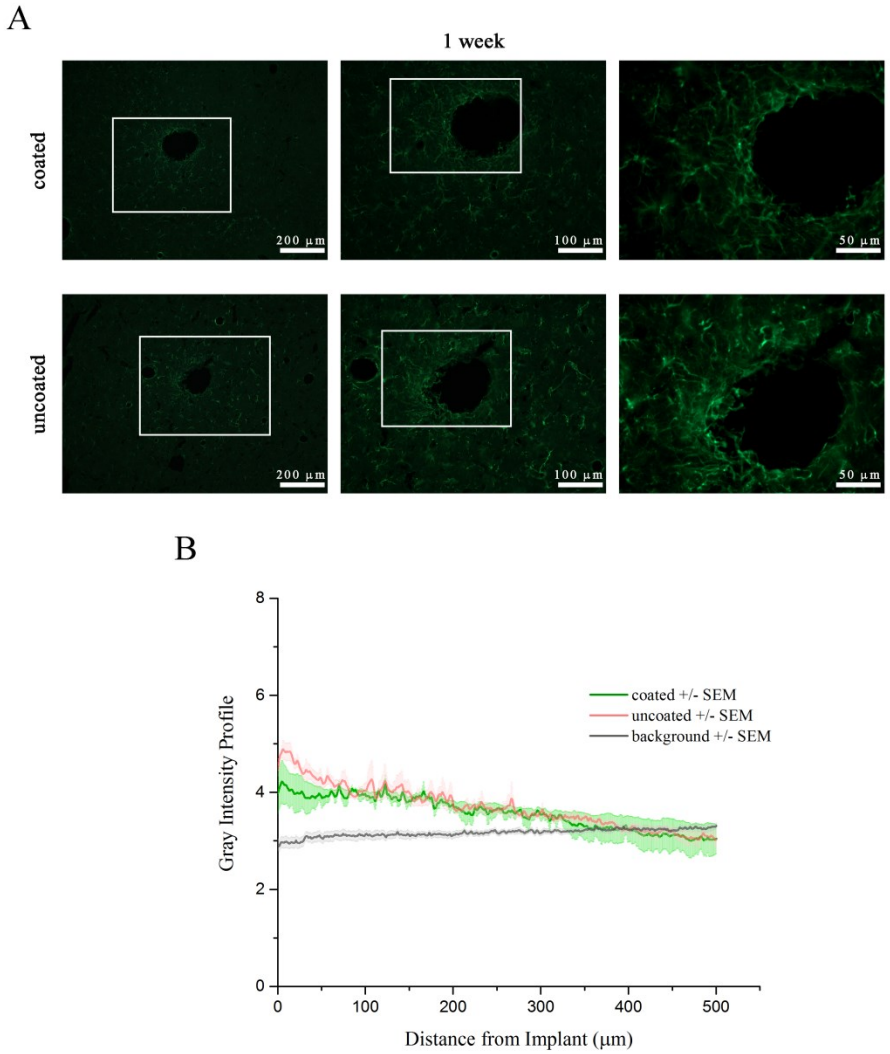

Figure 10. (A) Representative fluorescent images of GFAP immunolabeling showing astrocytes after 1 week of cell-coated (upper panel) and uncoated (lower panel) microelectrode implants. Black holes identify microelectrode traces. Different magnifications allow to observe reactive astrocytes proximal to implants. (B) Gray intensity profile of GFAP immunoreactivity as a function of distance from the implant. Each profile is the total average plot values (± SEM) of intensity curves obtained from five animals per group.

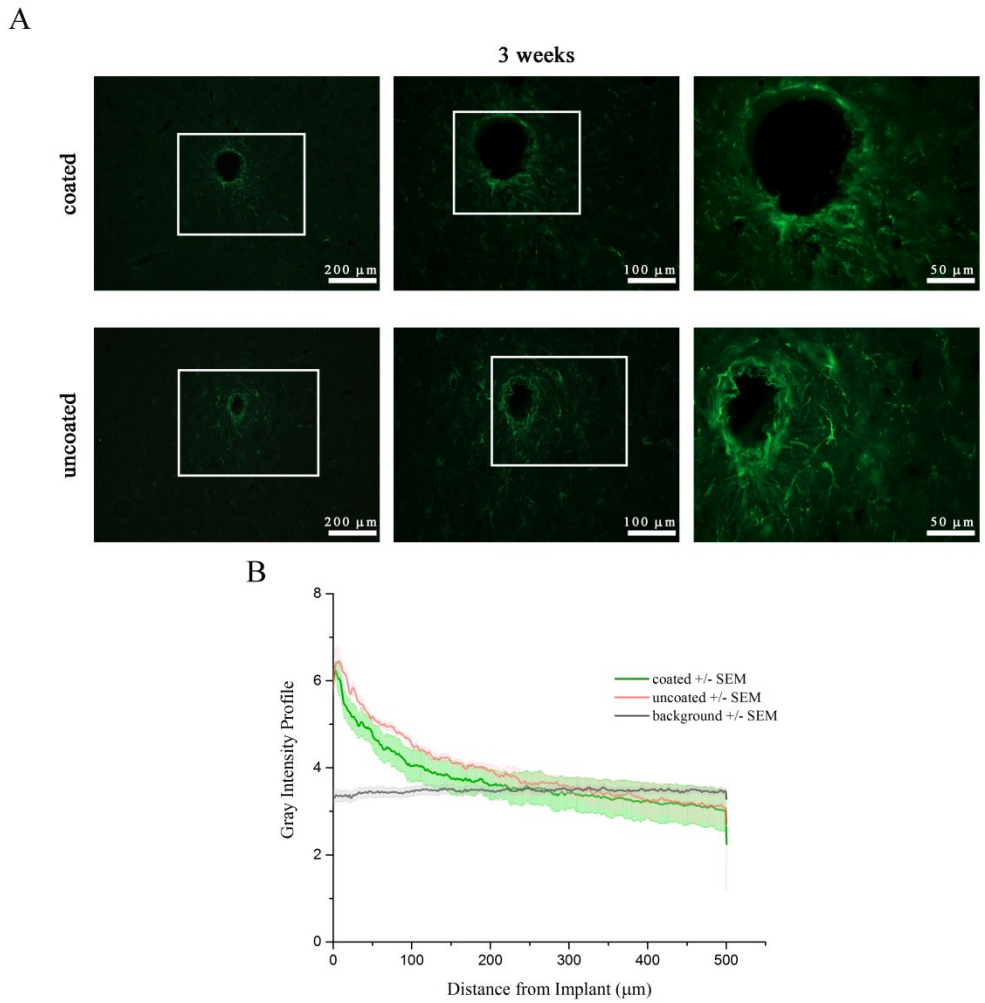

Figure 11. (A) Representative fluorescent images of GFAP immunolabeling showing astrocytes after 3 weeks of cell-coated (upper panel) and uncoated (lower panel) microelectrode implants. Black holes identify microelectrode traces. Different magnifications allow to observe reactive astrocytes proximal to implants. (B) Gray intensity profile of GFAP immunoreactivity as a function of distance from the implant. Each profile is the average plot values (± SEM) of intensity curves obtained from five animals per group.

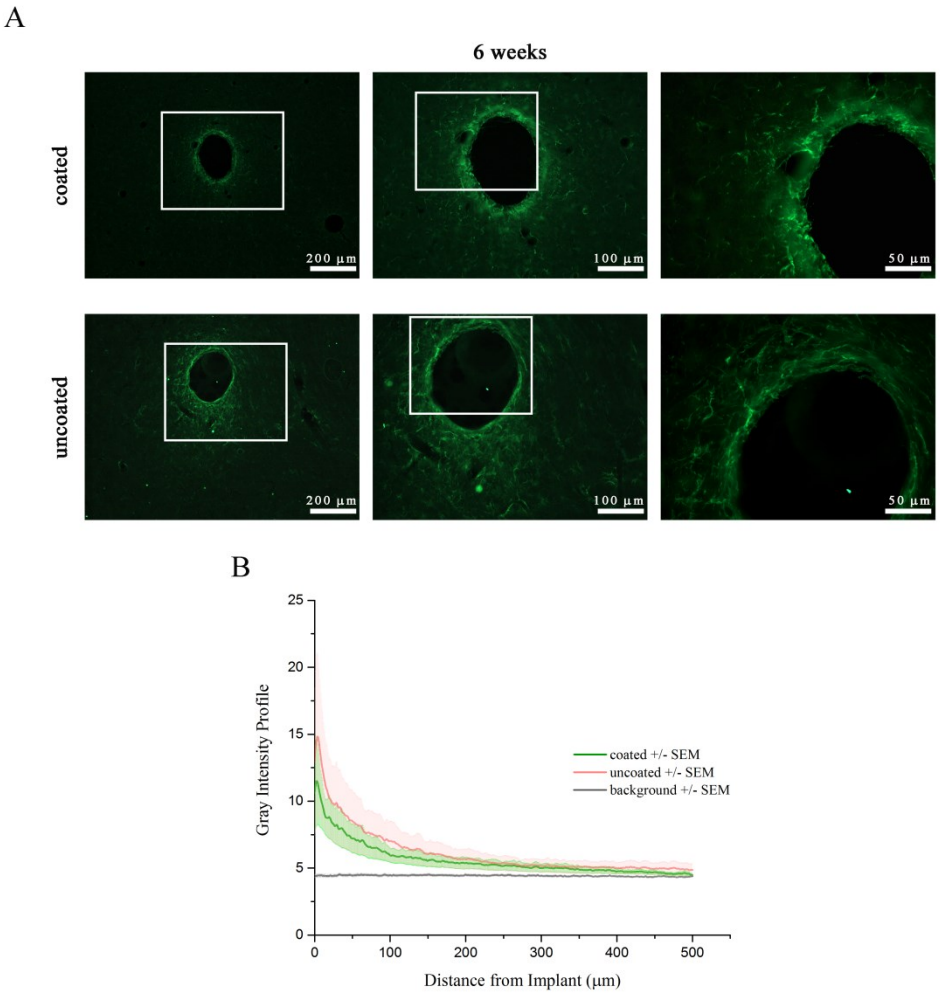

Figure 12. (A) Representative fluorescent images of GFAP immunolabeling showing astrocytes after 6 weeks of cell-coated (upper panel) and uncoated (lower panel) microelectrode implants. Black holes identify microelectrode traces. Different magnifications allow to observe reactive astrocytes proximal to implants. (B) Gray intensity profile of GFAP immunoreactivity as a function of distance from the implant. Each profile is the average plot values (± SEM) of intensity curves obtained from five animals per group.

The morphological changes reported here are consistent with what found in literature and with the different phases of the inflammatory response. Importantly, the bio-hybrid electrodes allow to minimize the FBR mainly in the first week and, despite the difference at the chronic stage is not statistically different, this attenuated initial response improves the overall glial reaction against the cells coated probes instead of the uncoated wires.

To assess the microglia/macrophage reaction elicited by cell-coated and uncoated microelectrodes, the brain sections were labeled also with ED-1 antibody directed against CD68 protein, a transmembrane glycoprotein specifically found in the cytoplasmic granules of activated microglia and macrophages. ED-1 positive cells, exhibiting the

characteristic amoeboid morphology of reactive macrophage-like microglia, were localized inside the immediate perimeter of the electrodes traces and no evidence of microglia/macrophage activation was observed in other more distant brain region. As shown in **Figure 13**, few ED-1 positive cells, identified with white asterisks, were found in proximity of the cell-coated microelectrodes traces while the ED1 immunoreactivity was stronger in proximity of the uncoated microelectrodes implant sites at 1, 3 and 6 weeks after implantation.

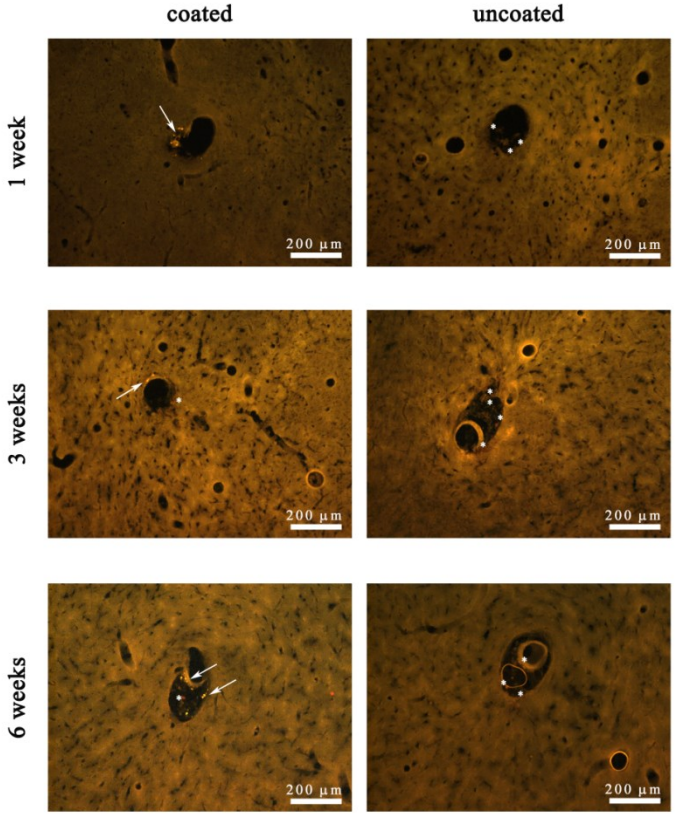

Figure 13. Representative fluorescence microscopy images of tracks for cell-coated and uncoated microelectrodes showing the localization of ED-1 positive cells (white asterisk) at 1, 3 and 6 weeks after implants. Arrows indicate the endothelial cells used as electrodes coating.

2.4.2 NEURONAL RESPONSE: COATED VS UNCOATED MICROELECTRODES

Intracortical microelectrodes are usually used to record from single or groups of neurons near the tip of the devices and the survival of neuronal cells after implant is a crucial aspect. Unfortunately, at the site of microelectrode insertion there is a decrease of neuronal density due to the trauma of implantation and to the glial scar formation that cause a

distancing of neurons from the recording area. The neuronal distribution at the interface is shown in **Figure 14A** and the result of the quantitative analysis of neuronal loss in function of distance from the implant is shown in **Figure 14B** and **Table 4**.

Compared to the non-penetrated tissue, there is a statistically significant reduction in NeuN density within ~100 µm from both coated and uncoated microelectrodes insertion area (for each time point) and this decreased neuronal immunoreactivity is more pronounced when comparing the uncoated probe to the background. In addition, a significant difference in NeuN count between coated and uncoated microelectrodes tissue implanted is present after 6 weeks. The neuronal displacement is inevitable following probe insertion, but the development of electrodes capable to maintain a close contact with neurons is fundamental. This data suggests a good interaction between the endothelial cells laying over the microelectrodes and the neurons in the surrounding tissue and this result is very promising in view of the use of bio-hybrid electrodes in chronic recording session.

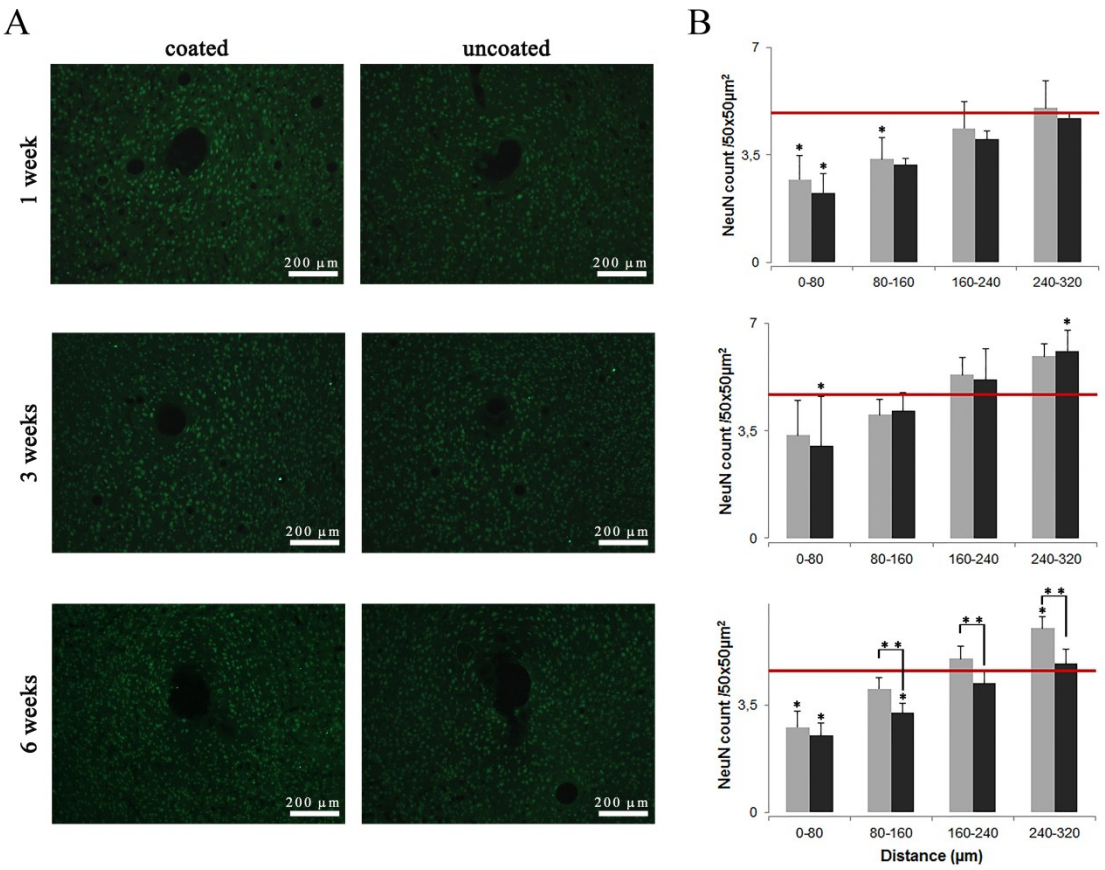

Figure 14. (A) Representative fluorescence images of NeuN immunolabeling showing neuronal nuclei density near the implanted microelectrodes at the different time points analyzed. (B) Normalized neuronal density expressed as NeuN count per area (50x50 µm^2) as a function of the distance from the implant with standard error. Each bar refers to the average number of NeuN nuclei of 4 implants/group + SD. Gray bars = coated microelectrodes; Black bars = uncoated

microelectrodes. The red lines show the mean value of neuronal nuclei counts within non-penetrated tissue regions. (*) = *p value* < *0.05* with respect to the background; (**) = *p value* < *0.05* coated vs uncoated.

	1 week	**3 weeks**	**6 weeks**
Coated vs Uncoated			
0 to 80 µm	0.2076	0.3976	0.1296
80 to 160 µm	0.6229	0.5883	*0.0005**
160 to 240 µm	0.5063	0.5597	*0.0020**
240 to 320 µm	0.5078	0.5510	*0.0075**
Coated vs Background			
0 to 80 µm	*0.0032**	0.0664	*0.0159**
80 to 160 µm	0.0759	0.2614	0.2501
160 to 240 µm	0.4610	0.1726	0.2760
240 to 320 µm	0.8384	0.0692	*0.0138**
Uncoated vs background			
0 to 80 µm	*0.0006**	*0.0439**	*0.0073**
80 to 160 µm	*0.0256**	0.1541	*0.0539**
160 to 240 µm	0.1236	0.2182	0.2748
240 to 320 µm	0.7638	*0.0159**	0.6160

Table 4. Statistical comparisons for neuronal nuclei (two-sample unrelated two-tailed t-test; * = *p value* < *0.05*)

3. CONCLUSIONS

A number of research groups has reported about bio-electrodes and the different ways to reach a higher biocompatibility facing the problems related to intracortical microelectrodes applications but none of them report a real application.

Here, for the first time, we present fully functional bio-hybrid electrodes, characterized regarding both electrochemical and immunological properties. We provide a new method to manufacture a bio-hybrid device starting from standard microelectrodes and modifying the probe surface with a living cell coating.

Thus, instead of approaching the issue by creating ex-novo bio-electrodes, we chose to improve the performance in terms of biosafety of existing devices. In literature, some papers consider the use of neuronal and non-neuronal cells such as microglia and astrocytes, in general aiming to replace the death and loss of cellular populations originated from the probe insertion trauma. Conversely, we used primary endothelial cells from rat aortic rings to wrap and create a vessel-like structure around the microelectrodes. The neural tissue is highly vascularized and this bio-hybrid aims to mimic the biological environment, deceiving the cells involved in the inflammatory response in order to prevent the FBR that is the main responsible of the intracortical microelectrodes failure over time. Endothelial cells have the ability to proliferate and organize in tubular structures and, starting from the work of Yevick *et al.*, we developed a method to cultivate endothelial cells directly adhering to the wires. Plating endothelial cells upon silicone slab, they were able to proliferate around the entire length of the microwires aligned on the edge of the support and in few days a bio-hybrid electrode is made. Moreover, with this approach the quantity of cells adhering to the wire was much higher than using a suspension cell culture as previously reported. At the beginning, the growth method was tested using polyimide capillaries and different types of electrodes insulating materials. The promising results obtained, led to the use of Thomas Recording microelectrodes, in-house manufactured, in order to create real working bio-hybrid electrodes, highly biocompatible and tissue integrated. We have successfully extracted endothelial cells from the rat aorta, that is an abundant source of this kind of cells, easy to recover and to culture in vitro. In this work we used heterologous cells but there are good perspectives for clinical and translational application, since there are several accessible sources to gather autologous cells from a human subject. We decided to use endothelial cells since the principal aim was to mimic the biological environment present in the brain instead of the possibility to restore some damaged group of neurons.

The analysis of tissue response to chronically implanted coated and uncoated microelectrodes showed a good reduction of brain tissue damage for the cell-coated microelectrodes in comparison to bare wires. We used histological techniques to assess the FBR since it represents the major method adopted in literature[17–19]. In particular, we focused on the GFAP reaction. As the glial cells play a key role in the development of the inflammatory response it is possible to follow the FBR progress analyzing the change in morphology of these cells and the expression level of the GFAP. We monitored the body reaction at different time points to be able to make a "snapshot" of the cells behavior at the critical FBR phases (acute - 1 week, progressive - 3 weeks and chronic/persistent - 6 weeks phases).

In conclusion, our results indicate that chronic tissue response could be reduced using a new kind of device, cell-friendly and highly biocompatible. Moreover, we tested the functionality of this kind of electrodes, providing good prospects for their future clinical use. Further research should be done to improve the cellular coating as well as to apply the technique to other types of intracortical probes. To this end, we are currently optimizing the isolation and culture protocol of brain microvascular endothelial cells that should allow the possibility of recreating an endothelium similar to that of the blood-brain barrier and thus to develop a totally seamless device.

BIBLIOGRAPHY

1. Klueh, U. *et al.* Enhancement of implantable glucose sensor function in vivo using gene transfer-induced neovascularization. *Biomaterials* **26,** 1155–1163 (2005). doi:10.1016/j.biomaterials.2004.04.017

2. Rejali, D. *et al.* Cochlear implants and ex vivo BDNF gene therapy protect spiral ganglion neurons. *Hear. Res.* **228,** 180–187 (2007). doi:10.1016/j.heares.2007.02.010

3. Prichard, H. L. *et al.* IFATS Collection : Adipose-Derived Stromal Cells Improve the Foreign Body Response. *Stem Cells* 2691–2695 (2008). doi:10.1634/stemcells.2008-0140

4. Kennedy, P. R. The cone electrode : a long-term electrode that records from neurites grown onto its recording surface. *J. Neurosci. Methods* **29,** 181–193 (1989).

5. David, S. & Aguayo, A. J. Axonal Elongation into Peripheral Nervous System ' Bridges ' After Central Nervous System Injury in Adult Rats. *Science (80-.).* **214,** (1981).

6. Kennedy, P. R. & Bakay, R. A. E. Activity of single action potentials in monkey motor cortex during long-term task learning. *Brain Res.* **760,** 251–254 (1997). doi:10.1016/S0006-8993(97)00051-6

7. Kennedy, P. R. *et al.* Direct control of a computer from the human central nervous system. *IEEE* (2000). doi:10.1109/86.847815

8. Kennedy, P. R. & Bakay, R. A. E. Restoration of neural output from a paralyzed patient by a direct brain. *Neuroreport* **9,** 1707–1712 (1998).

9. Kennedy, P. R. *et al.* Computer Control Using Human Intracortical Local Field Potentials. *IEEE* **12,** 339–344 (2004). doi:10.1109/TNSRE.2004.834629

10. Cui, X. *et al.* Surface modification of neural recording electrodes with conducting polymer / biomolecule blends. *Journal of biomedical materials research.* (2001).

11. Richter, A. *et al.* Cellular modulation of polymeric device surfaces : promise of adult stem cells for neuro-prosthetics. *Front. Neurosci.* **5,** 1–10 (2011). doi:10.3389/fnins.2011.00114]

12. Juarez-hernandez, L. J. *et al.* Bio-hybrid interfaces to study neuromorphic functionalities : New multidisciplinary evidences of cell viability on poly (anyline) (PANI), a semiconductor polymer with memristive properties. *Biophys. Chem.* **208,** 40–47 (2016). doi:10.1016/j.bpc.2015.07.008

13. Purcell EK. *et al.* In vivo evaluation of a neural stem cell-seeded prosthesis. *J. Neural Eng.* **6,** (2009). doi:10.1088/1741-2560/6/2/026005

14. Azemi E. *et al.* Seeding neural progenitor cells on silicon-based neural probes. *J. Neurosurg.* **113,** 673–681 (2010). doi:10.3171/2010.1.JNS09313

15. Yevick, H. G. *et al.* Architecture and migration of an epithelium on a cylindrical wire. *PNAS* **112,** (2015). doi:10.1073/pnas.1418857112

16. Williams, J. C. *et al.* Complex impedance spectroscopy for monitoring tissue responses to inserted neural implants. *J. Neural Eng.* **4,** (2004). doi:10.1088/1741-2560/4/4/007

17. Lee, H. C. *et al.* Histological evaluation of flexible neural implants ; flexibility limit for reducing the tissue response ? *J. Neural Eng.* **14,** (2017). doi:10.1088/1741-2552/aa68f0

18. Ersen A. *et al.* Chronic tissue response to untethered microelectrode implants in the rat brain and spinal cord. *J. Neural Eng.* **12,** (2015). doi:10.1088/1741-2560/12/1/016019

19. Winslow, B. D. & Tresco, P. A. Quantitative analysis of the tissue response to chronically implanted microwire electrodes in rat cortex. *Biomaterials* **31,** 1558–1567 (2010). doi:10.1016/j.biomaterials.2009.11.049

CHAPTER 2

HOW FLEXIBILITY AND PROBE SIZE INFLUENCE CHRONIC PERFORMANCE: *IN VIVO* STUDY ON POLYIMIDE-BASED INTRACORTICAL ARRAYS

For short and long term neural applications, it is desirable to reduce or ideally eliminate the foreign body response to the implanted devices. As already discussed, different approaches exist to minimize this issue. If, on the one hand, this improvement can be achieved by exploiting biological approaches as described in Chapter 1, another way to do so comes from material science and involves minimizing the size of the device and the bending stiffness of the implant affecting the soft brain tissue.

One of the main problems that hinders the sustained functionality of neural devices is indeed the mechanical mismatch between the soft neural tissue and the rigid neural probe, which results in initial local trauma that leads to the establishment of the inflammatory response. To overcome this issue, materials with lower Young's moduli (E) than that of the traditional silicon, for example polyimide (E ~ 2.5 GPa[10]) and paryleneC[1] (E ~ 2.8 GPa[11]), have been employed as probe substrate. Polyimide is a very promising material since it is thermally stable, mechanically durable, non-cytotoxic and biocompatible[2,3], although not yet approved by FDA. However, it should be noted that these materials are still six order of magnitude stiffer than the brain tissue (E ~ 5.51 kPa[12]). A more tissue-compliant device could be also obtained combining flexible materials with smaller overall dimensions of the probe. On the other hand, when the thickness of the polymer neural probe is reduced to diminish the encapsulation problem, the neural probe becomes extremely flexible. Stiff backbone layers[4], insertion shuttles[5] and biodegradable material coatings[6] have been employed to allow soft devices to be implanted into the brain and reach the desired position within the neural tissue.

Recent findings in the field of neural engineering have led to the development of ultra-thin and ultra-flexible intracortical electrode arrays, aiming to become "invisible" to the host tissue and unable to trigger a noticeable immune response in long-term applications[7,5]. However, reduced probe size comes at the cost of fewer individual electrodes, more challenging handling and fabrication, as well as mechanical properties less suited for

chronic *in vivo* experiments. It is therefore important to better understand which design parameters offer the best trade-off.

Among the several features that have been identified as useful for establishing a reliable neural-probe interface that minimizes the glial scar formation, one of the most important ones is the probe size, that should be comparable to that of cells and capillaries to reduce host perturbation[8]. Another key feature is device flexibility, that should be sufficient to permit maximal compliance to the brain tissue micromovements and minimal damage during insertion to allow for tissue recovery. Lastly, but maybe most importantly, the probe needs to be mechanically and electrically functional and robust for long-term operation under physiological conditions.

In this chapter, I compare two kinds of polyimide-based electrode arrays which differ only in their width: one kind is only 30 μm wide while the other has a width of 100 μm. Both device types are 12 μm thick and display electrodes 20 μm in diameter, spaced so that they target each one of the six cortical layers in rats. The devices were chronically implanted into the brain of adult rats and different time points were selected for immunohistochemical evaluation and quantification of the differences of the immune response elicited in the brain. Some of the probes were also used for long term recordings of electrophysiological activity. The wider probes (100 μm width) featured a pair of identical electrodes per cortical layer (instead of a single one) with the aim to achieve a better reconstruction of the neuronal configuration and status around the probe.

The work aims to systematically investigate the influence of selected geometrical parameters on the performance of thin-film polyimide based neural prostheses *in vivo*. The study is part of a larger project (CAPRI project) which involves different research groups and has started during my period abroad at the Albert Ludwing University Medical Center in Freiburg (Germany). The project is focused on a long-term investigation of the mechanical, electrochemical, cellular and molecular changes at the interface between implanted probes and brain tissue. It involves a multi-scale approach including implant manufacturing and pre-clinical *in vivo* probe implantation and testing, histological and cellular analysis of the tissue reactions and subcellular and molecular approaches to identify key molecules, e.g. genes, proteins and factors, responsible for the tissue injury. The goal is to better understand the signals that lead to neuroglial activation and find ways to perform targeted intervention to control the glial response, reduce reactions and maintain an ideal environment for the brain-electrode interface. Thus, CAPRI is fully dedicated to the probe/tissue interaction challenge and is designed to make a significant progress in this particular field by finding a clear answer to the question “how small does a

neural probe have to be to become invisible for the host tissue and yet remain capable of recording long-term high-quality signals?". In particular, in this chapter I will focus on the glial response evaluation and on the ability of these small devices to record neuronal signals in chronic *in vivo* experiments.

1. EXPERIMENTAL SECTION

All the experimental procedures were carried out in accordance with the guidelines established by the European Communities Council (Directive 2010/63/EU of September 22nd, 2010).

1.1 ELECTRODES FABRICATION AND DESIGN

Briefly, in collaboration with the Institute of Microsystem Technology in Freiburg, the fabrication of the devices (**Figure 1**) starts with the spinning of the first polyimide layer (U-Varnish-S, UBE, 4 µm) and the subsequent lithography step for patterning the first metallization layer (first layer of tracks, MET1). After, the first metal deposition is performed (100 nm of evaporated Pt) and the metal layer is insulated by a second PI layer (PI2, additional 4 um). Second metallization (additional tracks, MET2, again 100 nm of Pt) and a third PI layer (PI2, insulation for MET2, 4 µm) follow using the same protocol used for MET1 and PI2. Then, a photoresist (AZ 9260) is used to create the pattern for the devices' outlines and vias/access to the two metal layers underneath. Reactive-ion etching (RIE) is used to etch away the unwanted PI and, finally, the last metallization layer (MET3) is performed to create the electrode pads and make contact to the metal tracks underneath. Polyimide is always the outer layer.

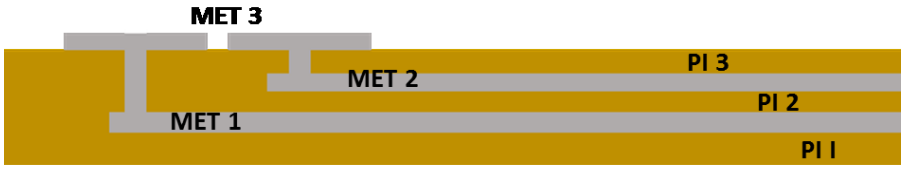

Figure 1. Capri device fabrication method. Metallization layers (MET 1-2-3) and polyimide layers (PI 1-2-3) are shown in gray and yellow respectively.

The two prototypes of polyimide-based electrode arrays (**Figure 2A**) differ only in their width: one kind is only 30 µm wide while the other has a width of 10 µm. Both device types are 12 µm thick and display electrodes 20 µm in diameter, spaced so that they target each one of the six cortical layers (**Figure 2B**) but the wider probes (100 µm width) featured a pair of identical electrodes per cortical layer while the tight one presents only six electrodes, one per neural level. The insertion hole at the end tip is designed to allow the

insertion into the brain with a shuttle device while a “big” metal pad (red rectangles in the sketches) is a reference mark for stopping the implantation at a controlled depth.

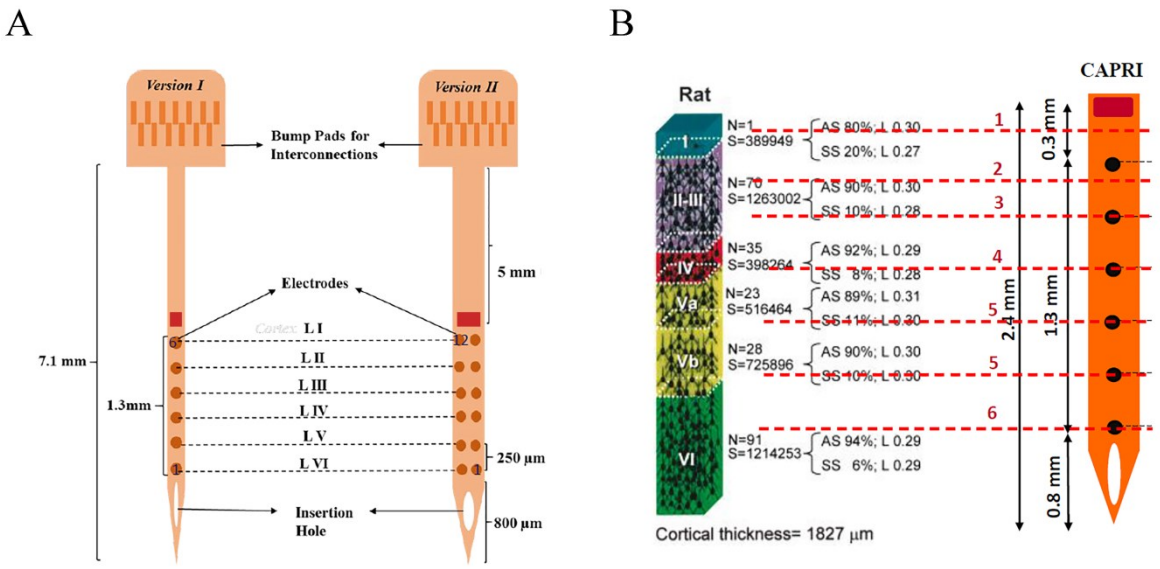

Figure 2. Capri prototypes and specifications. (A) Sketch of 100 µm and 30 µm wide devices showing probes specifications. (B) Schematic images showing the correspondence of the rat cortical layers with the electrodes placement.

1.2 Electrochemical characterization of the electrodes

The electrochemical properties of the 100 µm or 30 µm wide devices were studied via EIS in a physiological aqueous solution (0.9% NaCl) before implantation. During the EIS measurements, a sine wave (10 mV RMS) was superimposed onto the open circuit potential while varying the frequency from 10 to 10^5 Hz. The electrochemical characterization was carried out using a potentiostat/galvanostat (Reference 600, Gamry Instruments, USA) connected to a standard electrochemical cell used in a three-electrode configuration with a platinum counter-electrode and an Ag/AgCl reference electrode.

1.3 Animal surgery and array implantation for histological evaluation

To evaluate the foreign body reaction to 100 µm or 30 µm wide arrays, six Long Evans rats were used, two for each fixed time point (1, 2, 4 weeks) and two more animals, used for the recording sessions, were histologically analyzed after 16 weeks from the implant.

All rats were anesthetized with a mixture of Zoletil (Virbac, France; 30 mg/kg) and Xylazine (Bayer, Germany; 5mg/kg) administered intraperitoneally (i.p.). For the entire duration of the procedure, the depth of anesthesia was monitored by testing the absence of hind limb withdrawal reflex and was maintained by additional i.m. doses of anesthetic. The body temperature was maintained at 37–38 °C with a thermostatically controlled heating pad and lacrigel (Farmigea, Italy) was placed on the eyes to avoid dryness. After shaving and swabbing the head with ethanol, the anesthetized animal was placed in a stereotaxic apparatus (David Kopf Instruments, USA) equipped with Ear Bars (Model957 for small animals). An approximately 2 cm long incision was made along the midline of the cranium. The underlying muscle and connective tissue were retracted to expose the skull. A small craniotomy was made in both the hemispheres and a total of four arrays, two 100 μm arrays and two 30 μm arrays were inserted in each hemisphere. Sterile saline solution was applied while drilling to avoid any local heating and to keep clean the bone surface. The exposed dura mater was wetted with saline and carefully incised using surgical micro-scissors and the tip of a 24 G syringe needle to produce an opening both in the dura and in the pia mater that allows device penetration reducing pressure over the brain.

According to the manufacturer sheet, both types of device were stereotaxically inserted to a depth of about 2.5 mm: a big metal pad for halting the insertion allowed to precisely target the six cortical layer with each electrode (or couple of electrodes in the case of 100 μm array). In these procedures, the flexible neural probes were placed on the brain surface where dura and pia mater were previously removed. The shuttle device, a 80 μm diameter quartz wire, was vertically mounted on a stereotaxic arm and positioned over the insertion hole at the end of the probe. As the shuttle device traveled downward, it entered the hole and pulled the array into the brain tissue. Once the probe reached the desired depth, the shuttle device was retracted and the flexible array was released and left embedded into the brain tissue. The delivery process is extremely delicate due to the small size of both the devices and it needs to be well controlled and precise to avoid initial tissue damage. After insertion procedures, the surface of the implanted tissue was protected using Kwik-Sil silicone polymer (World Precision Instruments Inc, USA) and the skin was sutured.

1.4 HISTOLOGY AND QUANTITATIVE ANALYSIS

In order to investigate the foreign body reaction against the implanted arrays, immunohistological methods were used at 1, 2, 4 and 16 weeks after both 100 µm and 30 µm devices insertion. At the end of the determined time course, the animals were maintained deeply anesthetized and transcardially perfused with 300 ml of 0.9% saline solution at room temperature followed by 500 ml cold fixative solution of 2.0% paraformaldehyde, 1.25% glutaraldehyde and 2.0% sucrose (all from VWR, USA), prepared in 500 ml of 0.1 M sodium phosphate buffered solution (PBS, pH,7.4). Brains were then removed, post fixed overnight at 4 °C and placed in a 30% sucrose-buffered solution until they sank. They were then frozen and 50 µm-thick horizontal sections were cut using a sliding microtome (SM2000R; Leica Microsystems, Canada). The brain sections were stained to label the principal cell lines involved in the inflammatory tissue reaction using antibodies directed against reactive astrocytes detected by the production of glial fibrillary acidic protein (GFAP); activated microglia/macrophages detected by the membrane- bound CD68-antigen (clone-ED1); neuronal nuclei (NeuN) and total number of cell nuclei (DAPI). The adjacent sections were divided into two series, treated with blocking solution consisting of 4% (v/v) normal goat serum (Sigma Aldrich, USA), 0.5% (v/v) Triton-X-100 (Sigma Aldrich, USA), 2%(w/v) bovine serum albumin (BSA)(Sigma Aldrich, USA) in PBS for 1 h and then incubated in the primary antibodies overnight at room temperature. The first series was stained using mouse- anti-ED1 (1:300, Millipore, USA), while the second one using mouse-anti-GFAP (1:500, SigmaAldrich, USA) and rabbit-anti- NeuN (1:200, Millipore, USA). After 3 rinses in PBS (10 min per rinse) the sections were incubated with the anti- rabbit Alexa-488 and anti-mouse Alexa-568 conjugated secondary antibodies (1:500, Thermo Fisher Scientific, USA) for 3 hours in the dark, at room temperature. All mentioned antibodies were diluted in the blocking solution. Finally, after washing 3 times in PBS, the two series of sections were mounted separately onto microscope slides, counterstained with ProLong Gold Anti fade Mountant containing DAPI (Thermo Fisher Scientific, USA) and covered with a coverglass. The staining was observed using an Olympus BX51 microscope (Melville, USA) with 10×, 20× objectives (Olympus, Japan) and equipped with a X-Cite 120 fluorescence microscopy illumination system (EXFO, Canada) and a color videocamera CX-9000 (MicroBrightField, USA). The images of all the fluorescence tissue slices were acquired using NeuroLucida (MicroBrightField, USA) and ImageJ software (developed at the National Institutes of Health, USA) was used for the following analysis and to merge the different fluorescence

channels in order to obtain a single composite image for immunolabeling performed on the same slice (i.e. NeuN and GFAP staining).

Different horizontal sections were selected for each animal and image captured at different depths along the arrays penetration. Fluorescent images were captured under the same illumination level so that the overall background light intensities were comparable.
For astrocytes activation (GFAP expression) the following analysis was performed. For each image, three 500 x 50 μm rectangular shape windows (ROI = region of interest) starting from the edge of the hole created by the electrode were marked. The fluorescence intensity, directly related and proportional to glial activation, was then calculated as mean of the integrated density values of the 3ROIs per images and used to calculate the % increase of fluorescence after normalization with respect to the background (region far from the implant site). Furthermore, the staining intensities within the windows were quantified by averaging the pixel across the width of the rectangle and plotting them as a function of distance from the electrodes (longitudinal axis of the rectangle) using specific tools in ImageJ. A representative plot of the GFAP intensity over the distance for each time point was obtained. The tissue surrounding the probe was also characterized for the presence or absence of activated microglia/macrophage cells identified with ED1 immunostaining. GFAP immunoreactivity elicited by 100 μm and 30 μm devices was compared by a two-sample unrelated two-tailed t-test. The significance of the data was determinate at $p\ value < 0.05$.

1.5 ANIMAL SURGERY AND ARRAY IMPLANTATION FOR SIGNAL RECORDING

To test the ability of the devices to pick up neuronal signal, two Long Evans rats were used. We used for recording experiments only the 100 μm devices since they have a pair of identical electrodes per cortical layer (instead of a single one in case of 30 μm arrays), allowing to increase the statistical power. Indeed, the dimensions and properties of the electrodes of the two prototype arrays are the same. All the animals were treated as previously described. However, for chronic functional arrays implantation, the craniotomy was made on the left hemisphere and only one device for animal was stereotaxically inserted into the brain. In this case, the flexible neural probe was placed in contact with the brain surface where dura and pia mater were previously removed supported by a flexible arm attached to the connection board. At the same time, the shuttle device was vertically

mounted on a stereotaxic arm and positioned over the insertion hole at the end of the probe. As for the histological implants, the shuttle device traveled downward and as soon as it entered the hole, the array was pulled into the brain and inserted for about 2.5 mm inside the tissue. After implant, the tissue surface was protected using Kwik-Sil silicone polymer (World Precision Instruments Inc, USA) and the board support, excluding the connector used to interface it with the recording system, were cemented to the skull using dental acrylic (Jet Repair Acrylic; Lang Dental Manufacturing, USA). To hold in place the dental acrylic, four stainless steel screws were inserted into the skull and one of these was used as reference electrode. The skin was sutured around the cement, gentamycin cream (Mylan s.p.a., Italy) was spread over the wound and finally an antibiotic solution of Baytril 5% was administered (Bayer, Germany, 0.5 ml/10 Kg, i.m.).

1.6 *IN VIVO* IMPEDANCE MEASUREMENTS

The *in vivo* impedances of chronic implanted devices were analyzed through electrochemical impedance spectroscopy (EIS) using two electrodes configuration. The implanted intracortical arrays were referenced to a low impedance stainless steel bone screw inserted into the skull. The two-electrode method is suitable for measuring impedance performance from microelectrodes due to the large difference in impedance relative to the reference and the small current that passes through the circuit. During the EIS measurements, a sine wave (10 mV RMS) was imposed onto the open circuit potential while varying the frequency from 10 to 10^5 Hz. EIS was carried out using a potentiostat/galvanostat (Reference 600, Gamry Instruments, USA). Impedance spectra measurements were taken for each microelectrode of the arrays after each recording session from one to eight weeks after implant.

1.7 NEURAL RECORDING AND EVALUATION OF SIGNAL-TO-NOISE RATIO

Neural recordings from the six cortical layers were performed to characterize the electrical performance of the small and flexible arrays *in vivo*. Electrophysiological data were acquired using TDT RZ-2 Processor and PZ2 preamplifier (Tucker-Davis Technologies, USA). To connect the arrays to the headstage, a custom support for ZIF-Clip (Tucker-

Davis Technologies, USA) was designed. The acquired neural signals were sampled at 24.414 Hz and bandpass filtered from 10 to 5000 Hz. Recorded data were stored and analyzed off-line using the Off-line Sorter (Plexon Inc, USA) and NeuroExplorer (Nex Technologies, USA) software.

In chronic recordings, data were weekly acquired for 20 min during 8 weeks after implant. The spikes detection and the evaluation of the SNR were performed with specific tools using Offline sorter software. Each acquired trace was high-pass digitally filtered above 250 Hz. The signal was wavelet decomposed and thresholded to 3.5 standard deviations (SD) above and below the mean of the sample distribution to discriminate signal from noise. A specific tool (Threshold Scan Graph) was also used to systematically step the threshold and perform a waveform extraction at each threshold value, helping to adjust the correct trade-off between a large number of spikes and a high SNR.

Waveforms were clustered using T-Distribution E-M algorithm method (Off-Line Sorter, Plexon Inc, USA). All the spikes with inter-spike-interval (ISI) smaller than the refractory period (2 ms) were removed. The SNR is computed as the ratio of (sigma squared within signal)/(sigma squared within noise), where the “signal” is taken to be all samples within extracted spikes, and the “noise” is all samples outside of extracted spikes.

2. RESULTS AND DISCUSSION

2.1 IMPLANTATION OF SMALL AND FLEXIBLE POLYIMIDE-BASED ARRAYS

The most straightforward way to reduce the stress at the probe/tissue interface is to create devices made of soft materials such as flexible polymers since their lower Young's modulus reduces the mechanical mismatch with the brain tissue. Likewise, reducing substrate thickness and width leads to greater compliance and the buckling force is significantly reduced thus allowing the probe to fit more closely to the cerebral cortex. However, from the surgical point of view, the more the substrate is small and flexible, the harder it is to penetrate the brain. To overcome this difficulty, several approaches have been developed. Most shuttle devices used in previous studies had dimensions larger than 100 μm[9], which are larger than the dimensions of the CAPRI probes and resulted in unrecoverable damage and persistent scarring. In our case, both the 100 μm and the 30 μm arrays have been designed with an insertion hole at the end tip and a 80 μm quartz fiber as shuttle device was chosen to support the penetration (**Figure 3**). With this method we successfully inserted both types of probes inside the brain, with no visible damage during insertion procedure. Histological evaluation of the brain tissue response elicited by the arrays will be discussed later.

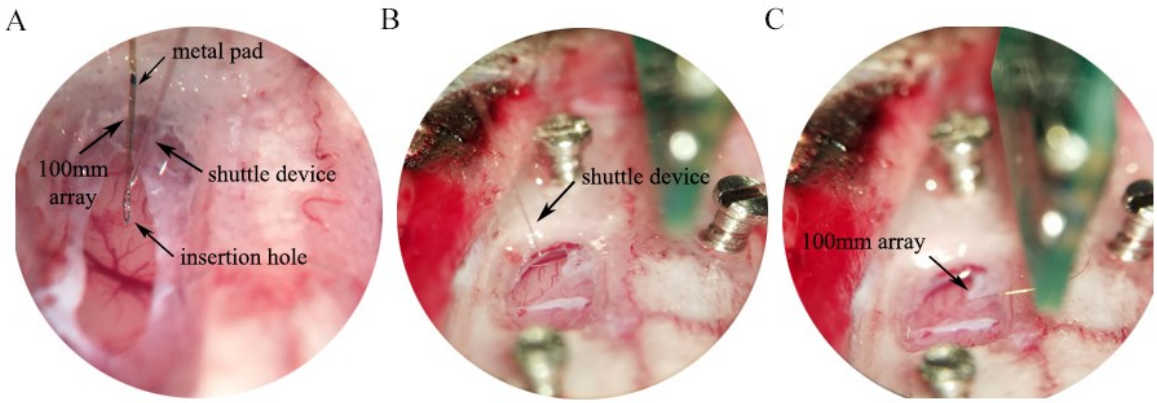

Figure 3. Representative images of implantation procedure for histological analysis (A) and for functional arrays recording analysis (B-C).

2.2 ELECTROCHEMICAL PROPERTIES OF SMALL AND FLEXIBLE ARRAYS

To evaluate the electrochemical performance of functional devices to use for chronic recording experiments, we performed the impedance spectrum measurement *in vitro* before implantation and after each recording session over eight weeks of implant. The impedance at 1 kHz is typically reported to predict neural recording performance[10] and as shown in **Figure 4A**, *in vitro* measurements reveal that all the small electrodes (20 µm in diameter) were good candidates for neural activity recording, with a mean impedance value of 6.47 ± 0.4 kΩ (n° total channels = 24). Indeed, typical materials used for recording electrodes including stainless steel, tungsten and platinum are tipically characterized by an electrical impedance that varies from approximately 50 kΩ to 1 MΩ. The mean impedance value calculated averaging all electrodes of two devices increases over time after chronic *in vivo* implantation (**Figure 4B**), reaching values between 1 MΩ and 10 MΩ after 8 weeks of implant. However, the electrodes were still working and they were able to record neural activity, as discussed below, while the rise of impedance could be associated with tissue remodelling and encapsulation that cause a decreased charge transfer between the electrode and the tissue.

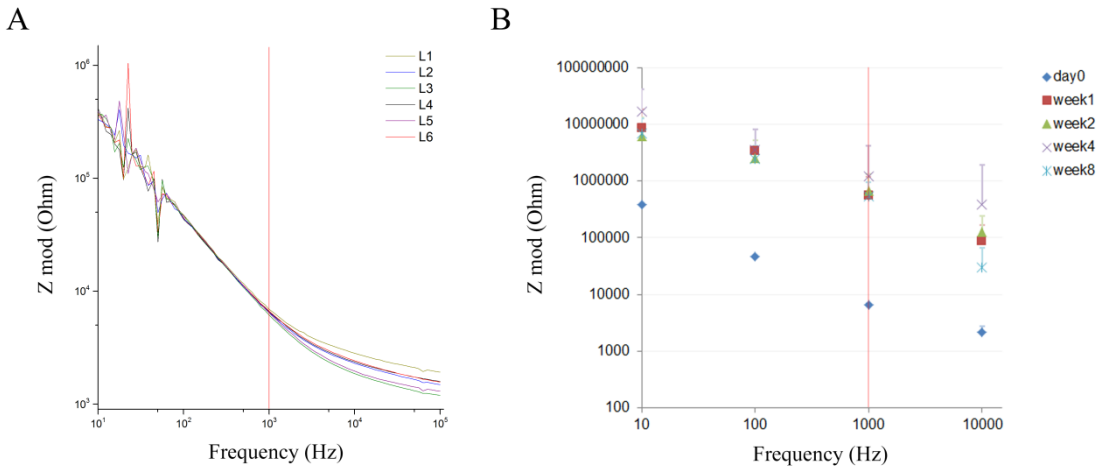

Figure 4. Electrochemical impedance spectroscopy. Impedance modulus (from 10^3 to 10^8 ohm), y-axis, with respect to the frequency window (from 10 to 10^5 Hz), shown in x-axis. (A) Representative impedance spectrum of one electrode per layer before array implant *in vitro*. (B) Mean impedance value (expressed in kΩ) ± standard deviation calculated *in vitro* (day0) and *in vivo* over time (week1-8) at 10kHz, 1kHz, 100Hz and 10Hz averaging the values of all channels of two devices (n=24). In A and B, the vertical red lines indicate the significant neurophysiological value of 1 kHz.

2.3 FUNCTIONAL PROPERTIES AND RECORDING QUALITY OF SMALL AND FLEXIBLE ARRAYS

In order to validate the recording capabilities of the flexible and small devices, two 100 µm arrays were chronically implanted within the cortex of two rats and 20 min of recording session were acquired weekly, up to 56 days, to allow spike sorting analyses. **Figure 5** reports high-pass filtered (cut-off 250 Hz) representative traces of spontaneous neural activity recorded *in vivo* with 100 µm array the day of implant (day 0) and at 7, 28 and 56 days after implant.

After the day of implant, where the spike amplitude appears lower due to the initial local trauma caused by the surgery and array penetration into the brain, the spiking activity remained relatively constant from 7 days to 8 weeks after implant.

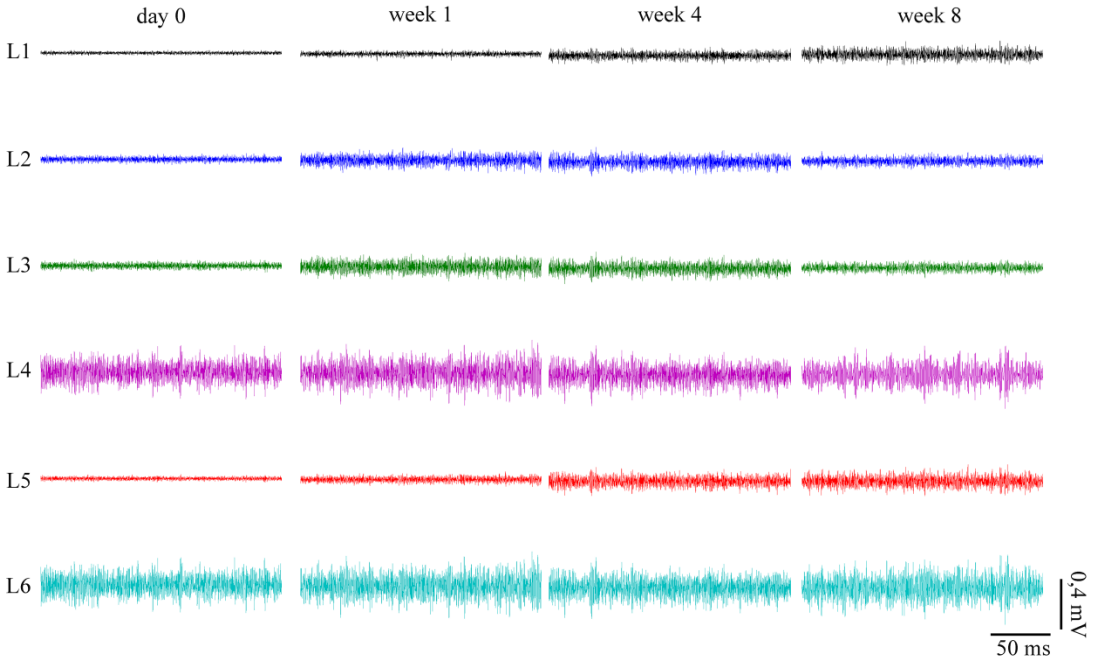

Figure 5. High-pass filtered (cut-off 250Hz) traces recorded from electrodes positioned at the six different cortical layers (L1-6) at different time points. The traces are representative of one electrode for layer followed over time.

One of the peculiarities of the arrays used in this study is the flexibility and the small dimensions flanked by a large number of functional electrodes. Indeed, each 100 µm device presents twelve electrodes, a couple of channels for each cortex neuronal layer and this could be useful to analyze the different behavior of neurons located at different levels. The ability of the two electrodes to pick up the same signal is graphically shown in **Figure 6,** that reports an example of the waveform comparison analysis performed for each channel in the array. Thus, the design of these ultra-small devices allows to record at the

same time from different neuronal populations and this ability is still visible after 56 days of implant.

Therefore, despite the small size, we were able to get a large number of functional electrodes and their defined position along the array opens the possibility to follow the behavior of single neuronal unit over time and to evaluate simultaneously how different neuronal populations could respond to specific treatments.

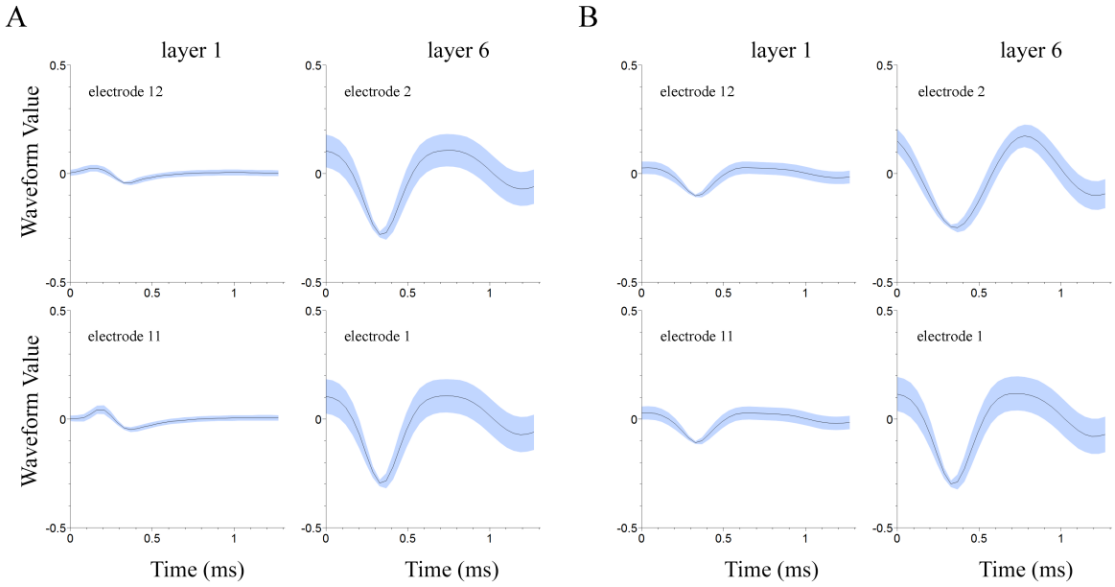

Figure 6. Action potential waveforms comparison. Representative images of the analysis performed for data recorded at 1 (A) and 8 (B) weeks after array implantation display the means (black line) and standard deviations (light blue background) of waveforms (1 ms = spike time window). In A and B, the couple of electrodes (12 - 11 and 2 - 1) of each layer is shown in two separate lines.

To quantify the recording quality of the electrodes, the signal-to-noise ratio was calculated over time for each layer of channels. The SNR is a common measure used to compare the level of a desired signal to the level of background noise and the higher is the ratio, the better is the recorded signal. As shown in **Figure 7A**, this value is near 2 with non negligible difference between different layers and it remains almost stable over time. However, a slight decrease is observed at one week from implant that could indicate the beginning of the inflammatory tissue response that could interfere with the signal detection. The spikes recording capability was also evaluated measuring the number of spikes detected over the duration of the recording session, reported in **Figure 7B**. Some differences can be noted between layers but the spiking activity remained relatively

constant from the day of implant to the eighth week with a small peak after 1 week. This high number is inversely proportional to the correspondent low SNR value and this is due to the fact that in this case many spikes were not so well distinguishable from the noise.

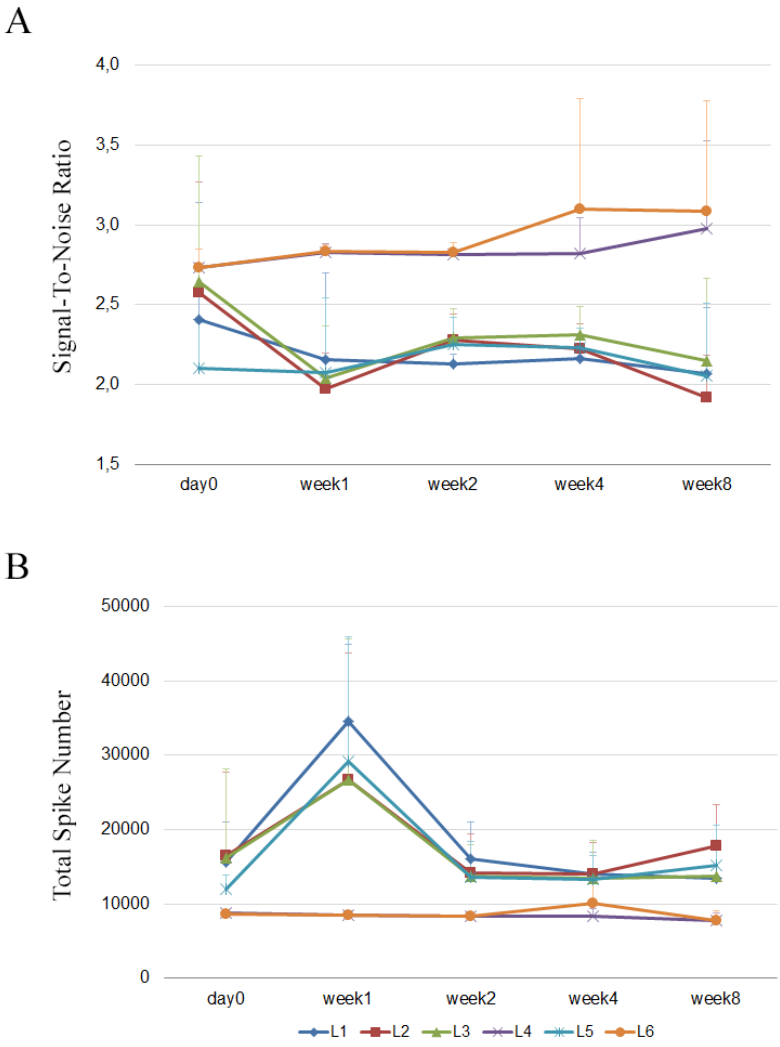

Figure 7. (A) Signal-to-noise ratio expressed as mean value per layer over two animals for each time point. (B) Mean values of spikes detected during the recording session (1200 sec) from two animals at implant day (day 0) and at 1, 2, 4 and 8 weeks after arrays implant.

2.4 IMMUNOFLUORESCENCE AND FOREIGN BODY REACTION

Immunofluorescence analysis was performed on four 100 µm and four 30 µm arrays at 1, 2, 4 and 16 weeks after implantation. The aim was to quantify the differences between the two devices in terms of immune response elicited in the brain and to verify the existence of a threshold, in terms of array thickness, below which the development of the glial scar becomes negligible.

The GFAP immunofluorescence is among the most used methods to assess the foreign body reaction since it directly correlates to glial cell activation and thus reflects the development of the inflammatory process.

After animals sacrifice, brains were removed and sectioned with the probe still inserted. This was possible due to the materials which the devices were made of, that could be easily cut by the microtome blade: the possibility to leave the device in situ during sectioning represents an advantage since limits the tissue damage due to probe extraction.

The immunofluorescence intensity of GFAP was measured with ImageJ software (see materials and methods for details), choosing three regions of interest starting from the device traces up to 500 µm away. The output results were used both to create representative intensity plots (**Figure 8**), useful for evaluating the extent of the glial response near the implanted site and to quantify the absolute GFAP immunoreactivity with respect to the background (region of brain distant from the track) and between 100 µm and 30 µm wide arrays.

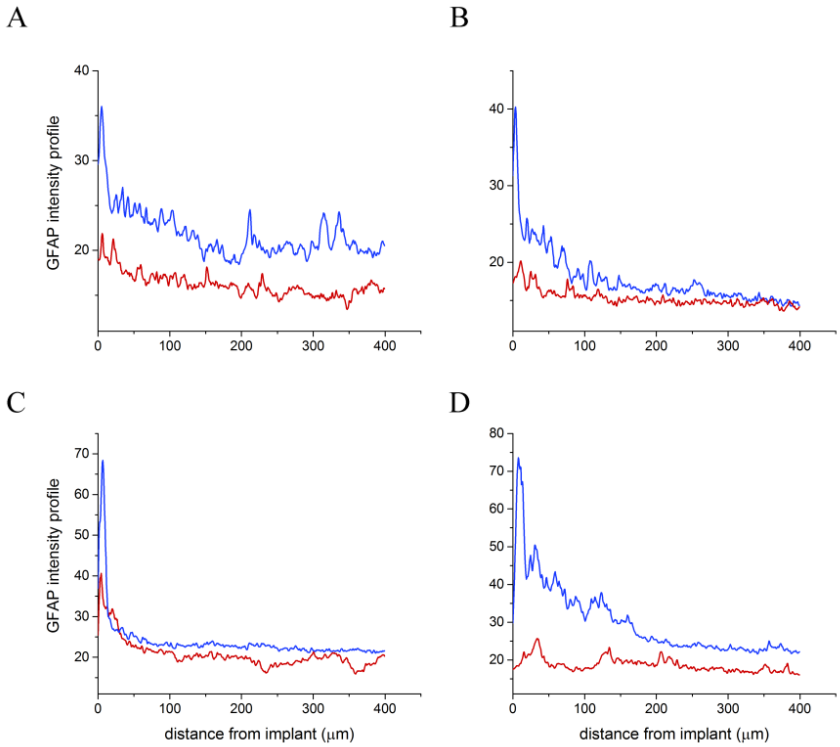

Figure 8. Graphs show representative GFAP intensity profile as function of distance from the implant at 1 week (A), 2 weeks (B), 4 weeks (C) and 16 weeks (D) after arrays implant. Red lines indicate the immunofluorescence profile in presence of 30 µm arrays, blue lines represent the intensity profile for 100 µm arrays.

As reported in **Figure 8,** at each time point analyzed, glial cells reactivity is localized 100 µm around the implant site while GFAP fluorescence intensity decays to background levels at a greater distance. This value however increases over time reaching the maximum intensity after 16 weeks for 100 µm arrays implants, meaning that also the foreign body reaction is at sustained levels. Moreover, differences in the GFAP intensity profile between 100 µm and 30 µm devices are visible at each analyzed time point. Interestingly, after more than 100 days from implant, the immune intensity profile of 30 µm arrays regresses to values similar to those found after the first week, indicating a weakening of the inflammatory response over time.

The absolute GFAP intensity values are reported in **Figure 9**. The 100 µm arrays elicit an immune response that slightly increases over the weeks and results statistically different from the one triggered by 30 µm arrays. The first two weeks after implant correspond to the acute immune response phase in which the glial cells are recruited near the site of implant and this cellular population become more reactive and compact over time with a visible increment of the fluorescence levels.

On the contrary, the GFAP expression levels in the presence of 30 µm devices are almost stable and moreover after 16 weeks of implant the immune response seems to be completely attenuated.

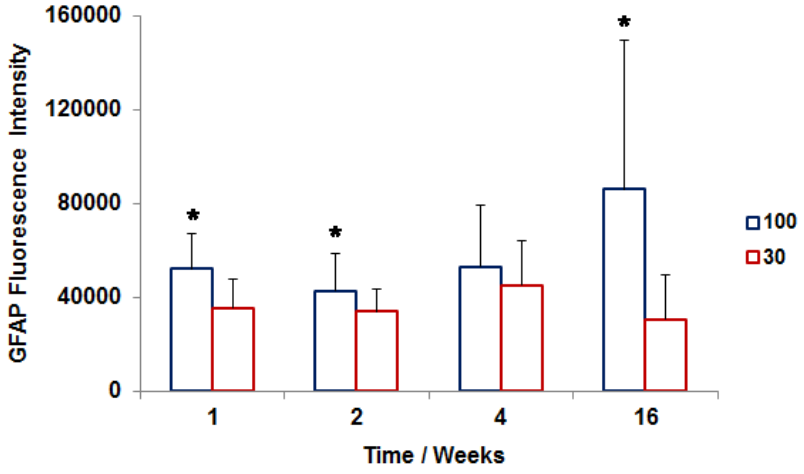

Figure 9. Quantitative analysis of GFAP immunoreactivity. The absolute GFAP fluorescence intensity values were calculated as mean of the integrated density values of the 3 ROIs per image, normalized with respect to the background. * *p value* < *0.05.*

The changes at the tissue-device interfaces were evaluated qualitatively by immunohistological imaging performed at 1 week, 2 weeks, 4 weeks and 16 weeks after implant. In the Figures 10-13 it can be noted the difference in behavior between the 100 µm and 30 µm flexible arrays. At high magnifications, reported on the right side of the panels, it is possible to clearly identify the different phases of the foreign tissue response (acute, progressive and chronic stages) and to highlight the morphology of the involved astrocytes. Indeed, while after 1 and 2 weeks the glial cells show ramified processes proximal to the electrode traces (**Figure 10** and **Figure 11**), after 4 weeks the astrocytes became more compact around the implant site (**Figure 12**) with the initial formation of the glial scar that is well visible and fully established after 16 weeks (**Figure 13**) from the implant of the 100 µm arrays.

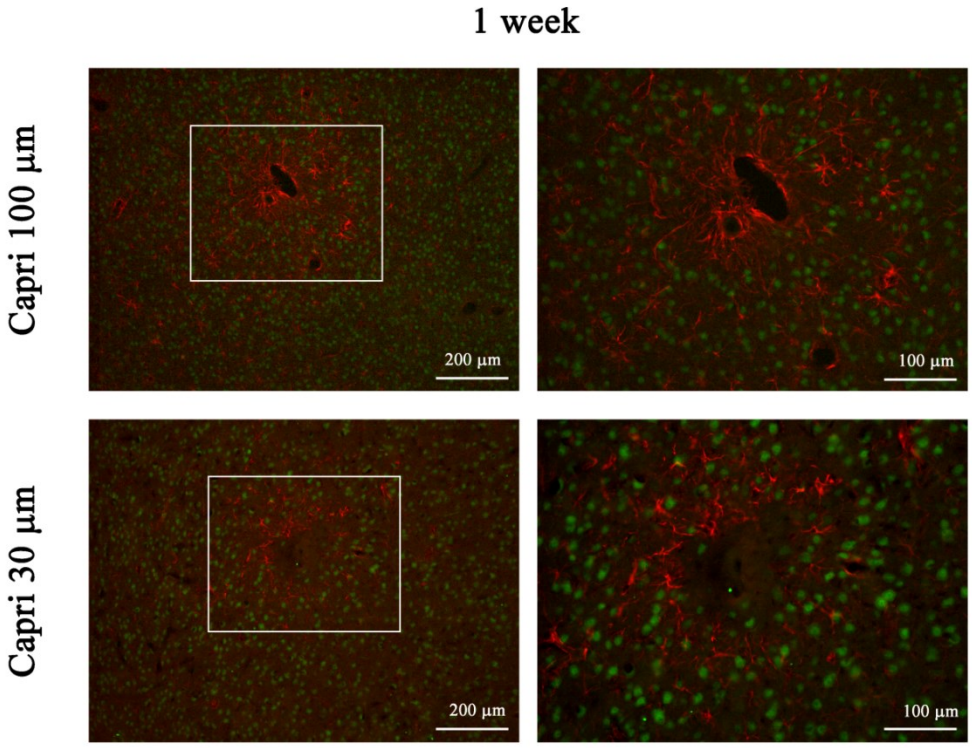

Figure 10. Immuno-histological staining for GFAP (red) and NeuN (green) at different magnifications after 1 week of implant with 100 µm or 30 µm flexible arrays.

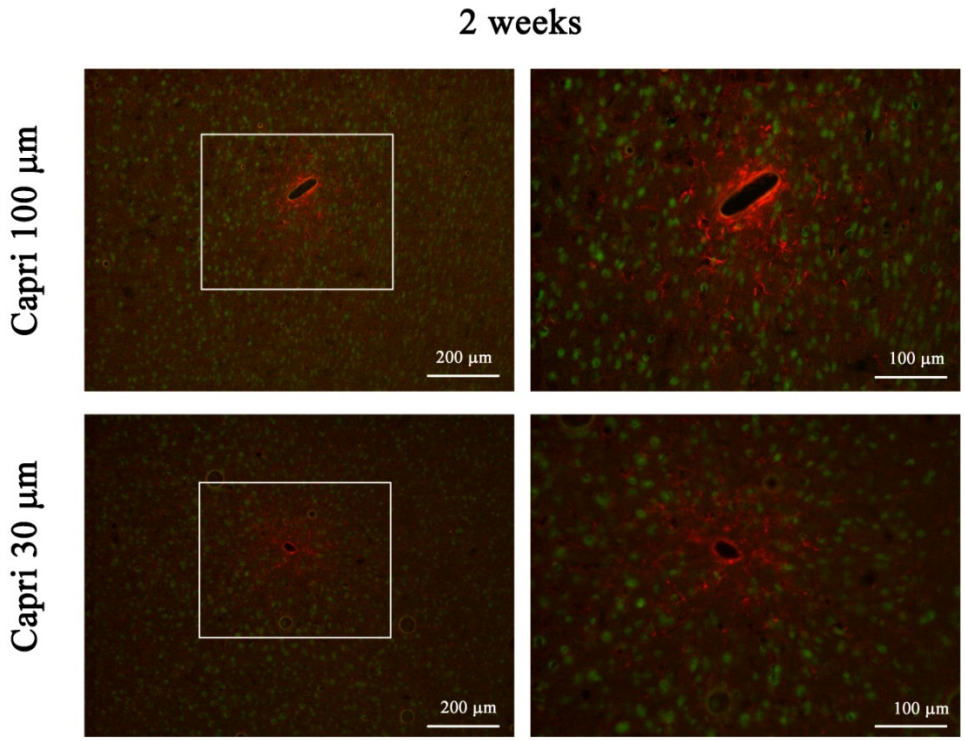

Figure 11. Immuno-histological staining for GFAP (red) and NeuN (green) at different magnifications after 2 weeks of implant with 100 µm or 30 µm flexible arrays.

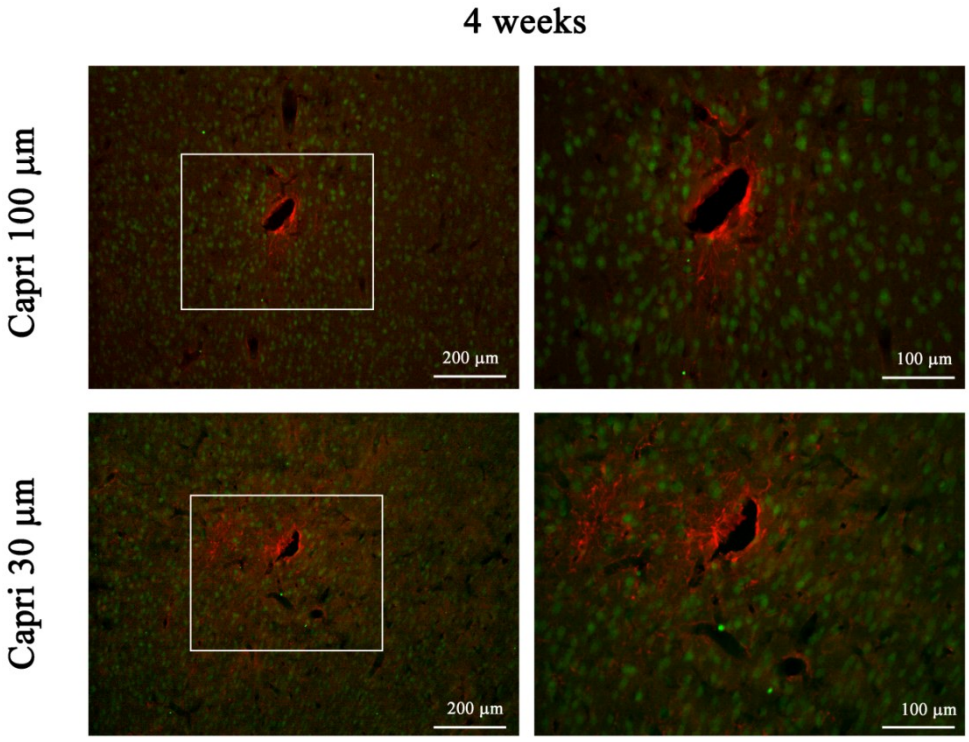

Figure 12. Immuno-histological staining for GFAP (red) and NeuN (green) at different magnifications after 4 weeks of implant with 100 µm or 30 µm flexible arrays.

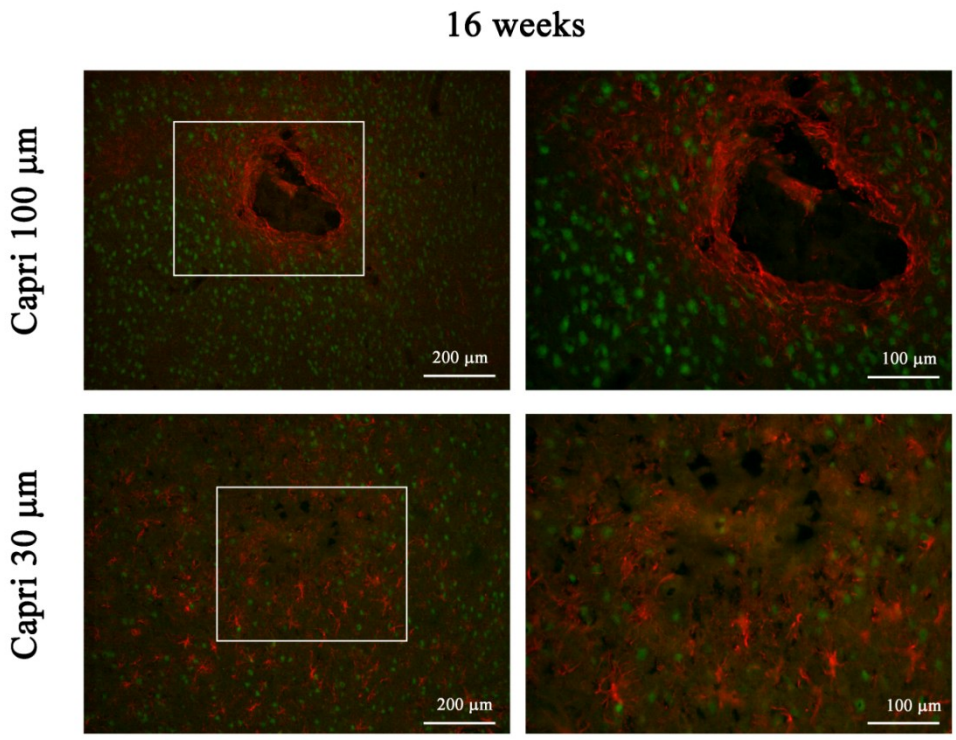

Figure 13. Immuno-histological staining for GFAP (red) and NeuN (green) at different magnifications after 16 weeks of implant with 100 µm or 30 µm flexible arrays.

The immunohistological staining after 16 weeks of implants revealed that the 30 µm arrays became almost "invisible" to the surrounding tissue. In fact, as shown in **Figure 13**, there is no evidence of scar tissue formation and also the astrocytes morphology appears more similar to the one of the early phase.

The brain tissue was also stained for the evaluation of activated microglia/macrophage cells identified with ED1 immunostaining. Few ED1-positive cells were observed at each time point in proximity of tracks for both types of array (**Figure 14**). Also in this case, at a chronic stage the difference between 100 µm and 30 µm arrays is clearly visible and the absence of ED1-positive cells is a further demonstration of the extremely reduced invasiveness reached with ultra-small devices.

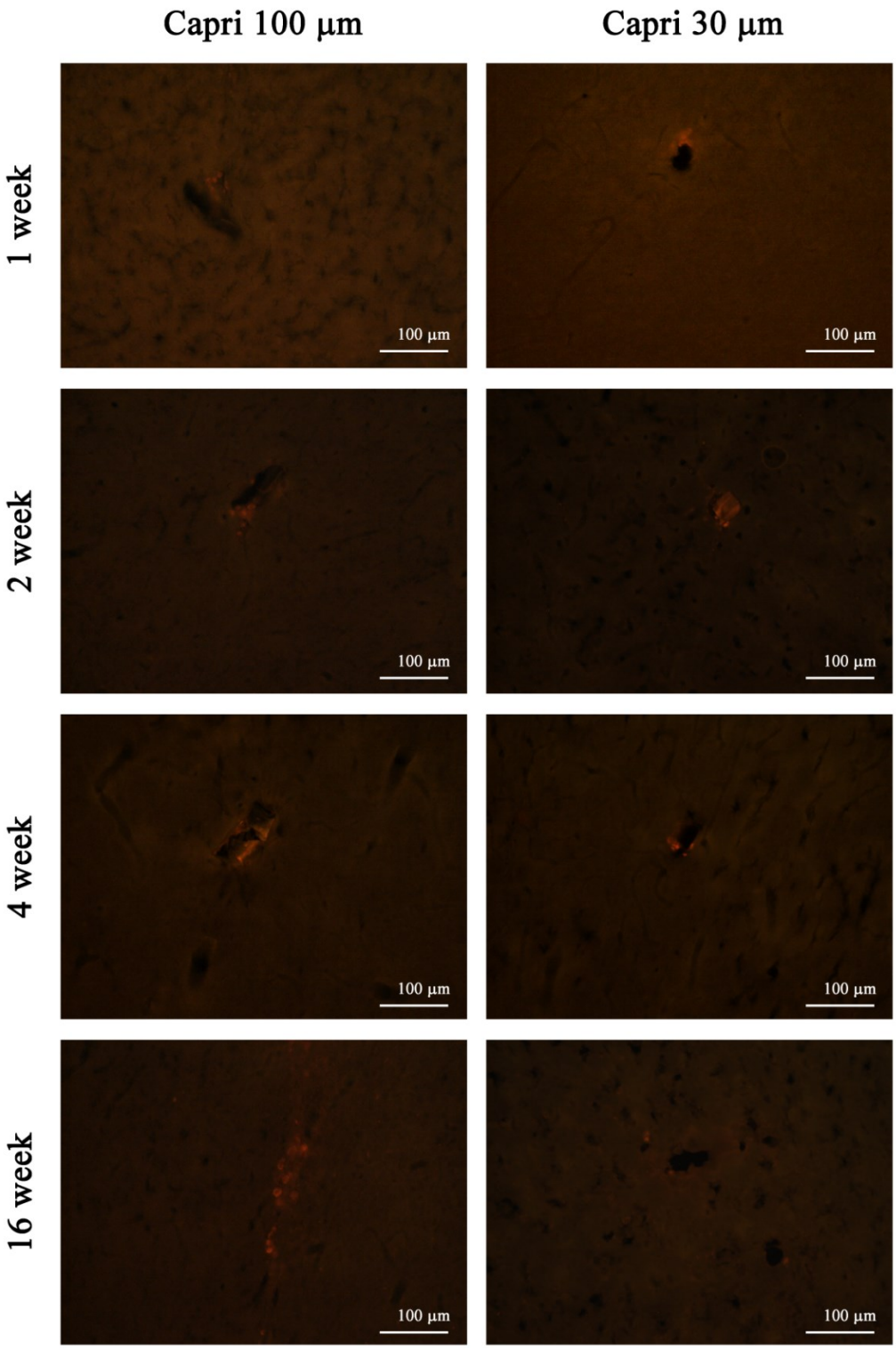

Figure 14. Immuno-histological staining for ED1-positive cells (red spots) after 1, 2, 4 and 16 weeks of implant with 100 µm or 30 µm flexible arrays.

3. CONCLUSIONS

In this work we have developed a protocol to produce hair-sized intracortical neural devices and we used these polyimide-based ultra-small and flexible arrays to evaluate both the foreign tissue response and the recording properties in *in vivo* chronic experiments, up to more than 50 days.

We have fabricated two kinds of array, both 12 μm thick, one 30 μm and the other 100 μm wide. Despite the small dimensions of the devices, they were featured with 6 and 12 electrodes 20 μm in diameter respectively that were ad-hoc organized in six layers to target the different cortex levels. Both devices are much smaller than traditional intracortical microelectrodes and their "invisibility" was tested *in vivo*, to define the threshold that combines the minimal foreign body reaction with a reliable and long-term stable functional implantation.

Initially, electrochemical measurements have provided an evaluation of the functionality of all the small electrodes and their ability to be used for neural recording application was assessed. Using our newly developed multilayer flex-probes we were able to obtain stable recordings over 8 weeks in rodent cortex and the spiking activity recorded over this time frame remained relatively constant. The signal picked up by different electrodes reflects the multilayer organization of neurons and this is a feature that could encourage the use of such arrays for studies that involve treatments in specific cortex areas. This chapter described the neurophysiological recording performed with the 100 μm arrays and these preliminary results are going to be implemented also with recording sessions using 30 μm arrays. Both types of device are characterized by electrodes with same specifications and thus, we expect to obtain promising, even better results also with the thinner arrays. It is known that changes at tissue level interfere with electrical and recording performance of implanted devices and the negligible inflammatory response elicited by the 30 μm arrays could be translated into good recording performance.

The inflammatory response surrounding the probes was quite higher for the 100 μm wide probes compared to the 30 μm arrays up to 4 weeks. Interestingly, after 16 weeks a substantial difference between the two array prototypes could be seen. While the 30 μm probe appeared to be seamlessly integrated, the tissue surrounding the wider probe exhibited the typical morphology of the glial scar. This could have a positive feedback in terms of signal picked up by the former devices.

Thus, even when devices are highly flexible and made thinner than a human hair, probe dimensions have still a substantial influence on the tissue surrounding the implant zone over longer times.

This work has provided preliminary results on the actual existence of a critical threshold in eliciting the FBR to chronically implanted intracortical neural devices, and at the same time has validated the possibility of developing very flexible and small but functional neural interfaces. Following these promising results, the project will continue testing also the recording capability of the 30 μm probes and to relate the functional performance of the electrodes with changes at the tissue/probe interface. Moreover, the tissue response will be thoroughly studied also at molecular level to identify the underlying molecular mechanism responsible for inducing scar formation, microglial reactivity or inflammation.

Indeed, although in the majority of studies immunostaining has been used to characterize the response of glial cells and the extent of cell death or cellular density in brain tissue surrounding the implanted electrodes, a more comprehensive study at sub-cellular level could provide interesting implications to direct the research into increasingly integrated neural interfaces systems.

BIBLIOGRAPHY

1. Kuo, J. T. W. *et al.* Novel flexible Parylene neural probe with 3D sheath structure for enhancing tissue integration. *Lab Chip* **13,** 554–561 (2013).

2. Stieglitz, T. *et al.* Flexible , Polyimide-Based Neural Interfaces. *IEEE* (1999). doi:10.1109/MN.1999.758853

3. Richardson R. R. *et al.* Polyimides as biomaterials : preliminary biocompatibility testing. *Biomaterials* **14,** (1993).

4. Seymour, J. P. *et al.* Novel multi-sided , microelectrode arrays for implantable neural applications. *Biomed. Microdevices* (2011). doi:10.1007/s10544-011-9512-z

5. Luan, L. *et al.* Ultraflexible nanoelectronic probes form reliable , glial scar – free neural integration. *Science Advanced,* **3,** (2017). doi:10.1126/sciadv.1601966

6. Xiang, Z. *et al.* Ultra-thin flexible polyimide neural probe embedded in a dissolvable maltose-coated microneedle. *J. Micromechanics Microengineering* **24,** (2014).

7. Du, Z. J. *et al.* Ultrasoft microwire neural electrodes improve chronic tissue integration. *Acta Biomater.* 46–58 (2017). doi:10.1016/j.actbio.2017.02.010

8. Seymour, J. P. & Kipke, D. R. Fabrication of Polymer Neural Probes with Sub-cellular Features for Reduced Tissue Encapsulation. *Conf Proc IEEE Eng Med Biol Soc*, 4606–4609 (2006). doi:10.1109/IEMBS.2006.260528

9. Kozai, T. D. Y. *et al.* Chronic tissue response to carboxymethyl cellulose based dissolvable insertion needle for ultra-small neural probes. *Biomaterials* **35,** 9255–9268 (2014). doi:10.1016/j.biomaterials.2014.07.039

10. Williams, J. C. *et al.* Complex impedance spectroscopy for monitoring tissue responses to inserted neural implants. *J. Neural Eng.* **4,** (2007). doi:10.1088/1741-2560/4/4/007

CHAPTER 3

BIOCOMPATIBILITY OF INNOVATIVE NEURAL ELECTRODE MATERIALS

To date, we discussed about different ways to deal with the chronic challenge, mainly aiming to improve the foreign body response elicited by implanted intracortical devices and carrying out interventions involving both material and biological sciences. Indeed, one of the main goals of my research was the design and development of new neural electrode generations, as much as possible bio-inspired, with reduced invasiveness, high resolution and sensitivity, functionally reliable and stable over time. Importantly, the great effort in improving the performance of traditional and novel microelectrodes has the final goal to translate research into medical applications. The same ultimate purpose of a *brain-machine interface* is to provide a practical support to human subjects affected by neurological diseases.

The performance of a medical device is controlled by two sets of characteristics, those which determine the ability of the device to perform the appropriate and specific function and those which determine the compatibility of the materials within the body. Indeed, as these devices have direct contact with the tissues and cells of the body, they not only require good physical and chemical properties, but must also have good biocompatibility.

Among the biocompatibility tests, the cytotoxicity assay is frequently used as a pilot project test and as an important indicator for the evaluation of medical devices as it is simple, fast, has a high sensitivity and can save animals from toxicity. The cytotoxicity test uses cells *in vitro* to observe the cellular growth and reproduction, detect the changes in the number of cells and morphological effects by the medical devices.

Referring to this, during the PhD school I was continuously involved in the study of cellular biocompatibility of different innovative devices and materials. In this chapter I will briefly report the scientific papers produced during these years, which highlight both the work done regarding the biocompatibility field (**3.1 – 3.4**) and the different approaches adopted to improve the performance of the intracortical electrodes (**3.5 – 3.6**), in addition to the two main projects previously discussed in detail.

Neural interfaces have intimate contact with the brain tissue, thus such devices should have a good interaction with the biological components, in order to limit the inflammatory reaction and toxicity. The in vitro study of biocompatibility is an important requirement for the safe use of implantable devices and cell culture systems are a simple but effective method that allows to directly measure the cytotoxicity and to determine the effect of a material on cellular growth. In order to verify the non-cytotoxicity of our new devices and substrate materials, cell viability assays were performed at different time points, before implantation into animal model, over several microelectrode arrays reported in the following works by monitoring fibroblasts survival and proliferation.

For each study, primary fibroblast cells were obtained from culture of adult rat tail specimens, according to the following procedure. Briefly, tail biopsies (≈1 cm in length) were obtained from the latter half of the intact tail after skin sterilization with 70% ethanol. Biopsies were further washed in PBS 1× (Thermo Fisher Scientific, US) and cut into small squares (2 × 2 mm approx.) under sterile conditions. Five to ten skin pieces were placed in the center of a six-well plate covered by a glass coverslip and cultured in advanced Dulbecco's modified eagle medium (Thermo Fisher Scientific, USA) supplemented with 10% fetal bovine serum (Sigma-Aldrich, Italy), 1% penicillin/streptomycin (Thermo Fisher Scientific, USA) and 1% L-glutamine (Thermo Fisher Scientific, USA) at 37 °C in a humidified atmosphere of 5% CO_2 in air. The medium was changed every 3 days. Upon confluence, the coverslips were removed and the cells were detached from the plate using 0.25% trypsin-ethylenediaminetetraacetic acid (EDTA) (Thermo Fisher Scientific, USA) 5 min at room temperature (RT). After centrifugation (1500 rpm, 5 min, RT) the cells concentration was established by counting them in Burker chamber using 0.4% Trypan blue (Thermo Fisher Scientific, USA) as vital dye. Fibroblasts were then plated on glass coverslips (control samples) or over the microelectrode array (devices) after surfaces sterilization for 30 min in 70% ethanol followed by washes with PBS. The cell viability was analyzed at different time points, established for each study, by triple staining with propidium iodide (PI; Sigma-Aldrich, Italy; 5 μg mL^{-1}), fluorescein diacetate (FDA; Sigma-Aldrich, Italy; 15 μg mL^{-1}) and Hoechst-33342 (Sigma-Aldrich, Italy; 3.3 μg mL^{-1}) 3 min at RT in Ringer–Locke solution. After incubation, samples were washed once in Ringer-Locke solution and immediately imaged. Dead cells were visible in red, viable ones appeared in green while total nuclei were stained in blue. Generally, at least ten different fields of view are acquired for each sample. Images were acquired using an Olympus BX51 fluorescence microscope (Melville, USA) equipped with X-Cite 120 fluorescence illumination system (EXFO, Canada), with a color CX-9000 digital camera

(MicroBrightField, USA) coupled with the NeuroLucida software (MicroBrightField, USA). Images were processed and merged using ImageJ (open source NIH image processing software). The percentages of surviving cells (mean ± standard deviation) were calculated based on the ratio of total (Hoechst-positive) nuclei minus PI-positive nuclei (dead cells) divided by the total nuclei. The obtained viability values were normalized with respect to the percentage of surviving cells observed over the respective control samples.
The significance of the data (*P value < 0.05*) was evaluated either using one-way ANOVA followed by the Bonferroni post hoc test or performing a two-sample (control and device) unrelated two-tailed t-test, depending on the experimental design.

Biocompatibility assays were mainly performed over different substrates like conductive polymer Poly(3,4-ethylenedioxythiophene) (PEDOT) and Glassy Carbon. They were found to be very promising materials for the development of neural interfaces both in terms of cytocompatibility, forming a dense layer of viable and proliferating cells, and electrochemical stability and mechanical properties, compared to conventional electrodes made of naked gold or platinum.
Moreover, we investigated the use of materials in combination with anti-inflammatory drugs such as Dexamethasone and the Tauroursodeoxycholic acid (TUDCA) and the biocompatibility of these composite materials was also tested. Several studies report the delivery of Dexamethasone from implanted substrates, while drug delivery systems based on the incorporation of TUDCA within conductive polymers has not been reported before, nor is its application as a potential anti-inflammatory agent for in vivo neural studies. However, it exerts anti-inflammatory activity by reducing microglia and astrocytes activation by involving the same activation pathway following neural device implantation and could thus represent an innovative and promising compound.
Indeed, aiming at modifying the biological environment rather than the probe itself, the delivery of anti-inflammatory drugs has been described as another strategy for attenuating chronic immune reactions. This approach, independent of probe geometry or type, offers the possibility to directly influence the cellular reactions in the close vicinity of the implanted probe and represents one of the strategies that we are currently exploiting to improve the tissue/probe interaction over time.

Lastly, I will briefly report another approach that we use to improve the performance of intracortical microelectrodes, combining in a single device several techniques for improving long-term reliability of neural interfaces and stability of recordings. These aims have been reached thanks to (1) the use of gold nanostructured microspheres

electrochemically grown at the free end of a thin tether; (2) the use of high surface area PEDOT-PSS-CNT coatings; (3) the encapsulation of the PEDOT-PSS-CNT coated microspheres with a soft, synthetic and permanent biocompatible hydrogel.

3.1

HIGHLY STABLE GLASSY CARBON INTERFACES FOR LONG-TERM NEURAL STIMULATION AND LOW-NOISE RECORDING OF BRAIN ACTIVITY.

Sci Rep. 2017 Jan 13; 7:40332. https://doi.org/10.1038/srep40332

Vomero M, Castagnola E, Ciarpella F, Maggiolini E, Goshi N, Zucchini E, Carli S, Fadiga L, Kassegne S, Ricci D.

We report on the superior electrochemical properties, in-vivo performance and long term stability under electrical stimulation of a new electrode material fabricated from lithographically patterned glassy carbon. For a direct comparison with conventional metal electrodes, similar ultra-flexible, micro-electrocorticography (μ-ECoG) arrays with platinum (Pt) or glassy carbon (GC) electrodes were manufactured. The GC microelectrodes have more than 70% wider electrochemical window and 70% higher CTC (charge transfer capacity) than Pt microelectrodes of similar geometry. Moreover, we demonstrate that the GC microelectrodes can withstand at least 5 million pulses at 0.45 mC/cm2 charge density with less than 7.5% impedance change, while the Pt microelectrodes delaminated after 1 million pulses. Additionally, poly(3,4-ethylenedioxythiophene)-poly(styrenesulfonate) (PEDOT-PSS) was selectively electrodeposited on both sets of devices to specifically reduce their impedances for smaller diameters (<60 μm). We observed that PEDOT-PSS adhered significantly better to GC than Pt, and allowed drastic reduction of electrode size while maintaining same amount of delivered current. The electrode arrays biocompatibility was demonstrated through in-vitro cell viability experiments, while acute in vivo characterization was performed in rats and showed that GC microelectrode arrays recorded somatosensory evoked potentials (SEP) with an almost twice SNR (signal-to-noise ratio) when compared to the Pt ones.

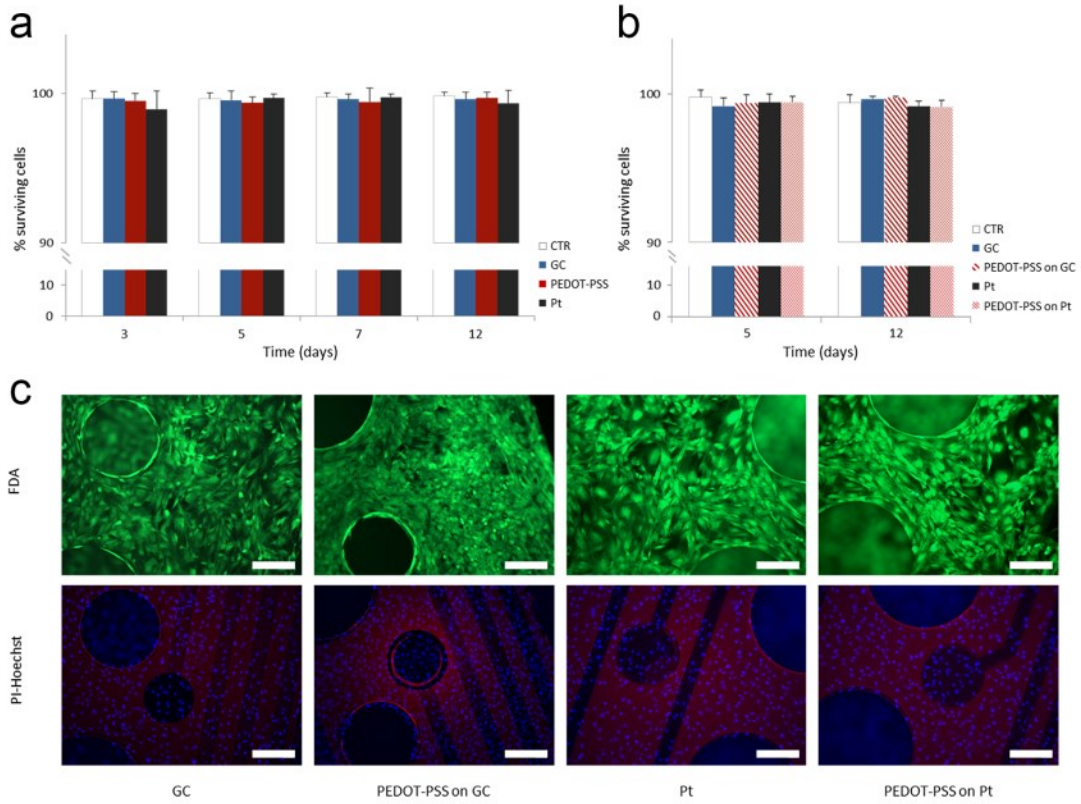

Figure 1 - extracted from paper 3.1:

Figure 7. Electrode biocompatibility tests. (a) Quantitative analysis of the viability of fibroblasts cultured on glass coverslip as control sample (CTR, white bars), glassy carbon (GC, blue bars), PEDOT-PSS (red bars) and platinum (Pt, black bars) substrates at 3, 5, 7, and 12 days *in vitro*. (b) Quantitative analysis of the viability of fibroblasts cultured on glass coverslip as control sample (CTR, white bars), glassy carbon (GC, blue bars), PEDOT-PSS on GC (thick diagonal red lines), platinum (Pt, black bars) and PEDOT-PSS on Pt (thin diagonal red lines) devices at 5 and 12 days *in vitro*. In a and b the percentages of surviving cells (means ± SD) were calculated based on the ratio of total (Hoechst-positive) nuclei minus dead cells (PI-positive) nuclei divided by the total nuclei. (c) Representative images of fibroblasts grown on the four different types of device at day 5 stained with FDA (green-viable cells marker), Hoechst-33342 (blue-total cells nuclei marker) and PI (red-dead cells nuclei marker). Scale bar: 200 μm.

3.2

A DIRECT COMPARISON OF GLASSY CARBON AND PEDOT-PSS ELECTRODES FOR HIGH CHARGE INJECTION AND LOW IMPEDANCE NEURAL INTERFACES.

Advances in Science and Technology, Vol. 102, pp. 68-76, 2017
https://doi.org/10.4028/www.scientific.net/AST.102.68

Vomero M, Castagnola E, Maggiolini E, Ciarpella F, Rembado I, Goshi N, Fadiga L, Kassegne S, Ricci D.

For neural applications, materials able to interface with the brain without harming it while recording high-fidelity signals over long-term implants are still sought after. Glassy Carbon (GC) and Poly (3,4-ethylenedioxythiophene)-poly (styrenesulfonate) (PEDOT-PSS) have proved to be promising materials for neural interfaces as they show – compared to conventional metal electrodes - higher conductivity, better electrochemical stability, very good mechanical properties and therefore seem to be very promising for in vivo applications. We present here, for the first time, a direct comparison between GC and PEDOT-PSS microelectrodes in terms of biocompatibility, electrical and electrochemical properties as well as in vivo recording capabilities, using electrocorticography microelectrode arrays located on flexible polyimide substrate. The GC microelectrodes were fabricated using a traditional negative lithography process followed by pyrolysis. PEDOT-PSS was selectively electrodeposited on the desired electrodes. Electrochemical performance of the two materials was evaluated through electrochemical impedance spectroscopy and cyclic voltammetry. Biocompatibility was assessed through in-vitro studies evaluating cultured cells viability. The in vivo performance of the GC and PEDOT-PSS electrodes was directly compared by simultaneously recording neuronal activity during somatosensory stimulation in Long-Evans rats. We found that both GC and PEDOT-PSS electrodes outperform metals in terms of electrochemical performance and allow to obtain excellent recordings of somatosensory evoked potentials from the rat brain surface. Furthermore, we found that both GC and PEDOT-PSS substrates are highly biocompatible, confirming that they are safe for neural interface applications.

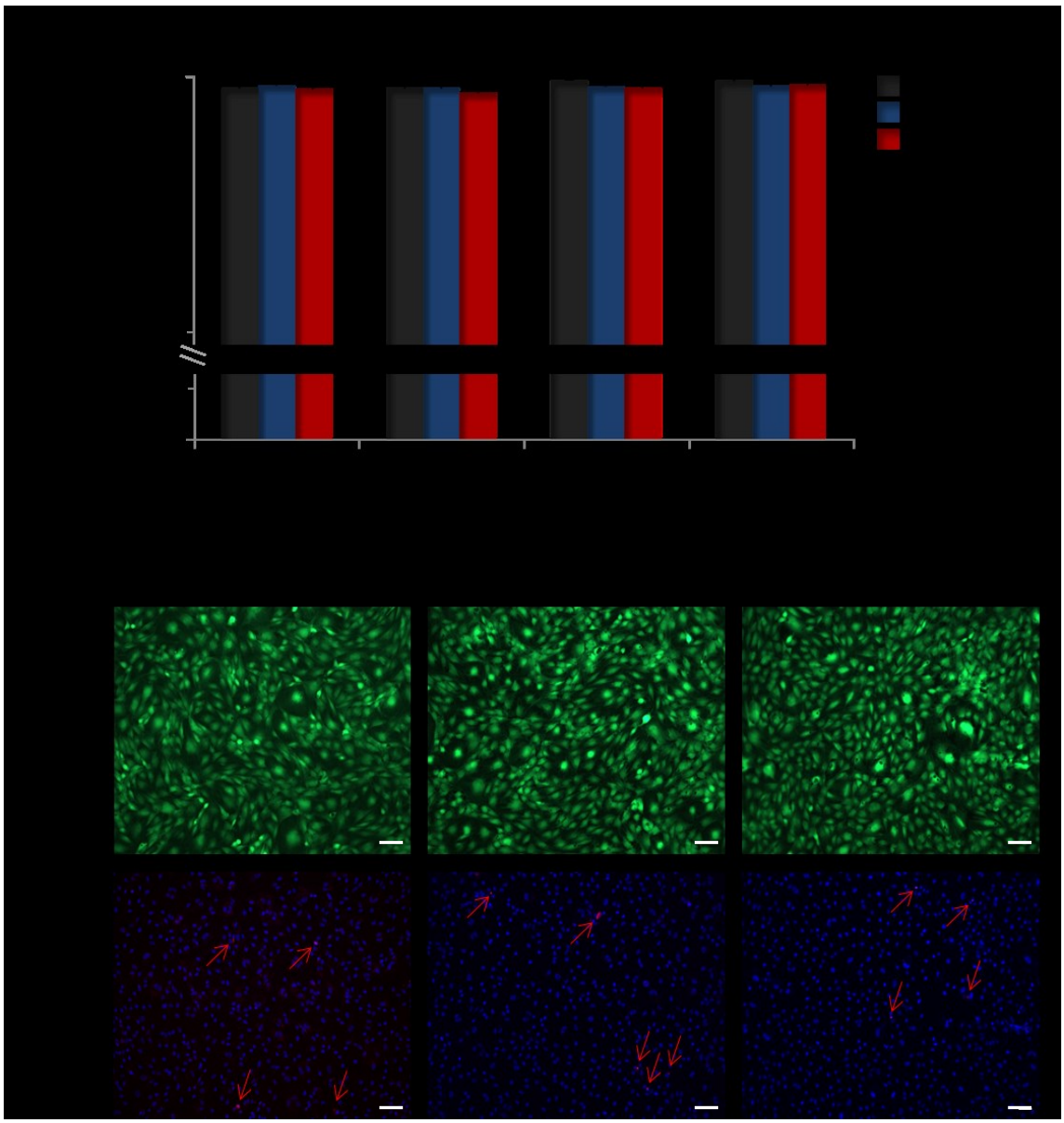

Figure 2 - extracted from paper 3.2:

Figure 4. (A) Quantitative analysis of the viability of fibroblasts cultured on glass coverslip as control sample (CTR, black bars), glassy carbon (GC, blue bars) and PEDOT-PSS (red bars) substrate at 3, 5, 7, and 12 days in vitro. The percentages of surviving cells (means ± SD) were calculated based on the ratio of total (Hoechst-positive) nuclei minus PI-positive nuclei divided by the total nuclei. (B) Representative images of fibroblasts grown on control glass coverslip (CTR), glassy carbon (GC) and PEDOT-PSS at day 12 stained with FDA (green-stained viable cells), Hoechst-33342 (blue-stained total cells nuclei) and PI (red-stained dead cells nuclei). Red arrows indicate the PI-positive nuclei. Scale bar: 100 μm

3.3

INCORPORATION OF SILICON CARBIDE AND DIAMOND-LIKE CARBON AS ADHESION PROMOTERS IMPROVES *IN VITRO* AND *IN VIVO* STABILITY OF THIN-FILM GLASSY CARBON ELECTROCORTICOGRAPHY ARRAYS.

Advanced Biosystems, Vol. 2, Issue 1, January 2018, 1700081 https://doi.org/10.1002/adbi.201700081

Vomero M, Castagnola E, Ordonez JS, Carli S, Zucchini E, Maggiolini E, Gueli C, Goshi N, Ciarpella F, Cea C, Fadiga L, Ricci D, Kassegne S, Stieglitz T.

Thin-film neural devices are an appealing alternative to traditional implants, although their chronic stability remains matter of investigation. In this study, a chronically stable class of thin-film devices for electrocorticography is manufactured incorporating silicon carbide and diamond-like carbon as adhesion promoters between glassy carbon (GC) electrodes and polyimide and between GC and platinum traces. The devices are aged in three solutions—phosphate-buffered saline (PBS), 30×10^{-3} and 150×10^{-3}M H_2O_2/PBS—and stressed using cyclic voltammetry (2500 cycles) and 20 million biphasic pulses. Electrochemical impedance spectroscopy (EIS) and image analysis are performed to detect possible changes of the electrodes morphology. Results demonstrate that the devices are able to undergo chemically induced oxidative stress and electrical stimulation without failing but actually improving their electrical performance until a steady state is reached. Additionally, cell viability tests are carried out to verify the noncytotoxicity of the materials, before chronically implanting them into rat models. The behavior of the GC electrodes in vivo is monitored through EIS and sensorimotor evoked potential recordings which confirm that, with GC being activated, impedance lowers and quality of recorded signal improves. Histological analysis of the brain tissue is performed and shows no sign of severe immune reaction to the implant.

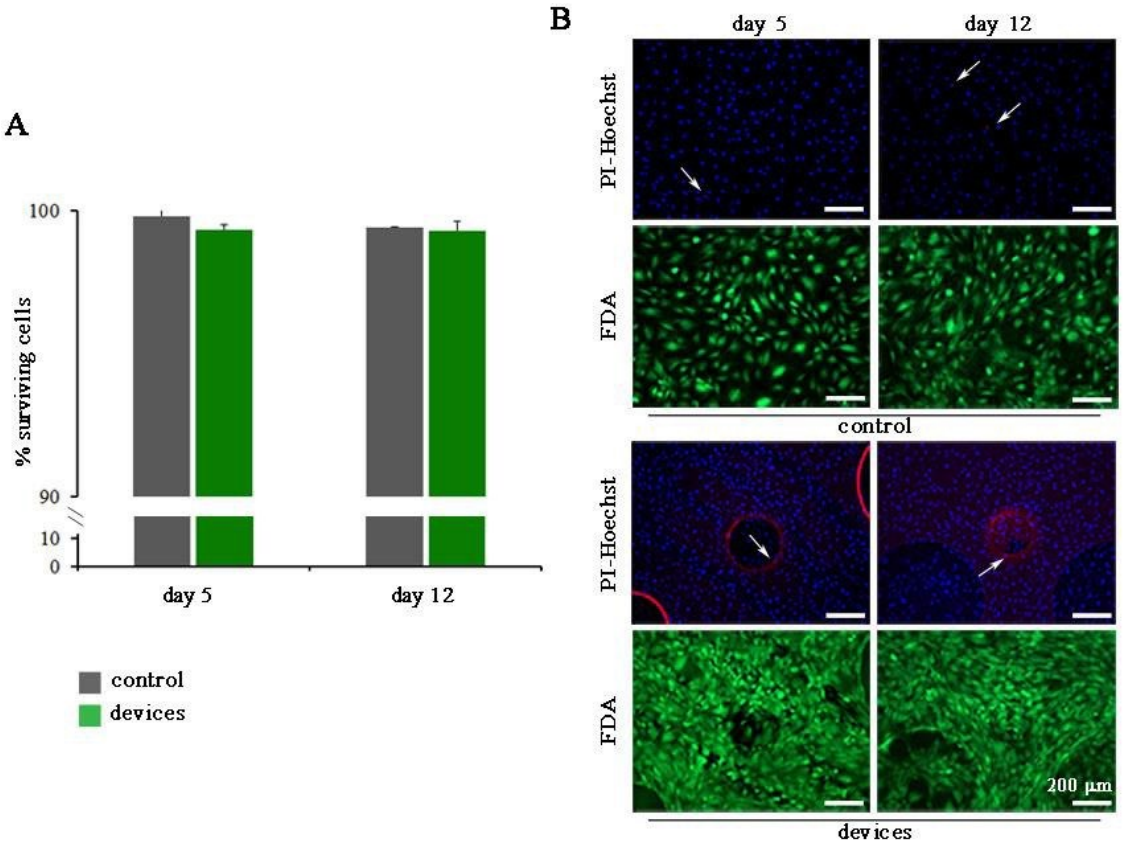

Figure 3 - extracted from paper 3.3:

Figure 8. (A) Quantitative analysis of the viability of fibroblasts cultured on glass coverslip as control sample (CTR, grey bars) and devices (green bars) at 5 and 12 days in vitro. The percentages of surviving cells (means ± SD) were calculated based on the ratio of total (Hoechst-positive) nuclei minus dead cells (PI-positive) nuclei divided by the total nuclei. (B) Representative images of fibroblasts grown on glass coverslip (control, upper panel) and devices (lower panel) at day 5 and day 12 stained with FDA (green-viable cells marker), Hoechst-33342 (blue-total cells nuclei marker) and PI (red-dead cells nuclei marker). White arrows indicate the PI-positive nuclei. Scale bar: 200 µm.

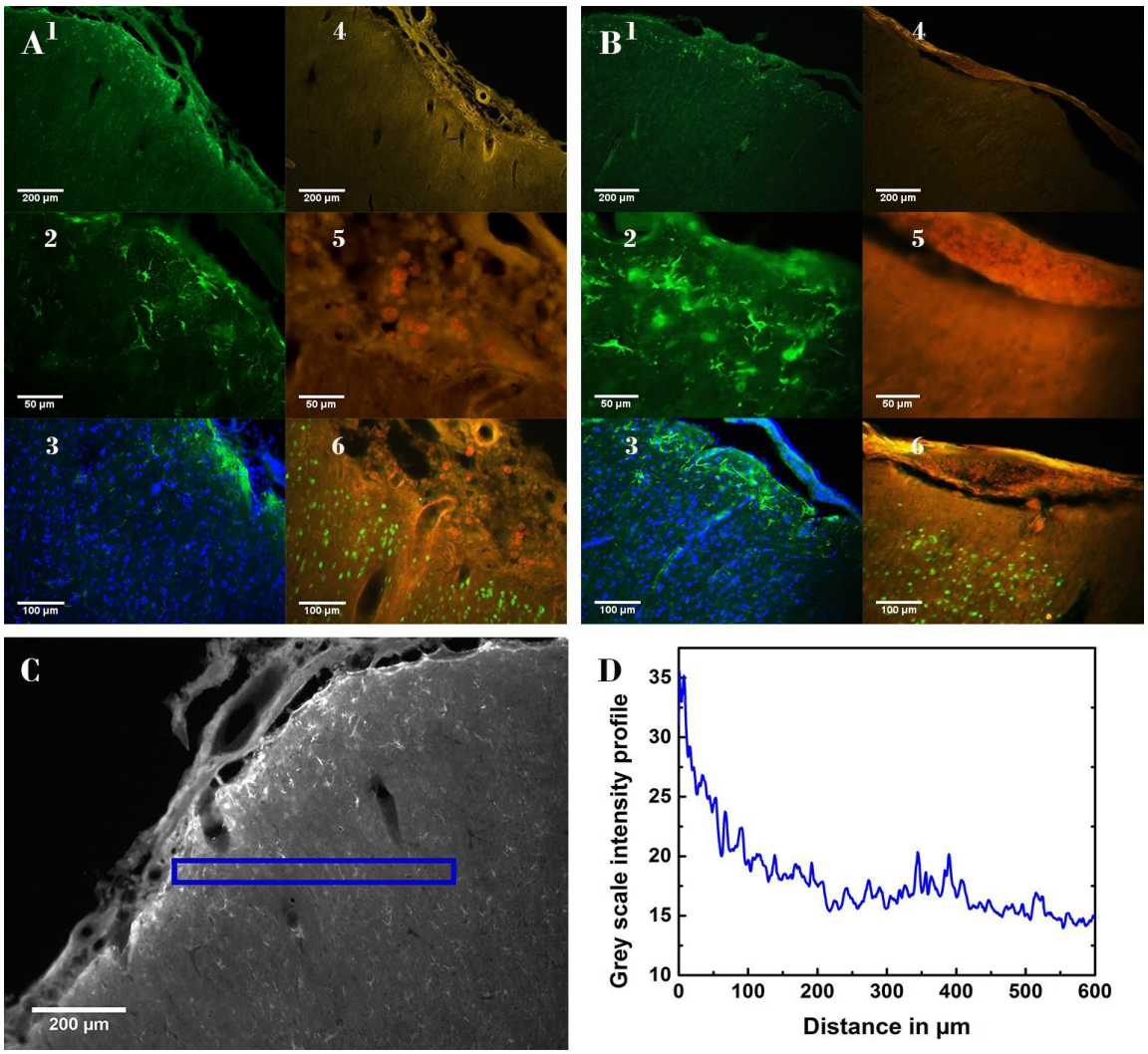

Figure 4 - extracted from paper 3.3:

Figure 11. A, B: Fluorescence microscopy images of the implanted cortex area for the experimental rat (A, ECoG electrode array implant) and for the control rat (B, just dental acrylic and screws implant). 1, 2: The images show the GFAP-positive cells (green) at 10x and 40x to underline respectively the morphology of the cortex and of the astrocytes. 3: The images show the cell nuclei (blue) merged on GFAP staining (green) to show the density of DAPI. 4, 5: The images show the ED1-positive cells (red) at 10x and 40x to underline respectively the morphology of the cortex and of the macrophages. 6: The images show the neuronal nuclei (green) merged on ED1 staining (red) to show the density of the neurons under the implanted cortex area. C, D: Fluorescence microscopy image (C) and the related graph (D) showing an example of the fluorescence (grey scale) decay following the distance from the brain surface calculated for the blue box area (50 x 600 µm) shown in panel C.

3.4

SINGLE WALLED CARBON NANOHORNS FOR NEURAL SENSING AND STIMULATION.

Sensors and Actuators B: Chemical, Vol. 271, pp. 280-288, 2018 https://doi.org/10.1016/j.snb.2018.05.083

Carli S, Lambertini L, Zucchini E, Ciarpella F, Scarpellini A, Prato M, Castagnola E, Fadiga L, Ricci D.

Oxidized single walled carbon nanohorns (ox-SWCNH) were electrodeposited onto gold microelectrode arrays in conjunction with poly(3,4-ethylenedioxythiophene) (PEDOT) and polystirenesulfonate (PSS), and the properties of the new composite material for neural recording and stimulation were assessed. PEDOT/ox-SWCNH composites were compared with films prepared with one of the most notorious carbonaceous material in this field, the oxidized multi-walled Carbon Nanotubes (ox-MWCNT). The PEDOT/ox-SWCNH exhibited superior charge transfer capability, reflecting greater electroactive surface, as confirmed by SEM and EIS characterizations. As a consequence, a charge injection limit of 11.6 mC/cm^2 was observed for the new composite, which is higher than the one of PEDOT/ox-MWCNT (8.7 mC/cm^2). Having confirmed comparable neural recording performance, the PEDOT/ox-SWCNH composite results very promising for improving therapeutic electrical stimulation in the central and peripheral nervous systems.

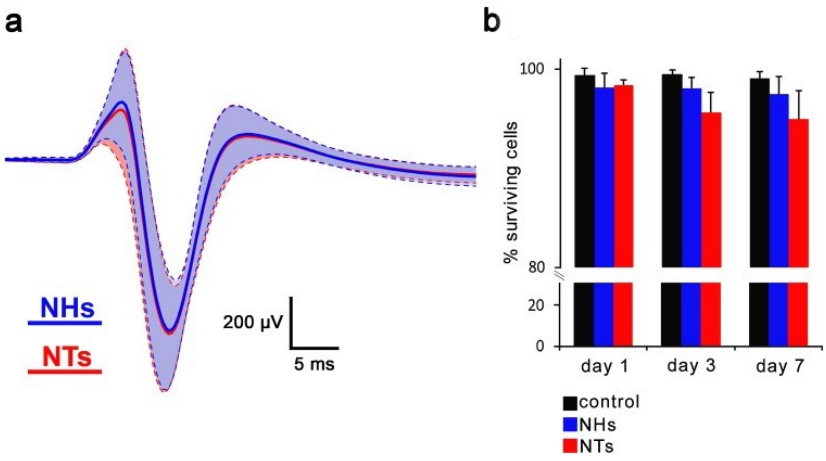

Figure 5 - extracted from paper 3.4:

Figure. 6. a) SEPs acquired by both types of electrodes (in blue NHs electrodes and in red NTs electrodes). Data are presented as mean (solid lines) ± SD (dashed lines) of all channels in 4 different locations (N = 32); b) Quantitative analysis of the viability of fibroblasts cultured on glass coverslip as control sample (control, black bars), over FTO coated with NHs (blue bars) and NTs (red bars) at 1, 3 and 7 days of *in vitro* culture. The percentages of surviving cells is represented as samples mean value ± SD.

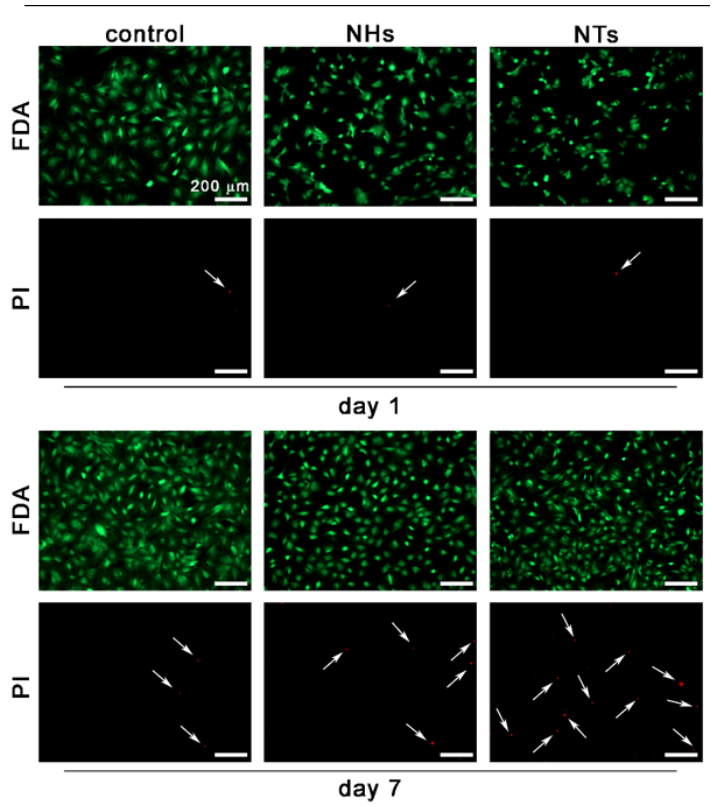

Figure 6 - extracted from paper 3.4:

Figure S12. Representative images of fibroblasts cultured on glass coverslips (control), over FTO coated with NHs and NTs at day 1 (upper panel) and day 7 (lower panel) stained with FDA (green-viable cells marker) and PI (red-dead cells nuclei marker). White arrows indicate the PI-positive nuclei. Scale bar: 200 µm.

3.5

DRUG DELIVERY SYSTEM BASED ON TAUROURSODEOXYCHOLIC ACID AND PEDOT.

Chemistry - A European Journal – *Article accepted for publication*

Carli S, Fioravanti G, Armirotti A, Ciarpella F, Prato M, Ottonello G, Salerno M, Scarpellini A, Perrone D, Marchesi E, Ricci D, Fadiga L.

One of the main concerns related to chronically implanted intracortical neural microelectrodes is the adverse reaction of the surrounding tissue and the modulation of this response represents one of the main goals to be reached in order to account for long-term use of neural intracortical implants. In this context, localized drug delivery from biocompatible poly(3,4-ethylenedioxythiophene) (PEDOT) coated on neural probes, is one of the most powerful tools to reduce the foreign body response as well as to overcome the well-known issues related to the systemic administration of high dosage of glucocorticoids. For this purpose, the use of potent synthetic anti-inflammatory Dexamethasone phosphate (DEX) is widely reported. Recent studies suggest that Tauroursodeoxycholic acid (TUDCA) may have cytoprotective and anti-apoptotic action, with potential neuroprotective activity. Moreover, anti-inflammatory properties of TUDCA toward acute neuroinflammation on an animal model were reported: in particular, TUDCA exerts its anti-inflammatory neural activity by reducing the microglial and astrocytic cells activation which represents the same activation pathway due to neural device implantation. Surprisingly, to the best of our knowledge, drug delivery systems based on the incorporation of TUDCA within conductive polymers has not been reported hitherto, nor is its application as a potential anti-inflammatory agent for in vivo neural studies. Hence, for the first time, we incorporated TUDCA within PEDOT backbone through the ionic-approach, which is expected to promote an electrochemically controlled delivery of the drug. Furthermore, we compared the new PEDOT-TUDCA composite with the well-known DEX-P conjugate (PEDOT-DEX) in terms of electrochemical as well as morphological and biocompatibility properties.

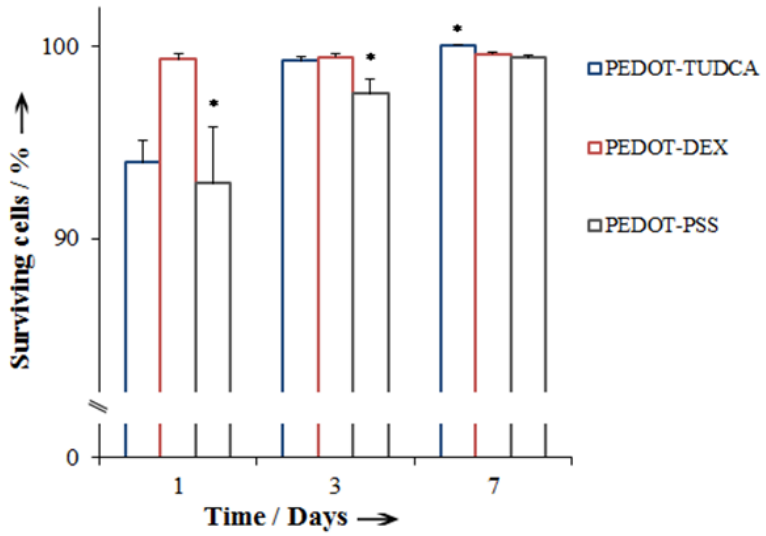

Figure 7 - extracted from paper 3.5:

Figure 8. Quantitative analysis of the viability of fibroblasts cultured on PEDOT-TUDCA (blue bars), PEDOT-DEX (red bars), PEDOT-PSS (gray bars) substrate at 1, 3, and 7 days in vitro. The percentages of surviving cells (means ± ER) were calculated based on the ratio of total (Hoechst-positive) nuclei minus PI-positive nuclei divided by the total nuclei. *: *p value* < 0.05.

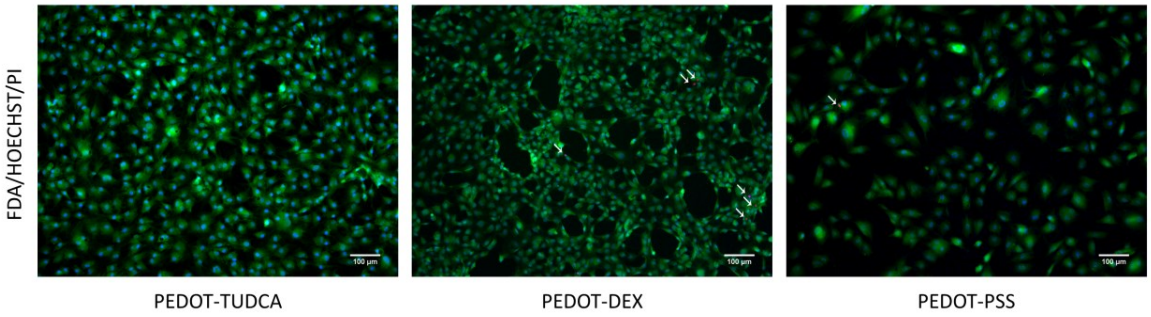

Figure 8 - extracted from paper 3.5:

Figure S4. Electrode cytocompatibility: representative images of fibroblasts grown on the three different types of coating at day 7 stained with FDA (green-viable cells marker). Arrows indicate death cells.

3.6

pHEMA Encapsulated PEDOT-PSS-CNT Microsphere for Recording Single Unit Activity in the Brain.

Front Neurosci. 2016 Apr 18;10:151. https://doi.org/10.3389/fnins.2016.00151

Castagnola E, Maggiolini E, Ceseracciu L, Ciarpella F, Zucchini E, De Faveri S, Fadiga L, Ricci D.

The long-term reliability of neural interfaces and stability of high-quality recordings are still unsolved issues in neuroscience research. High surface area PEDOT-PSS-CNT composites are able to greatly improve the performance of recording and stimulation for traditional intracortical metal microelectrodes by decreasing their impedance and increasing their charge transfer capability. This enhancement significantly reduces the size of the implantable device though preserving excellent electrical performance. On the other hand, the presence of nanomaterials often rises concerns regarding possible health hazards, especially when considering a clinical application of the devices. For this reason, we decided to explore the problem from a new perspective by designing and testing an innovative device based on nanostructured microspheres grown on a thin tether, integrating PEDOT-PSS-CNT nanocomposites with a soft synthetic permanent biocompatible hydrogel. The pHEMA hydrogel preserves the electrochemical performance and high quality recording ability of PEDOT-PSS-CNT coated devices, reduces the mechanical mismatch between soft brain tissue and stiff devices and also avoids direct contact between the neural tissue and the nanocomposite, by acting as a biocompatible protective barrier against potential nanomaterial detachment. Moreover, the spherical shape of the electrode together with the surface area increase provided by the nanocomposite deposited on it, maximize the electrical contact and may improve recording stability over time. These results have a good potential to contribute to fulfill the grand challenge of obtaining stable neural interfaces for long-term applications.

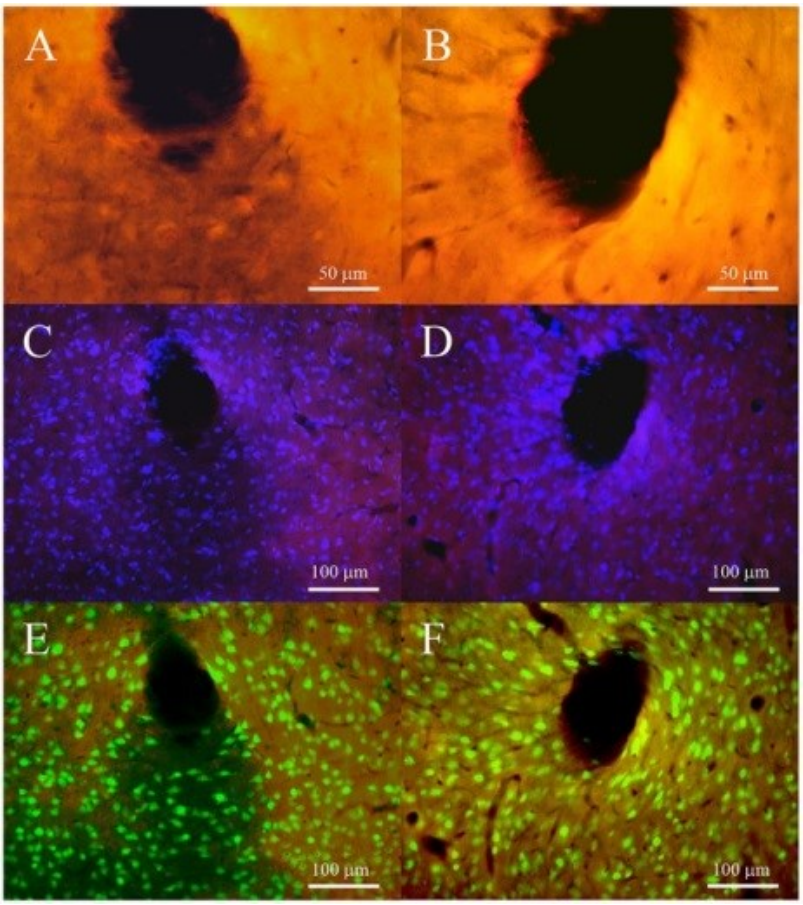

Figure 9 - extracted from paper 3.6:

Figure 9. Fluorescence microscopy images of tracks for non-encapsulated (left panels) and pHEMA-encapsulated (right panels) microspheres at 2 weeks after implant. (A, B) show the GFAP-positive cells (red) at 40× to underline the morphology of astrocytes; (C, D) cell nuclei (blue) merged on GFAP staining to show the density of DAPI surrounding tracks; (E, F) neuronal nuclei (green) merged with GFAP staining to show the presence of neuronal bodies surrounding the track.

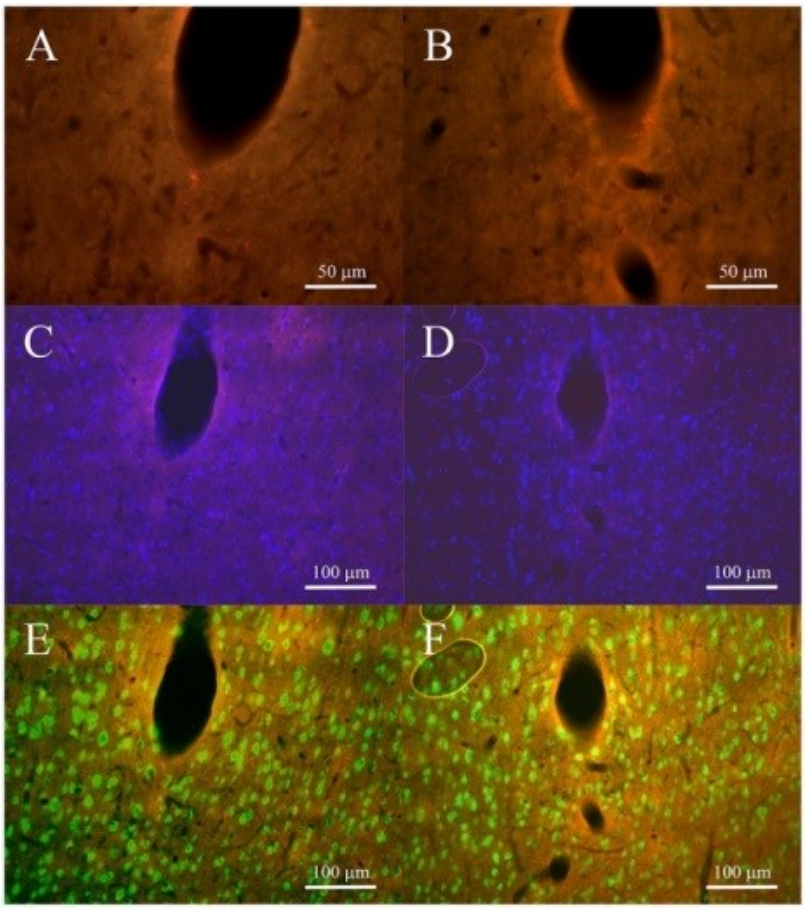

Figure 10 - extracted from paper 3.6:

Figure 10. Fluorescence microscopy images of tracks for non-encapsulated (left panels) and pHEMA-encapsulated (right panels) microspheres 4 weeks after implant. (A, B) show the GFAP-positive cells (red) at 40× to underline the morphology of astrocytes; (C, D) cell nuclei (blue) superimposed on GFAP staining to verify the density of DAPI surrounding the tracks; (E, F) neuron nuclei (green) superimposed on GFAP to show the presence of neuronal bodies surrounding the tracks.

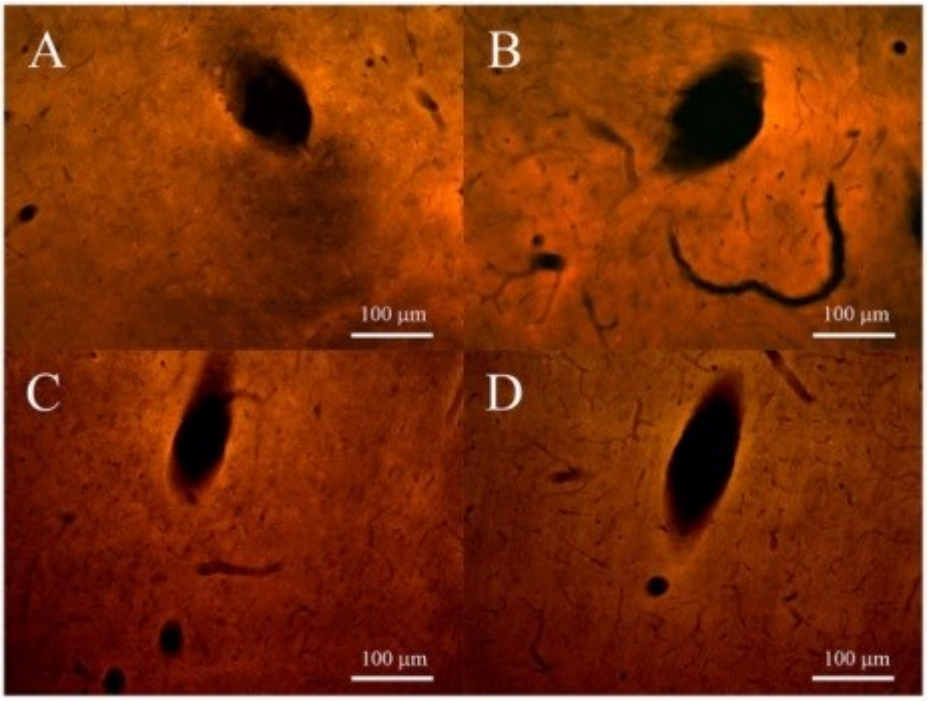

Figure 11 - extracted from paper 3.6:

Figure 11. Fluorescence microscopy images of tracks for non-encapsulated (left panels) and pHEMA-encapsulated (right panels) microspheres, 2 and 4 weeks after the implant. (A, B) show the ED1-positive cells (red) at 20× at 2 weeks; (C, D) show the ED1-positive cells (red) at 20× at 4 weeks.

CONCLUSIONS AND FUTURE PERSPECTIVE

This thesis has accounted the main projects carried out during my doctorate, linked together by a common key goal that was the development of a new kind of neural devices, able to overcome the issues that so far limit the use of implantable microelectrodes for durable applications.

The reason why we focused on intracortical microelectrode arrays lies in the several advantages they offer, such as the ability to selectively access individual or small groups of cortical neurons and the possibility to deliver high-resolution spatiotemporal patterns of stimulation. Intracortical microelectrodes could represent very promising devices for dealing with many disorders of the nervous system. However, one of the main concerns related to implanted intracortical microelectrodes is the adverse reaction of the surrounding tissue, that can lead to the phenomena of electrode encapsulation and chronic inflammatory response resulting in loss of neuronal recording/stimulating ability. Thus, new approaches should be investigated to mitigate these reactions.

In this framework, biocompatibility and long-term viability are crucial questions for chronic applications of implanted devices and a seamless integration of the human made devices with the nervous system is desirable both to revolutionize our understanding of the brain and to significantly enhance the quality of life in individuals with compromised neural function due to disease or trauma.

Here, we have explored the use of innovative materials testing their non-cytotoxicity by *in vitro* methods and, along the chapters, I have presented some of the intervention strategies we investigated in order to maintain the integrity of both the probe and the tissue as much as possible.

We show that the brain tissue foreign body reaction could be attenuated by the development of a biocompatible and biomimetic coating made of living-cells and that the recording consistency and lifetime of implanted arrays could be improved by a more cell-friendly design, with ultra-small dimensions and flexibility as much as possible compliant with the soft nature of the brain. Additionally, pharmacological interventions through the embedding and release of anti-inflammatory molecules from devices materials have been investigated to reduce harmful cellular reactions elicited by implanted arrays.

Considering the ultimate goal of my research, a great effort is done in identifying the most potent strategies for improving microelectrode performance and this probably requires to implement and integrate multiple strategies together. Furthermore, it is also essential to better understand the signals that lead to neuroglial activation and to create a targeted intervention strategy to prevent or at least to control this response. From this perspective, we are currently working on cutting-edge production techniques, on a more comprehensive molecular examination of the tissue reaction and on the development of an entirely compatible electrode, capable of long-term clinical applications.